Kasdi Merbah University – Ouargla –
Faculty of Hydrocarbons, Renewable Energies, Earth Sciences, and Universe
Department of Drilling and Mechanics of Oil Fields

Dissertation
Professional Master

Domain: Science and Technology

Field: Hydrocarbons

Specialty: Professional drilling

Submitted by

Assil Lidia Ramdani

Taha Kheir eddine Khelaifia

Abdelbadie Bouziza

Title

Contribution to the use of SWD technology: Simulation Study of a Comparison between VSP and drill bit stick-slip vibration

Publicly defended On
06/06/2024

Academic year
2023 / 2024

Dedication

*I am so proud to dedicate this thesis to my amazing mother **S. Benaissa**, who has been my rock and the driving force behind my success. My accomplishments would not have been possible without your steadfast love, selfless giving, and unshakable support. I am inspired daily by your fortitude and tenacity.*

*I also want to dedicate it to my dearest grandfather **M. Benaissa** and my three wonderful sisters, **Hadil Linda**, **Karisse Lilia** and **Ranime Hazare** who have been my pillars of support and my greatest cheerleaders. Your unfailing confidence in me and your unceasing support have given me the willpower and endurance I need. This endeavor would not be feasible without your help, but it has also been extremely fulfilling.*

*To my incredible friends **Nadjoua Chikhi** and **Taha Kheireddine Khelaifia**, whose unwavering friendship and relentless support have been a beacon of strength and motivation throughout this journey.*

I am so grateful for all of your constant love, inspiration, and support. This achievement is proof of your influence and the significant impact you have made on my life and academic career!

Assil Lidia Ramdani

Dedication

First and foremost, I thank Almighty and Merciful Allah for giving me the courage, strength, and patience to accomplish this work.

*I dedicate my thesis to my life's role model, my dear father **Abdel Moudjoud**. Your guidance and support have shaped my personality, and I am proud to follow in your footsteps. May Allah bless you as the crown above my head; you are the person I aspire to become.*

*To my dear mother **Samira**, the bright side of my life, your endless sacrifices, late nights, and selfless devotion have paved the way for me to pursue my dreams and reach this significant milestone. Your encouragement during moments of doubt and your celebrations during moments of triumph have shaped me into the person I am today. Thank you for being an essential part of my life and the reason for my success.*

*I also dedicate this work to my beloved siblings: my sister **Amira**, my brother, my look-alike **Aymen**, my brother and my close friend **Marwan**, your love, continuous support, and unwavering appreciation have been invaluable to me.*

*To my caring aunts, **Zohra** and **Fouzia**, thank you for your endless support. Your words of encouragement have been a constant source of motivation during challenging times.*

*To my dear brother **Naim Lallali**, your unwavering friendship, encouragement, and belief in me have been a constant source of strength and inspiration. Thank you for being a good friend and another brother for me.*

*Finally, I want to dedicate this work to a special person, **Assil Lidia Ramdani**, whose brightness got me through my worst times. I appreciate everything you've done for me, including your constant presence and support.*

Thank you all!

Taha Kheir eddine Khelaifia

Dedication

*To my beloved family, my foundation and my strength: my mother and father, for their endless support and encouragement; my siblings **Kawther**, **Issam**, **Abdelmounim**, and **Fatima Zohra**, for their unwavering belief in me and their constant love.*

*To my dear friend **Selman** and all my friends, for their companionship and support throughout this journey.*

To my cherished homies of the university residence, I'll miss the unforgettable days we've shared together.

To the members of the Petroleum Club SPE, with whom I spent three incredible years growing, learning, and achieving together.

And to the wonderful team at Pastry Bouchra, thank you for your kindness and support.

This thesis is dedicated to all of you.

Abdelbadie Bouziza

Gratitude

We would like to express our gratitude to Almighty God for bestowing upon us the strength, courage and patience to undertake this work.

We would like to extend our gratitude to ***T. Bourechak****, for his guidance whenever we needed it and providing us with invaluable advice about our thesis.*

Our profound gratitude goes out also to ***H. Saaler****,* ***L. Hammache****,* ***B. Hafsi****,* ***Z. Sadi*** *and* ***Redouane*** *for their significant advice and direction about our thesis and for their continuous assistance during our project, "Thank you for your generosity".*

Our sincere gratitude goes out to our supervisors, ***Mr. Elhadi Atlili****, and* ***Mr. Khelifa Cherif****, for their steadfast assistance and knowledge. Their advice and perceptive criticism have been helpful for completing this study.*

Furthermore, we convey our appreciation to the jury members for their invaluable time, perceptive observations, and helpful criticism during the development of our thesis.

Finally, we are pleased to thank everyone who helped in any way. We really appreciate your contributions, encouragement, and continuous backing, all of which have made it possible for us to finish this thesis. We would be negligent to overlook the priceless help we were given in finishing this thesis.

Abstract

Seismic technologies have the potential to significantly enhance the exploration of subterranean layers in search of oil and gas reserves. In this context, this thesis discusses the practicality and advanced application of Seismic While Drilling technology, with a particular focus on stick-slip vibrations, which represent another kind of seismic source. The study commences with a fundamental exposition of methodologies such as vertical seismic profiling and borehole imaging, and it elucidates the intricacies inherent to these seismic imaging techniques. The study contributes to the ongoing discourse on the utilisation of stick-slip vibrations in SWD processes by synthesising theoretical insights with practical applications, with a particular focus on advanced techniques. Finally, it employs Python and MATLAB simulations to corroborate theories and demonstrate their possibility to be applied in complex geological settings, with a particular focus on the Algerian oilfields. This thesis demonstrates how SWD technology can revolutionise real-time subsurface imaging and drilling performance, thereby significantly advancing seismic exploration procedures.

Keywords: Seismic While Drilling, stick-slip vibrations, vertical seismic profiling, borehole imaging, Algerian oilfields, drilling performance, seismic exploration methods.

Résumé

Les technologies sismiques ont le potentiel d'améliorer considérablement l'exploration des couches souterraines à la recherche de réserves de pétrole et de gaz. Dans ce contexte, cette thèse traite de l'aspect pratique et de l'application avancée de la technologie de forage sismique, en mettant l'accent sur les vibrations de type stick-slip, qui représentent un autre type de source sismique. L'étude commence par un exposé fondamental des méthodologies telles que le profilage sismique vertical et l'imagerie de forage, et élucide les subtilités inhérentes à ces techniques d'imagerie sismique. L'étude contribue au discours actuel sur l'utilisation des vibrations de type stick-slip dans les processus SWD en synthétisant les idées théoriques avec des applications pratiques, avec un accent particulier sur les techniques avancées. Enfin, elle utilise des simulations Python et MATLAB pour corroborer les théories et démontrer leur possibilité d'application dans des contextes géologiques complexes, avec un accent particulier sur les champs pétrolifères algériens. Cette thèse démontre comment la technologie SWD peut

révolutionner l'imagerie de la subsurface en temps réel et les performances de forage, faisant ainsi progresser de manière significative les procédures d'exploration sismique.

Mots-clés: Seismic While Drilling, stick-slip vibrations, vertical seismic profiling, borehole imaging, Algerian oilfields, drilling performance, seismic exploration methods.

ملخص

تحسِّن التقنيات الزلزالية بشكل كبير من استكشاف الطبقات الجوفية بحثًا عن احتياطيات النفط والغاز. في هذا السياق، تناقش هذه الأطروحة التطبيق العملي والمتطور لتقنية الزلازل أثناء الحفر، مع التركيز على الاهتزازات الانزلاقية اللاصقة التي تعد نوعاً آخر من المصادر الزلزالية. وتبدأ الدراسة بشرح أساسي لطرق مثل التنميط الزلزالي الرأسي والتصوير الآبار، وتسلط الضوء على التعقيدات التي تنطوي عليها تقنيات التصوير الزلزالي هذه. تقدم الدراسة الحديث عن استخدام الاهتزازات الانزلاقية اللاصقة في عمليات التصوير الزلزالي العمودي من خلال دمج الفهم النظري مع التطبيق الواقعي والتركيز على التقنيات المتقدمة. وفي النهاية، تدمج الأطروحة محاكاة باستخدام برنامج Python وMATLAB لتأكيد النظريات وإثبات قابليتها للتطبيق في المواقف الجيولوجية المعقدة، وتحديداً المتعلقة بحقول النفط الجزائرية. تسلط هذه الأطروحة الضوء بشكل أساسي على الكيفية التي يمكن أن تُحدث بها تقنية SWD ثورة في التصوير تحت السطح في الوقت الحقيقي وأداء الحفر، وبالتالي إحداث تقدم كبير في إجراءات الاستكشاف الزلزالي.

الكلمات المفتاحية: الحفر الزلزالي أثناء الحفر، الاهتزازات الزلزالية اللاصقة، التنميط الزلزالي العمودي، التصوير الزلزالي للآبار، حقول النفط الجزائرية، أداء الحفر، طرق الاستكشاف الزلزالي.

Table of contents

CHAPTER II: Stick-Slip vibration during drilling

CHAPTER III: **Drill bit stick-slip vibration and SWD**

List of Figures

CHAPTER I: Overview of Borehole imaging and VSP

CHAPTER II: Stick-Slip vibration during drilling

CHAPTER III: Drill bit stick-slip vibration and SWD

CHAPTER IV: Simulation using Python and MatLab

List of Tables

CHAPTER I: Overview of Borehole imaging and VSP

CHAPTER II: Stick-Slip vibration during drilling

CHAPTER III: Drill bit stick-slip vibration and SWD

CHAPTER IV: Simulation using Python and MatLab

List of Abbreviations

VSP : Vertical Seismic Profiling

P wave : Primary waves

S wave : Secondary waves

ZVSP: Zero-offset Vertical Seismic Profiling

FB : First Break

API : American Petroleum Institute

CREWES: Consortium for Research in Elastic Wave Exploration Seismology

SAC : Seismic Analysis Code

SEG-Y: Standard Exchange format for Geophysical data

MWD: Measurement While Drilling

SSV: Stick Slip Vibration

RPM: Rotation per minute

BHA: Bore hole assembly

PDC: Polycrystalline Diamond Compact

TVM: Torsional Vibration Mitigation

WOB: Weight on bit

ROP: Rate of penetration

SNR: Signal to Noise Ratio

ARMA: The autoregression and moving average

GENERAL INTRODUCTION

General Introduction

Seismic While Drilling (SWD) represents a groundbreaking advancement in the field of geophysical exploration, providing real-time seismic data acquisition during the drilling process. This innovative technique capitalizes on the vibrations produced by the drill bit, utilizing them as a seismic source to generate continuous subsurface images. By integrating seismic data collection with drilling operations, SWD aims to enhance the efficiency and safety of hydrocarbon exploration and production.

Among the various sources of vibrations during drilling, stick-slip vibrations have emerged as a particularly promising candidate for SWD. This dynamic phenomenon occurs when the rotational movement of the drill string alternates between periods of sticking and slipping, resulting in high-amplitude, low-frequency oscillations. These oscillations can generate seismic waves capable of penetrating the surrounding geological formations, providing valuable seismic information without the need for additional seismic surveys.

The primary objective of this research is to evaluate the viability of stick-slip-based SWD in the Algerian oilfields, taking into account the specific geological and operational challenges. Through a combination of theoretical analysis and practical field assessments, this study aims to identify the limitations and potential solutions for implementing this technique in a region known for its complex subsurface conditions.

This thesis will delve into the mechanics of stick-slip vibrations, the propagation of seismic waves through various geological formations, and the methodologies for real-time seismic data acquisition and interpretation.

The chapters will establish a comprehensive framework for understanding the fundamental principles and technical considerations of using stick-slip vibrations as a seismic source. It will focus on the specific challenges encountered in the Algerian oilfields and assess the impact of geological factors such as salts and anhydrite on seismic wave transmission and the overall effectiveness of stick-slip-based SWD. Field data and simulations will be used to evaluate the feasibility of this technique under real-world conditions.

CHAPTER I

Overview of Borehole imaging and VSP

1. Introduction

The concept of "borehole imaging" describes a method used in petroleum engineering and geophysics for imaging the subsurface formations and structures surrounding a borehole. Using specific instruments or sensors, this procedure entails drilling a borehole to obtain comprehensive photographs of the nearby geological formations.

Borehole imaging is a useful tool for geological interpretation, reservoir characterization, and wellbore stability research because it offers important details on the lithology, structure, fractures, and fluid content of the subsurface. The imaging tools used in borehole imaging typically employ various technologies, including acoustic, electromagnetic, and optical methods, to generate images of the borehole wall and surrounding formations. Additionally, we have a vertical seismic profiling (VSP) is used to extract high-resolution seismic data from wells or boreholes.

In contrast to traditional surface seismic surveys, which use seismic sources and receivers on the surface to collect images of the subsurface, vertical seismic profiling (VSP) uses seismic sources and receivers down a borehole to obtain data directly from the subsurface. This makes it possible to obtain higher resolution and accuracy images, particularly of areas with difficult-to-access areas or complex surface geology.

2. Vertical Seismic Profile

One important method in geophysical exploration is vertical seismic profiling, or VSP. It entails monitoring both upgoing and down going seismic wavefields along a stratigraphic succession. Not too long after the initial attempts at surface reflection seismology, in which sources and receivers were situated at the surface.

In general The VSP has four important roles to play in assessing the rock and fluids close to the borehole:

- To provide in situ rock properties in depth, particularly seismic velocity, impedance, anisotropy, and attenuation,
- To assist in understanding seismic wave propagation (e.g., source signatures, multiples, and conversions),

- To make well understood reflectivity images in depth,
- To use all of the above in further surface seismic data processing and interpretation. [1]

The basic components of a VSP survey are a seismic source, wireline and downhole receiver array, and a recording/wireline truck [1]. In vertical seismic profiling, the energy source is placed on the surface; however, the geophones are placed down a borehole at equally spaced depth intervals (typically 50 to 100 ft) and several seconds of data are recorded. In this way, the source pulse can be followed within the subsurface. In most seismic measurements, both the energy source and the receivers are positioned on the earth's surface. The seismic-energy sources used for VSP can be impulsive (e.g. explosives), controlled (e.g., mechanical vibrator), or an active drill bit, and the source strength is site- and project-specific.

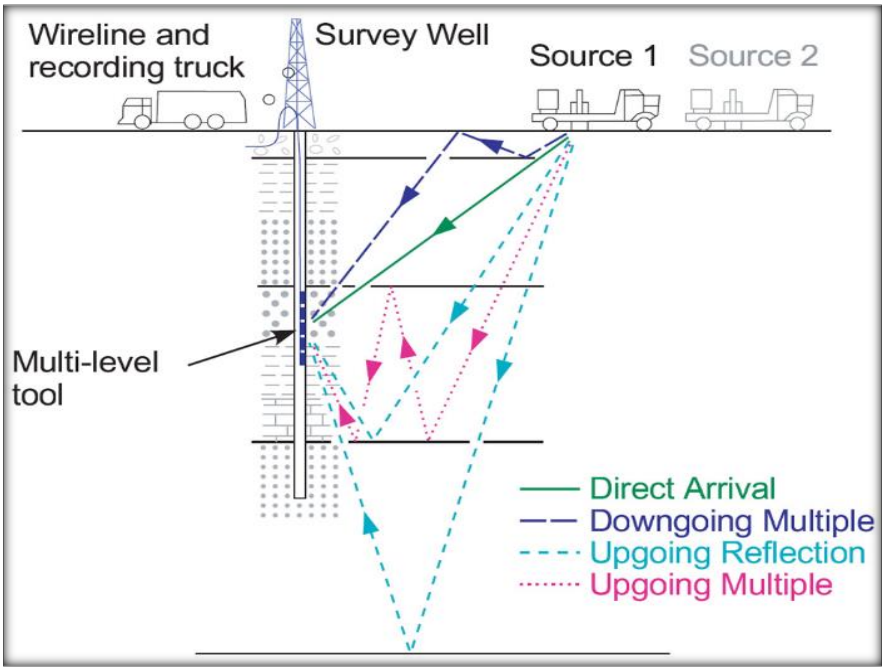

Figure I. 1. Schematic diagram of a VSP survey indicating a survey well, seismic source**,** receiver, wireline and recording trucks (from DiSiena et al., 1984).

2.1. VSP configurations

2.1.1 Near-offset VSP or zero-offset VSP

Refers to a geometrical configuration where the source and receiver locations are vertically aligned, or can be treated as such during processing. Near-offset VSPs are typically used to tie surface-seismic data to the subsurface geology and to differentiate primary reflections from surface-generated and interbed multiples. Figure (I. 2).

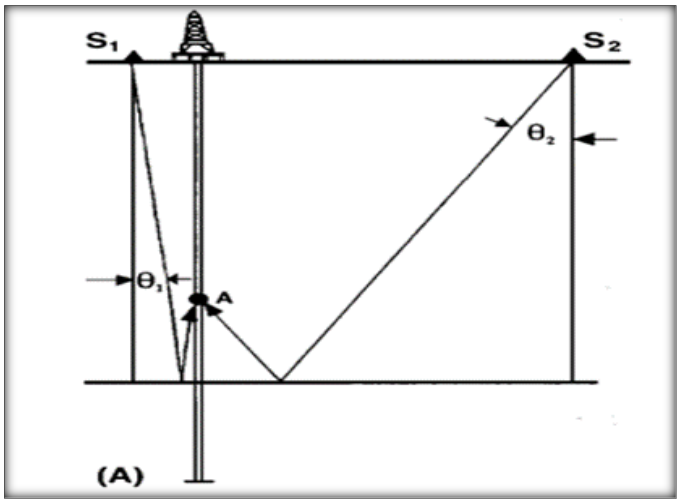

Figure I. 2. The field layout of the (zero) near- offset VSP surveys.

In (A), the surface source at S1 is at a zero-incidence location with respect to the geophone borehole sonde in the vertical non-deviated borehole. The up- and down going waves travel vertically down to the reflector and back to the receiver geophone sonde in the borehole. The source at S2 is a non-zero offset location as the source does not lie directly over the borehole geophone.

Example of Near-offset (Zero-offset VSP)

This example about the acquisition parameters used for the near-offset over-sea ice VSP.

Table I. 1 : Vertical Seismic Profile Acquisition Parameters

Survey type	Near-offset VSP
Offset	70 m in the structural up-dip direction from the drill-site
Source Type	Seismic Systems 210- in3 generator-injector air gun
Source Mode	Harmonic, generator and injector volumes of 105 in3 each
Air gun Position	18 m below the ice level
Air Gun Pressure	2000 psi
Top Depth	386m
Bottom Depth	1388m

Receiver Spacing	6 m
Air Gun Pressure	3.4 x 106 pa (2000 psi)
Sampling Rate	2 ms
Record Length	3 s
Borehole Inclination	~ 2.25 °.

2.1.2 Far-offset VSP or offset VSP (Cassell, 1984)

Refers to a geometrical configuration where the source and receiver locations cannot be treated as vertically aligned during processing. The configurations using source S2 and source S3 with receivers at either B or C (Figure I. 2) illustrate far-offset geometry.

Our preferred definition is that far-offset geometry exists whenever it is necessary to partition a wavefield in order to isolate a wavefield component onto a single data channel Far-offset VSPs are typically recorded to seismically image the subsurface away from the borehole in more detail, or when conditions preclude running a near-offset VSP.

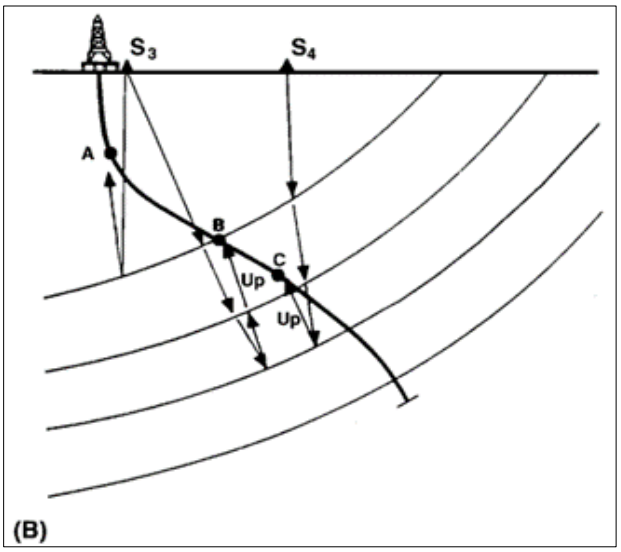

Figure I. 3. The field layout of the far-offset VSP surveys.

In (B) for the deviated borehole, source S3 is in a zero-offset configuration for the upper vertical (shallow depths) part of the borehole and (non-zero) far-offset for the deviated remainder of the borehole.

2.1.3 Check-shot VSP

Surface-recorded seismic data often comprise the largest database that must be dealt with in reservoir development. However, seismic data have one shortcoming that can limit their usefulness—the reflection events used to map the seismic sequences and the seismic facies that describe the areal and vertical distributions of reservoir and sealing units are measured as functions of seismic traveltime, not as functions of depth [2].

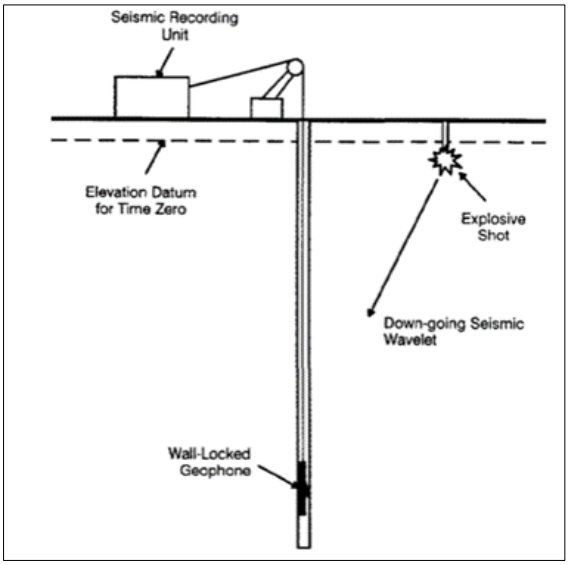

Figure I. 4. The source-receiver geometry check shot VSP surveys [2].

2.1.4 Multi-offset VSP (Walk-away VSP)

Walk away VSP entails a receiver array of five to seven geophones collect data from multiple surface source location along a line that extends from the well each line usually has hundreds of source positions. Reflections from each horizon below the geophone offer an umbrella- shaped coverage of the formation along-side and beneath the well [2], Figure (I. 5).

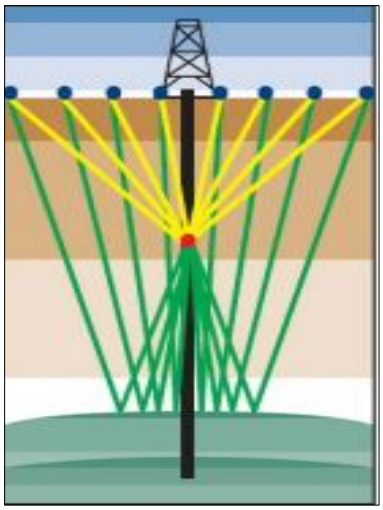

Figure I. 5. Walk-away VSP surveys [3].

Geophone position **Source position**

Up going ray path **Down going ray path**

2.1.5 Walk above VSP

This method takes into account a deviated well's geometry. Every receiver has a unique lateral position, and in every scenario, the source is directly above the receiver. These data offer a high-resolution seismic picture of the subsurface beneath the welding trajectory. [3] Figure (I. 6).

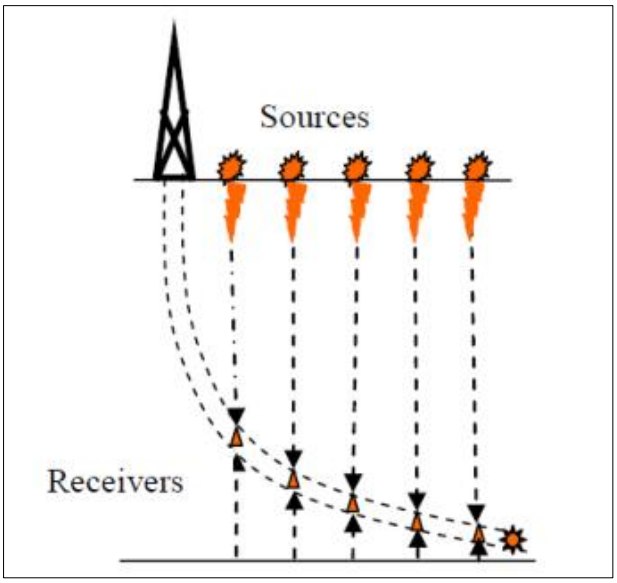

Figure I. 6. One-way travel time using Walkabove technique [4].

2.2 Operating Principle

We can find two specific ways in which VSPs can be applied to seismic exploration. First, seismic events observed at the surface of the ground can be traced, level by level, to their point of origin within the earth. Thus, one can tie a surface profile to a well log with an extraordinarily high degree of confidence. On the other hand, acoustic properties of a stratigraphic sequence can be measured and sometimes correlated to important exploration parameters.

The measurement basically involves recording the total upgoing and downgoing seismic wave fields propagating through a stratigraphic section P- and S-wave arrivals by means of geophones clamped to the wall of a drilled well. An essential part of VSP interpretation, due to the relatively small amplitudes (the separation of the up-going and the down-going wave components).

Figure I. 7. Schematic of conventional VSP. [5]

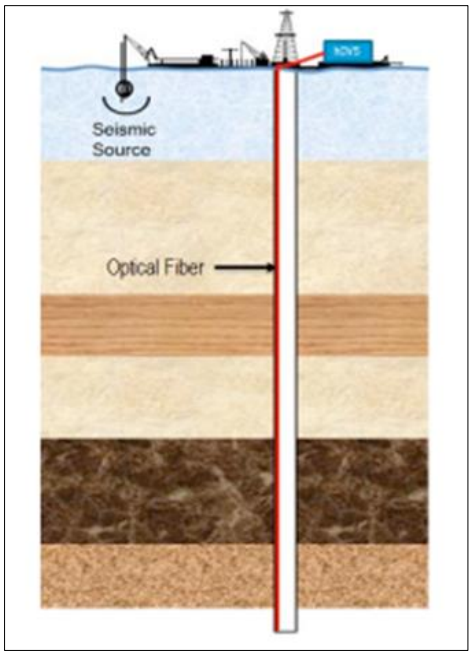

Figure I. 8. Schematic of optical fiber VSP. [5]

A seismic source located near or at the surface is energized, and an array of seismometers R is clamped in a well. All downward- and upward-traveling (reflected) events are recorded in sequence at every level in the hole.

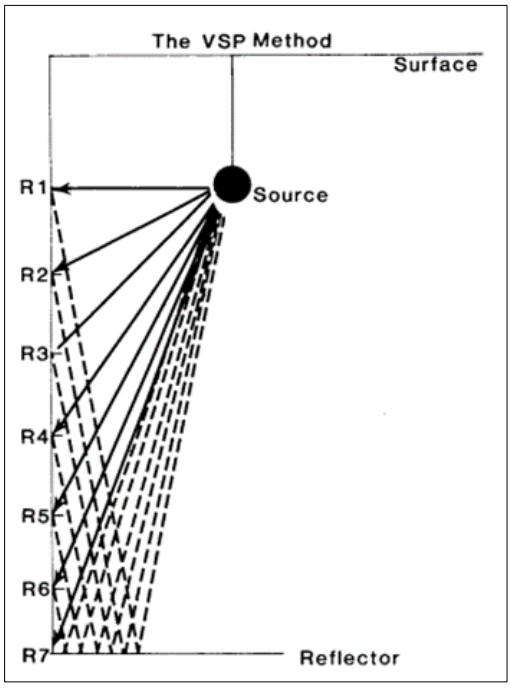

Figure I. 9. The VSP method. [5]

The important features of vertical seismic profiling are the following:

- The ability to produce a more dependable seismic trace at a borehole than one made from a seismogram combined with density and sonic curves.
- The capacity to facilitate the connection between borehole logs and surface seismic sections.
- When compared to surface seismic data, a VSP's shorter transit distances result in superior resolution.
- The capacity to record a signal from a reflector that doesn't require surface reception.
- The potential for corridor stacking, which involves stacking every upgoing event in order to identify the main reflectors and link them with the seismic data from the surface.

2.3 Seismic wave propagation in Borehole

Surface seismic methods can only record waves that are direct or that move along the air-surface contact, or that are reflected or refracted back to the surface. This is one of the main distinctions between VSP and surface seismic methods. As they pass through the borehole, however, we are able to record both reflected (up-going) and transmitted (down-going) wavefields using VSP.

A down-going wavefield that propagates normal to the surface and coincides with the borehole track will ideally result from a shot point at the borehole collar (zero-offset, or ZVSP) in a homogeneous, horizontally layered earth with a vertical borehole; the down-going Primary compressional wave (P-wave) is the first energy (First Break, or FB) arriving at the borehole receiver.

When ZVSP is operating optimally, the FB arrival time is linear with respect to depth, across all borehole receivers that reside within a common “elastic” layer. When our seismic traces are displayed in depth and time, the slope of the FB arrival times represents the velocity of the layer and in effect, represents the borehole in the space -time (x, y, t) domain.

The average (total travel time from source to receiver) or interval (travel time between receivers) P-wave velocity structure of the earth is determined using the FB travel times of ZVSP.

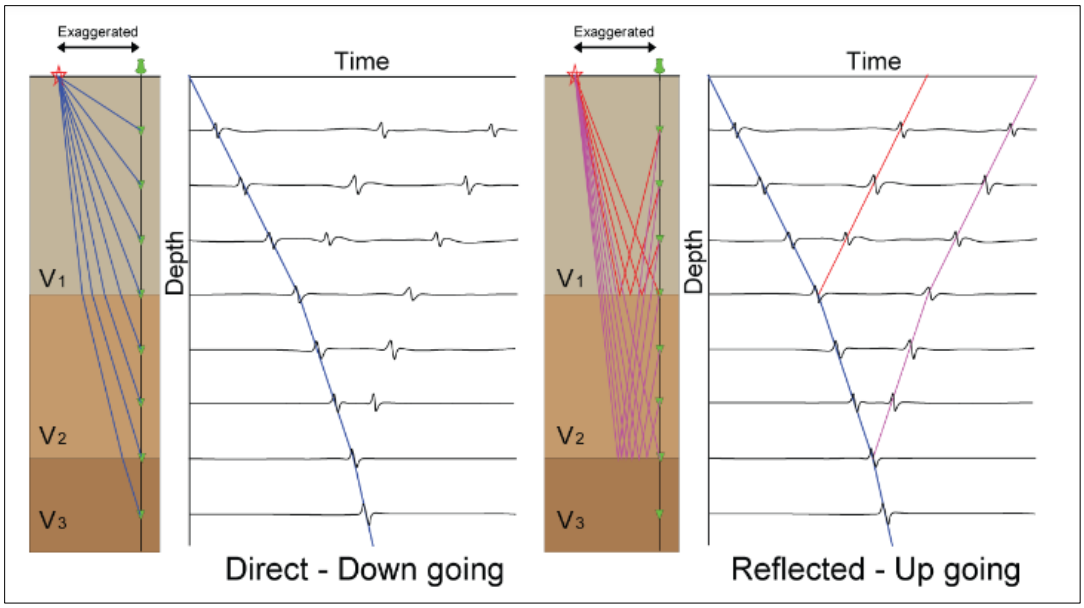

Figure I. 10. Principle of recording down-going and up-going wavefields in a VSP experiment [6].

2.4 Vertical Seismic Profiling (VSP) and Reversed Vertical Seismic Profiling (RVPS)

Similar seismic sections are produced using reverse vertical seismic profiling (RVSP) and conventional vertical seismic profiling (VSP), however RVSP data can be collected rapidly and economically.

A seismic source is positioned on the surface and a few receivers are positioned below ground in a traditional VSP. Receivers are positioned on the surface of an RVSP source, which is situated in the well. RVSP data should to match traditional VSP data that has been collected from different surface source locations [7].

Both VSP and RVSP have an advantage to surface seismic in that their energy traverses the earth at a shorter distance than that of surface seismic, and only once through the unconsolidated near-surface. This results in reduced attenuation of the signals, particularly at higher frequencies. Moreover, the signal-to-noise (SIN) ratio of RVSP data is larger than that of VSP data.

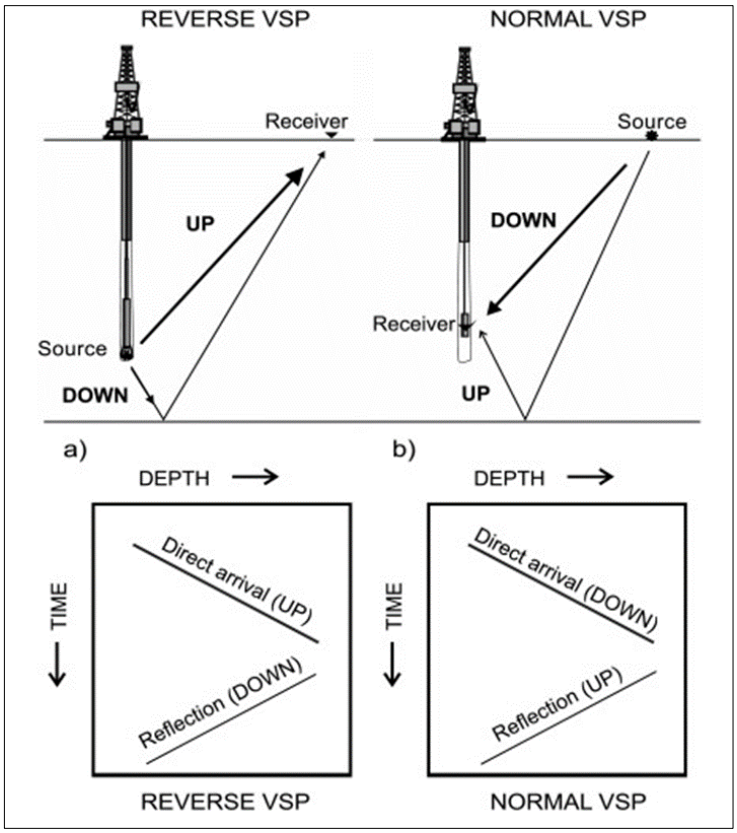

Figure I. 11. Wave-fields in reverse and normal VSP [8].

2.5 Utility and Advantages of the VSP

2.5.1 Application of technique VSP

- Integration with and expansion of seismic-reflection surface geophysical surveys.
- Monitoring of hydraulic fracturing.
- Improvement of reservoir characterization and fluid-drainage monitoring.
- Study of lithological and hydrocarbon effects on propagating wavelets.
- Imaging of subsurface geologic structures (e.g., faults, salt domes).

2.5.2 Advantages of VSP

- The VSP provides a direct observation of seismic waveforms propagating to various depths within the earth's subsurface.
- Allow us to precisely calculate anisotropy parameters, enable the creation of comprehensive velocity profiles, support advanced exploration techniques like imaging below the drill bit, and give a linkage between seismic and borehole images.

- Compared to surface seismic recordings, VSPs have a better resolution.
- The down-going and up-going wave-fields show the variation with depth of acoustic properties such as impedance and viscous damping.
- The relationship between acoustic impedance (Z) and velocity (V) of a material.
- VSP provides to decrease the reports of all seismic activity and limit the reports to just abnormal or extreme changes in seismic activity.
- Rock qualities can be understood by determining velocities through the direct down-going wave-field.

2.6 Limitations of the technique

- VSP is expensive to record many receiver offsets on the surface (multi-offset VSP), one way to make multi-offset VSPs more cost effective is to develop a receiver system that can cover the entire length of a well simultaneously.
- In many regions there are no regular waves on the seismograms at all (limitation of the effectiveness and the depth of investigation), making the appropriate interpretation of the VSP data difficult.
- Processing VSP data is complicated and necessitates specific equipment software and expertise, and any errors made when processing data may produce inaccurate or deceptive results.
- Risks are due to having the drill string out of the well for one or more days.

3. Borehole Seismic Imaging

Borehole seismic deals with recording seismic waves using geophone(s) in a borehole with the energy source either at surface or in the borehole. When it is recorded with the energy source at the surface, it is known as well seismic survey and recorded with source in another nearby borehole, is known as cross-well survey.

In order to determine the correct overburden velocity which is crucial for time-to-depth conversion and calibration of seismic reflections with wells the well seismic surveys comprise check-shot and VSP surveys. We use borehole seismic to including managing groundwater, planning the disposal of subsurface trash, evaluating geothermal areas, characterizing mining sites, assessing petroleum sites, monitoring CO_2 storage, and characterizing oil and gas

reservoirs. Borehole seismic surveys can be carried out in several different ways, (The Down-hole technique, Cross-hole technique and seismic tomography methodologies).

3.1. Borehole Seismic Technique

3.1.1 Down-hole technique

A class of borehole seismic measurements used for correlation with surface seismic data, for obtaining images of higher resolution than surface seismic images and for looking ahead of the drill bit; also called a VSP. Using geophones inside the wellbore and a source at the surface near the well [9].

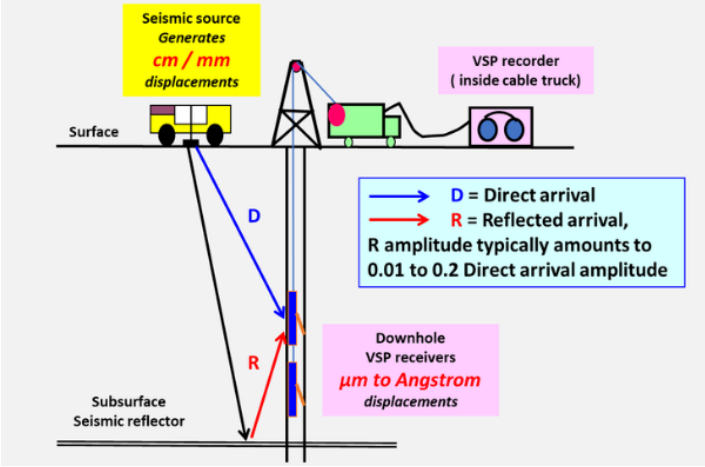

Figure I. 12. Downhole technique (VSP) [10].

3.1.2 Up-hole technique (Check-shot)

A technique to measuring seismic travel time from the surface to a specified depth using borehole seismic data. A geophone can be placed to each formation of interest, an energy source can be sent out from the Earth's surface, and the signal received can be recorded to determine the P-wave velocity of the formations contacted in a wellbore. Then, by making corrections to the sonic log and creating a synthetic seismogram, the data can be connected with seismic interpretations from the surface.

Comparison between techniques

The check shot just gives you a kind of 1D time–depth relationship, but in contrast, the VSP gives you an actual seismic image around a well and you can extend the area you can see around the borehole by using some more advance geometry acquisition; walk-away, 3D VSP.

3.1.3 Cross-hole technique

The Cross-hole technique uses a seismic source located in an adjacent borehole. In every case, a tri-axial geophone serves as the receiver. This makes it possible to acquire profiles of seismic velocities from both shear (S) and compressional (P) waves [9].

3.2. Advantages and utility of the approach for drilling process

3.2.1 Application

- Estimating the materials dynamic coefficients to determine the quality of the rock or concrete.
- Identification of bedrock faults and shear zones.
- Quality control tool for structural repairs.
- Detection of faults, shear zones and voids.
- Diagnosis of problem areas in 2-D or 3-D.

3.2.2 Advantages

- Reduces the overall cost of the seismic survey.
- The ability to obtain reliable structural data in zones of fractured or lost core.
- Borehole imaging can serve a number of purposes simultaneously with the collection of structural data. For example, it is widely used to detect thin beds and map bedding orientation, for borehole breakout analysis, and for casing inspection.
- Focus on deep targets.
- Prevent loss of resolution in near-surface weathering
- Borehole seismic imaging, in contrast to surface seismic technologies, directly measures seismic waves as they pass into the subsurface and provides precise information about the characteristics of the formations the borehole encounters.

Overall, borehole seismic imaging offers a powerful tool for subsurface characterization and exploration across various industries, including oil and gas, geothermal energy, mining, and environmental monitoring.

3.3 Technological Limitation

- **Depth limitations**

Borehole seismic imaging is effective for imaging structures and formations in the vicinity of the borehole. However, its imaging depth is limited compared to surface seismic methods. It may not provide a comprehensive picture of deeper structures or formations.

- **Resolution limitations**

The resolution of borehole seismic imaging is limited by factors such as the frequency and wavelength of the seismic waves used, as well as the spacing and orientation of sensors in the borehole. This can limit the ability to resolve small-scale features or details in subsurface structures.

- **Cost and complexity**

Borehole seismic imaging can be expensive and technically challenging to implement. It requires specialized equipment and expertise for drilling boreholes, deploying seismic sensors, and processing and interpreting the data.

- **Formation properties**

The effectiveness of borehole seismic imaging can be influenced by the properties of the formations being imaged, such as their composition, porosity, and fluid content. These properties can affect the propagation of seismic waves and the quality of the resulting images.

- **Noise and artifacts**

A number of noise and artifact causes, such as borehole conditions, equipment failures, and ambient influences, can affect borehole seismic imaging. These may deteriorate the imaging data's quality and make interpretation more difficult.

4. Conclusion

In summary, vertical seismic profiling (VSP) and borehole imaging are essential methods in the domains of subsurface exploration, petroleum engineering, and geophysics. These techniques have special benefits for identifying and visualizing subsurface structures, giving important information on fluid dynamics, reservoir characteristics, and geological formations.

High-resolution imaging of the borehole wall and surrounding formations is made possible by borehole imaging techniques like the acoustic borehole (BHTV) and optical imaging. These

techniques help with geological interpretation, reservoir modeling, and wellbore stability research.

By providing improved imaging resolution and accuracy, vertical seismic profiling (VSP) enhances surface seismic surveys. This is especially useful in regions with complicated underlying geology or restricted access. VSP data integration with other subsurface information allows for improved reservoir characterization, analysis, and optimization of drilling and production strategies in various industries, including oil and gas exploration.

Despite the challenges and limitations associated with borehole imaging and VSP, such as cost, complexity, and depth limitations, these techniques continue to play crucial roles in advancing our understanding of subsurface processes and optimizing the exploration and production of Earth's resources.

As technology and methodologies evolve, borehole imaging and VSP are expected to remain indispensable tools for subsurface characterization and exploration in the future.

CHAPTER II

Stick-Slip vibration during drilling

1. Introduction

The objective of oil and gas businesses is to achieve a balance between cost control and optimal drilling efficiency. It is of significant importance to acknowledge that vibrations may potentially impede the efficacy of this process.

It is typical for the drill bit to interact with the hole bottom to a significant extent and for the drill string components to make contact with the borehole walls throughout the drilling operation. These interactions are the consequence of deficiencies in the drilling process.

Oil field drillers frequently encounter the challenge of drill string vibration. It is widely acknowledged that this is the primary source of issues with drill string components, which can be challenging to resolve and result in a significant reduction in drilling efficiency. It has been reported that there may be an increase in drilling costs of up to 10% due to vibrations in the drill string. [11]

In addition to the significant risks associated with vibrations during drilling, this is a highly intricate issue that necessitates effective mitigation and rigorous control. This can only be achieved if all modes of vibration, their contributing factors and their impact on the drill string and therefore on the drilling process are carefully studied.

This chapter will examine the impact of mechanical vibrations on the drill string, with a focus on the stick-slip vibration mode and its simulation through a case study. Additionally, the chapter will explore the potential of the stick-slip vibration as a source of seismic registration.

2. Mechanical vibrations

Drillers are well aware of the issue of drill string vibration and must closely monitor certain drilling parameters that could potentially lead to resonance and reduced drilling efficiency. It should be noted, however, that typical drilling circumstances may still result in a considerable quantity of these vibrations.

The drill string may experience uneven and undesired pressures as a result of the many active forces and intricate geological structures it meets. These tensions may thus result in the emergence of dynamic events.

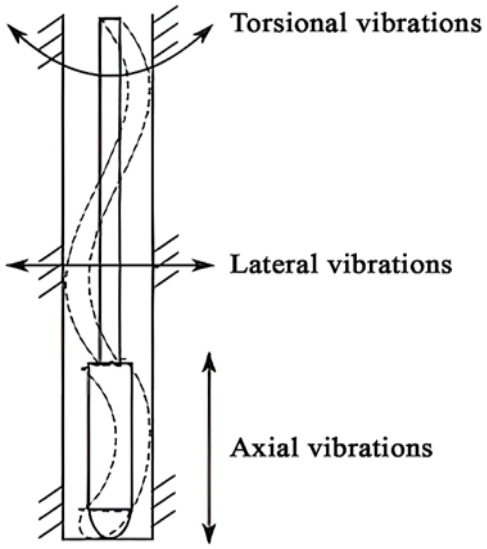

Figure II. 1. Three drill-string vibration motions [12].

It has been observed that oscillations occur during the drilling process, particularly in rotary drilling equipment. It is crucial to acknowledge that even minor self-excited disturbances may result in the drill string exhibiting unstable oscillations. It is important to note that the drilling process can be affected by a number of factors, including the following:

- A significant imbalance on a large scale.
- In mud motors, nutation or rotor wobbling within the stator can affect the cutting action of the drill bit.
- Misalignment, buckling or bending.
- The coefficient of friction between the drill bit and the borehole surface and between the column and the borehole wall must be considered.

It is not uncommon for petroleum wells to experience shock and vibration, particularly in offshore applications where the levels can be quite high. These vibrations have a significant impact on the ROP and overall drilling efficiency, and they can lead to fatigue [12].

The degree of intricacy of the terrain being drilled can influence the extent of vibration produced during the drilling process. The vibration and shock (V&S) level of the drill string can increase significantly in formations with poor drillability, deep and ultra-deep wells with lengthy drill strings, deep to ultra-deep water, coal and shale formations with unstable boreholes, and uneven borehole diameter and course.

Impacts

Drill string oscillations are damaging to the drilling process; it can lead to:

- Equipment on drilling rigs damaged too soon, resulting in fatigue failure.
- Overloading the mechanism.
- A drop in penetration rate that raises the cost of drilling operations.
- Tampering with drilling measurements and causing damage to measuring apparatus.
- A notable loss of energy.
- Loss of directional controls and instability of BHA.
- Stress corrosion cracking, which can lead to downhole tool failure, drill bit weakening, bolt fracture, and drill pipe fracture.

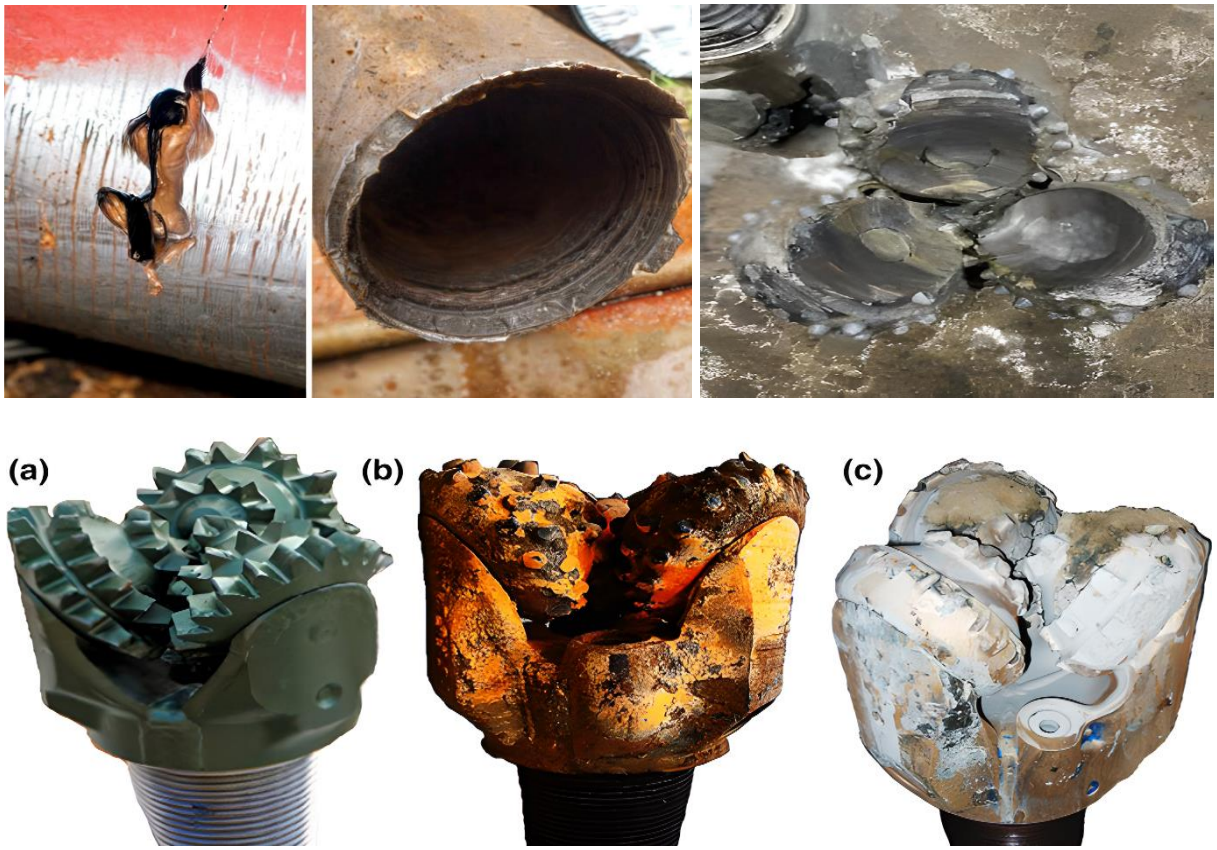

Figure II. 2. Damages resulted due to drilling vibrations [13].

Vibration mechanisms Drill bits and drill strings can perform a wide range of complex motions, but they can be divided into three main vibration types: axial (longitudinal), lateral

(transverse), and torsional (stick-slip). Each vibration type has a different pattern and is caused by a different source, which also results in a different set of related issues.

- Axial (longitudinal): motion occurring along the drill string axis.
- Lateral (transverse): Motion from side to side.
- Torsional (stick-slip): motion that creates twisting and torque.

Note: *It is worth noting that vibrations are often observed in multiple modes, which can be coupled, such as torsional-axial or torsional-lateral.*

2.1. Axial vibrations and Bit-Bouncing

Because the drill string carries the oscillations to the surface, axial vibrations may be felt at shallow depths. When drilling a well in a confined geological formation or employing down-hole axial generator equipment, this kind of oscillation is crucial [14].

The reported axial rate of acceleration is often much lower in the axial mode, which is thought to be less violent than the other two modes. This is due to the self-correction nature of drilling during this phase of the hole. It is important to take into account that the bit's interaction with the formation might have a significant impact on the axial vibrations' amplitude.

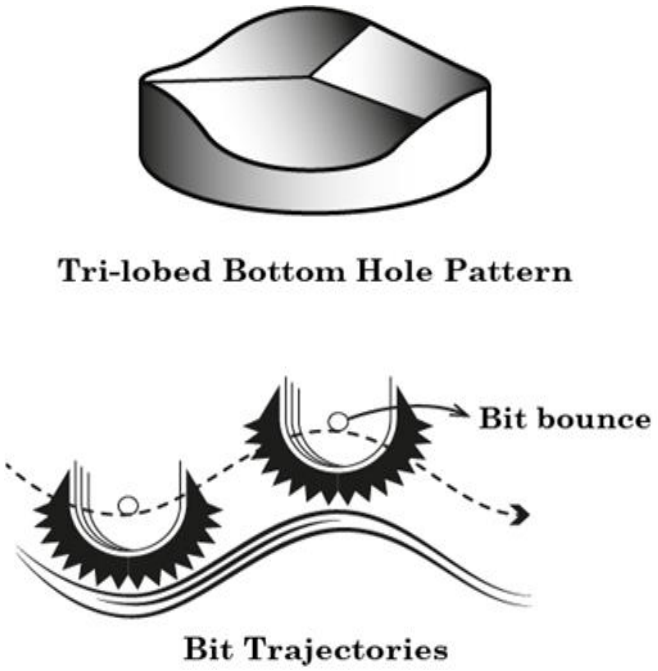

Figure II. 3. Bit bounce [12].

2.1.1 Identifications

- Vibration of the rig and equipment.
- Movement of the vertical pipes at the well's top.
- Changes in torque, bit weight, and penetration rate as the bit separates from the borehole bottom.

2.1.2 Impacts

Axial drill string vibrations may cause:

- Faster Bit Wear (Bit Dull Grading): damaged and fractured teeth, bearings
- MWD Failures
- Lowering the rate of penetration.
- Shorter bit runs
- Surface equipment damage

2.1.3 Bit-Bouncing

"Bit bouncing" can be brought on by axial vibrations. At this point, the bit breaks free from the rock and returns to the drilling direction.

Bit-bouncing, more common in hard rocks, can occasionally be caused by axial vibration and can be rather severe. It is commonly known that roller cone bits typically experience large amounts of axial vibration, and that tricone bits are susceptible to this phenomena. Tricone bits are frequently used to drill a well's uppermost parts. They have a distinctive three-lobed appearance on the bottom because they are made up of three cones that work together. Despite its somewhat disorganized appearance, this pattern has been shown to be successful in piercing a range of rock forms.

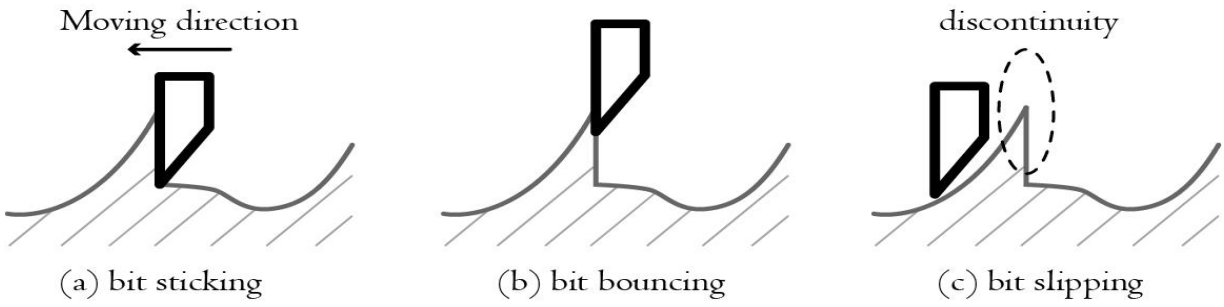

Figure II. 4. Bit-bounce phenomena [12].

2.1.4 Empirical monitoring

Common technologies for eliminating of axial vibrations fall into the two following technologies:

- **Software remedies**

Using the Delphi programming language, an algorithm has been created to ascertain the axial vibration's natural frequency. Through drilling parameter optimization, this approach may effectively reduce drill string fatigue. Notably, adjusting the drilling parameters for example, lowering the bit's weight and raising the angular velocity can also aid in preventing bit bouncing.

- **Hardware remedies**

While drilling, it is advised to take into account methods such using shock subs and non-aggressive drill bits to reduce axial vibration. It has been found that changing the hardware (using a shock sub, for example, or using somewhat less aggressive bits) eliminates axial vibrations more successfully than changing the drilling settings.

2.2. Lateral vibrations and Whirling

Among the primary modes of drill string vibration, the transverse mode is said to be responsible for 75% of drill string failures. [15]

Only in situations where the BHA has enough transversal mobility to bend and make contact with the hole wall can this movement occur. In extreme circumstances, coupled longitudinal and torsional vibration (also known as mode coupling) can result from lateral vibration. Due to disturbances from different directions, this process may produce small-scale resonance, which might seriously harm a drilling operation. Since they are thought to be the most intense kind, lateral vibrations have the capacity to do serious harm. It is important to note that because they do not spread to the surface via the drill string, they might be difficult to find.

2.2.1 Identifications

Lateral mode is difficult to detect at the surface, as it can be abruptly attenuated:

- Greater torque applied to the bit;
- Amplification of the overtones in the frequency spectrum.
- More torque applied to the bit's top.

2.2.2 Impacts

The whirling phenomenon can have several adverse effects on the drilling process.

- Lowers the rate of penetration.
- The formation of a borehole that is off-center, actuators, pipe joints, stabilizers, MWD equipment, and bit.
- In addition to the possibility of washout and twisting-off, as well as early bit wear.

2.2.3 Whirling

Drill string oscillations that whistle can be difficult to control since they often provide little to no surface indication. More deeply into the borehole, lateral vibration shocks may be produced by the rotating bottom hole assembly interacting with the hole wall. An offer-center borehole is created when objects collide with the borehole wall; stress may also damage BHA components and change the borehole's overall direction. [16]

Drill collar whirl is just the drill collar rotating and bending centrifugally. This bending results from the drill collar's center of gravity shifting away from the borehole's center line. Centrifugal force acts on the drill collar's center of gravity as it spins, bending it.

2.2.4 Types of Whirling

The most significant lateral motions are:

- **Backward whirl (most damaging):** Rolling along the borehole wall is the BHA. The centrifugal force of the motion itself stabilizes this motion. Gravity destabilizes motion in an angled borehole by drawing the BHA away from the high side of the borehole wall. Should this impact be sufficiently powerful, we can get:
  - **Chaotic whirl:** The BHA only rolls down the bottom side of the hole wall; it breaks touch with the wall at around the '01.30' location and then returns to make contact with it at '07.00'. This motion is highly regular, but it becomes more complex due to bending effects.
- **Forward (synchronous) whirl:** This BHA is unbalanced but stabilized. It is visible in the washing machine at home. Bit spin is the term for the phenomena that occurs when the drill bit's center moves in tandem with the drill string's rotation. Between the wall

and the bit gauge, this causes a constant sliding action. It ultimately causes a tiny hole to open up in the borehole wall. The bit cutters always rotate in a clockwise manner, which is important to note.

- **Bit-Whirl:** The term "bit whirling" refers to the movement of the bottom hole assembly out of center caused by an unbalanced drill bit. Uneven loading and harsh impacts on the cutters may result from this. Regrettably, it is challenging to eradicate this phenomena since it is rather stable.
- **Bending vibrations:** These are the lateral vibrations of a slender beam.

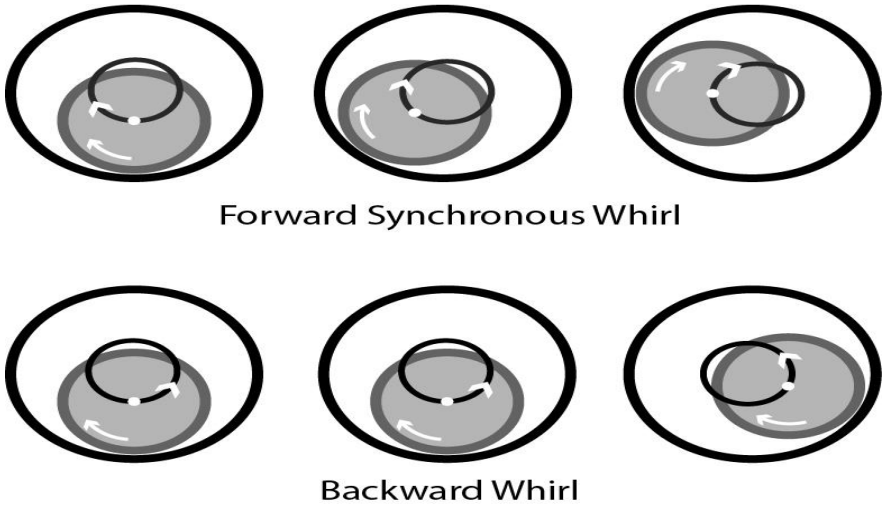

Figure II. 5. Backward and Forward Whirl [12].

2.2.5 Empirical monitoring

In order to alleviate the whirling phenomenon, various hardware and software solutions are being investigated:

- **Software remedies**

One of the main causes of the drill string's lateral non-uniform motion, which results in high levels of self-exciting vibrations, is resonances. A finite element approach for calculating the critical velocities. It is important to remember that transverse drill vibrations might come from other sources besides resonances. Consequently, it is advised to view avoiding critical velocities as only one aspect of the mitigating procedure.

- **Hardware remedies**

Buckling and eccentricity of the BHA are frequently blamed for lateral vibration. It is advised to carefully choose downhole equipment, such as bicentre bits and roller reamers, to handle eccentricity forces. These tools can assist reduce these concerns. [15]

There are several approaches that may be taken into consideration in order to handle lateral vibrations during drilling. These include altering the drilling process (e.g., lowering the work-over-burden and raising the angular velocity), improving the drilling fluid's lubricity, and employing stabilizers to make the BHA more rigid or switching to roller reamers in its place.

2.3. Torsional vibrations and Stick-Slip

According to downhole data, a set bit rate of rotation is not always the result of using a fixed surface rate of rotation. In actuality, a significant portion of the drilling period often exhibits a big amplitude fluctuation in the torsional speed downhole. The BHA's torsional stiffness intensifies the non-uniform vibration behavior, leading to bit stoppage or velocities up to 10 times the rotary table speed.

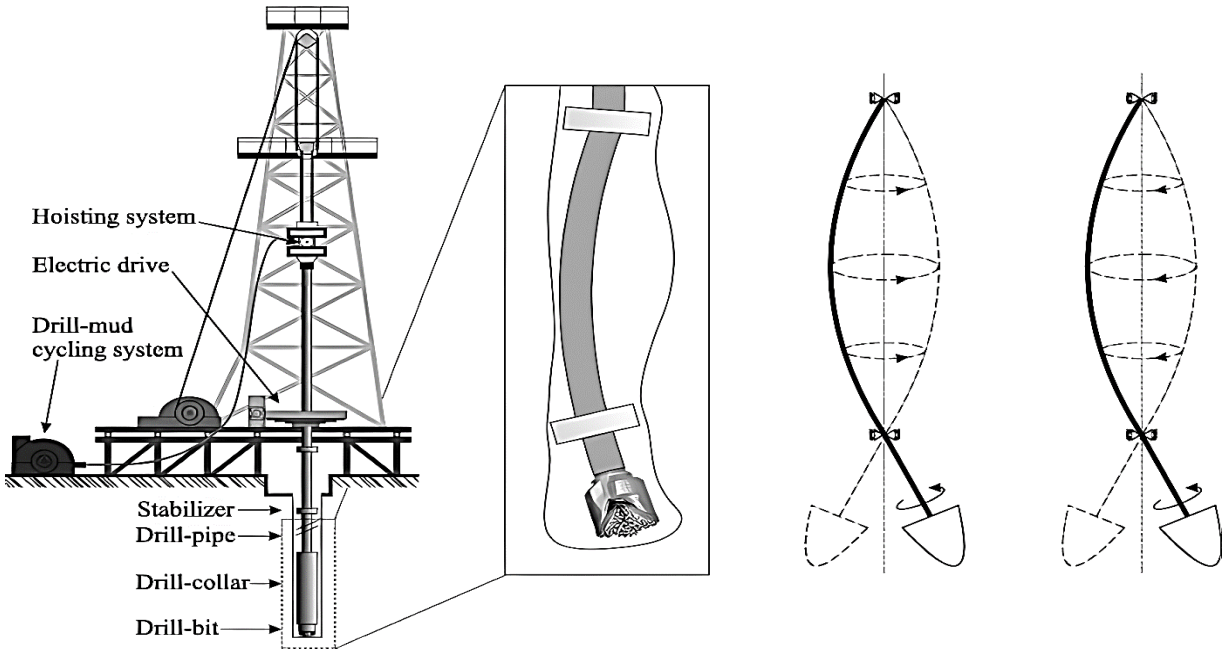

Figure II. 6. Drill-string Torsional motion while drilling [15].

Stick-slip is the main source of the twisting motions in the drill string that result in torsional vibrations. These vibrations are shown to happen when frictional tension on the bit and BHA causes the bit and drill string to periodically accelerate or decelerate. [11]

It has been shown that uneven downhole rotation can result from torsional vibrations. This phenomena happens when there are brief stoppages in the bit, which causes the drill string to occasionally twist before free spinning. Note that every time this movement occurs, the drill string is permanently marked.

Drilling operations frequently involve torsional and vibration modes, particularly in deep wells and wells with long laterals and high angles. Furthermore, it appears to be caused by the high WOB of aggressive polycrystalline diamond compact bits and hard formations or salt. It is observed, meanwhile, that friction against the borehole wall and the torsional stiffness of the BHA dampen the torsional vibration.

It is important to remember that torsional vibration damping is often less effective than axial vibration damping. The reason for this is that longitudinal rigidity is more important than torsional stiffness. Furthermore, uneven rotations are frequently caused by the flexibility of the drill string. The vibration mode is observed at surface as large variations in torque values. Even in deviated wells, torsional vibrations can be detected by surface measurements and reduced by the driller (Schlumberger, 2010). [16]

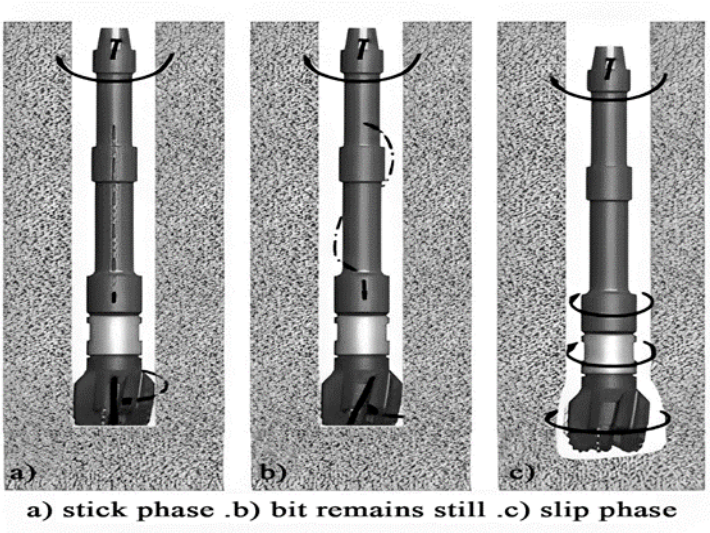

Figure II. 7. Drill-string Stick and Slip states. [16]

Note: *Torsional oscillations is a type of self-excited vibration which can occur in the drill string without an external periodic excitation force. The drill string has a unique natural resonant period. This depends on the drill string geometry, mass and friction with the borehole wall. You may sometimes hear a "humming" sound in the drive motor with a frequency of 0.1-1 Hz or 1-10 seconds.*

2.3.1 Identifications

Indicators that may indicate the occurrence of a torsional vibration include:

- A 20% boost in torque at the highest end.
- Take into account variations in the drill string's angular velocity.
- Rotating table and top drive jamming.
- Lower angular speeds,
- Unscrewing of pipe joints
- Increased torque at bolted joints, etc.

2.3.2 Impacts

There is several problems associated with this kind of vibration which are:

- Decrease in penetration rate
- Overtorque at the connection.
- Drill off twist in strings.
- Broken BHA components.
- Damage to PDC bits.
- Bit damage caused by impacts.
- Ruptures in screwed joints.

2.3.3 Stick-Slip

Torsional vibrations of the stick-slip variety can be quite damaging. It happens when the bit interacts with the formation frictionally in a non-linear way. This non-linearity causes the bit to alternate between two phases: an adhesive (stick) phase and a sliding (slip) phase.

The drill bit briefly stops rotating during the "stick" phase until the drill string generates enough torque to release it. The bit accelerates during the next phase, known as the "slip" phase. But finally, it slows down and stops once more. [17]

A torsional wave may be produced by the stick-slip action and travel up the BHA to the rotary table system. There, the drill string's large mass of inertia acts as a stationary end, reflecting the torsional wave back to the bit through the drill string. Then, this torsional wave cycle may be repeated. Stick duration raises the stick-slip's amplitude, and bit release significantly increases the drill string's rotational acceleration.

2.3.4 Empirical Control

- **Software remedies**

The effect of drilling settings on stick-slip vibrations is examined in this study. It was discovered that while stick-slip is lessened, penetration rate is decreased when the weight on bit is reduced. It is advised to reduce WOB by 15% or increase angular velocity in order to alleviate torsional vibrations. Pause the table and restart operations at a faster pace or with less weight on the table if stick-slip continues. Real-time torsional vibration magnitude display was achieved using Fourier spectrum analysis. [18]

- **Hardware remedies**

Other strategies to address torsional oscillation include: less aggressive bit designs to reduce bit torque; better wellbore quality and fewer stabilizers and diameter sizes to reduce drill string torque; and improved wellbore clean-up and mud lubricants to reduce drill string torque.

3. Simulation and Study case of NP12-X168 well in Jidong oilfield of China

3.1 Introduction

This work examines the bit and borehole stick-slip vibration behavior in a highly-deviated well, with an emphasis on the management strategy to lessen the vibration's size. A finite state model of a well which includes a drill string system, borehole, PDC bits, and a rock model is used in the study. Through modeling the effects of these behaviors, the study seeks to increase comprehension of these behaviors and improve drilling and well efficiency. Drilling efficiency

may be limited by the unsatisfactory results that standard PDC bits may not produce. The findings could serve as a basis for enhancing well efficiency and drilling performance.

This case effectively addresses interaction between drill string, wellbore wall, drill bit, and rock by simulating the bottom boundary condition of a drill string system in a highly-deviated well using real-time rock breaking simulation.

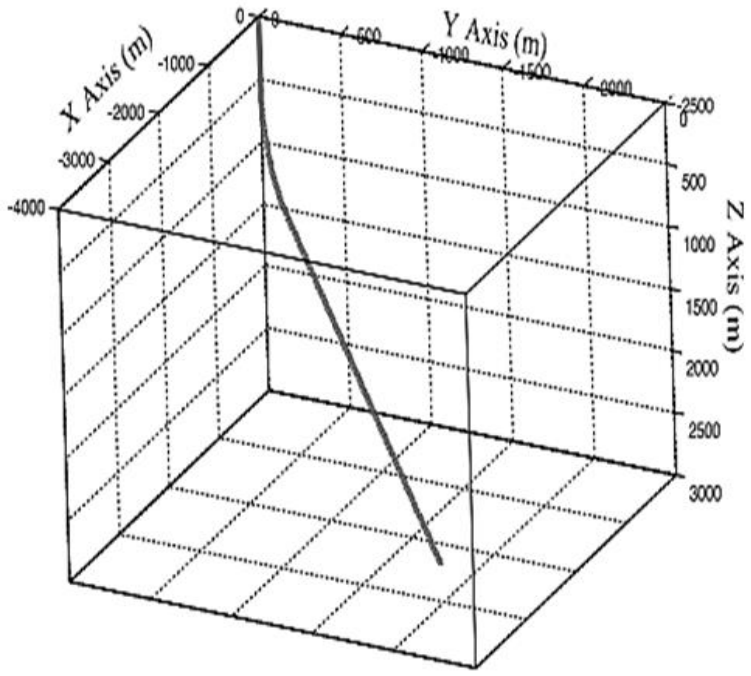

Figure II. 8. The spatial trajectory of NP12-X168 well [19].

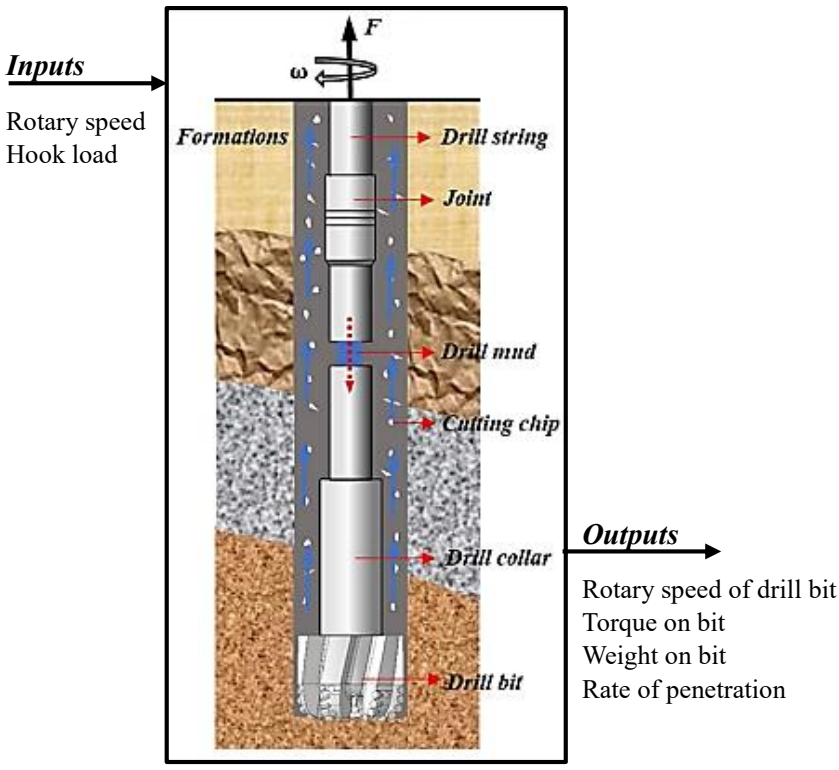

Figure II. 9. The schematic diagram of drilling string system. [19]

3.3. Numerical simulation modeling procedure

3.3.1. The numerical simulation modeling of highly-deviated well drilling string system

Plotting the geographical track of the NP12-X168 well, located in the Jidong oilfield in China, serves as an example. The NP12-X168 well's BHA is as follows:

Φ 311.1 mm PDC bit + *Φ* 310 mm stabilizer × 1.97 m + *Φ*203 mm DC (drill collar) × 9.1 m + *Φ*200 mm MWD (Measurement While Drilling) × 1.88 m + *Φ* 196 mm DC× 8.11 m + *Φ* 127 mm HWDP (Heavy Weight DrillPipe) × 85.15 m + *Φ* 139.7 mm DT (Drill string) × 2889.81 m. The type and mechanical parameters of drilling tools are listed in Table (I. 1).

The WOB is 40kN (4 tone), the hook load is 794kN, the rotary table rotates at 90 RPM (revolutions per minute), and the drilling density utilized in actual drilling is 1.25 g/cm3. Its viscosity is 60 s.

Table II. 1: Mechanical parameters of drilling tools.

Drilling tool type	Inner diameter (mm)	Elasticity Modulus (MPa)	Poisson's ratio	Density (Kg/m^3)
Φ 139.7 DT	88.9	2.10×10^5	0.3	7.86×10^3
Φ 127 HWDP	76.2	2.10×10^5	0.3	7.86×10^3
Φ 196 DC	73	2.10×10^5	0.3	7.86×10^3
Φ 203 DC	58	2.10×10^5	0.3	7.86×10^3
Stabilizer	71.4	2.10×10^5	0.3	7.86×10^3

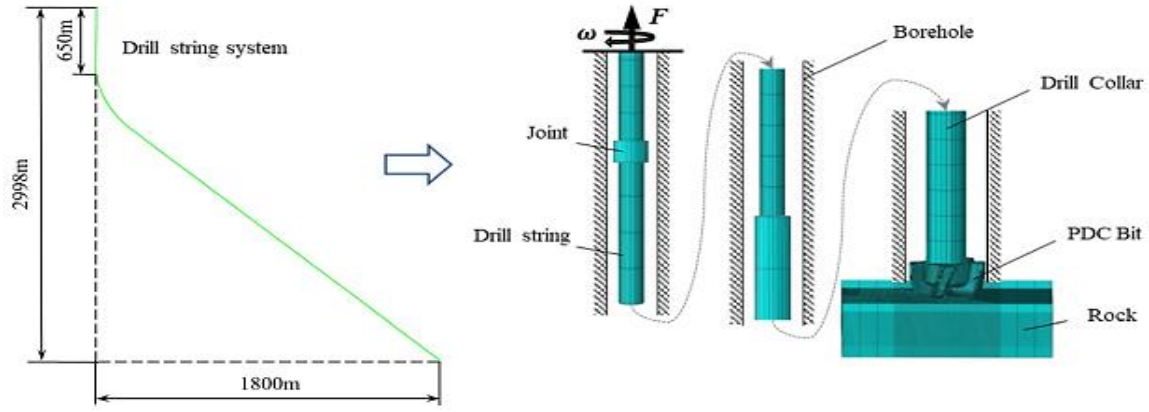

Figure II. 10. The nonlinear dynamic numerical simulation model of drill string system [19].

The erosion contact algorithm integrates a damage model, which is used to characterize the evolution of the material damage in the rock components using a damage parameter. In the simulation technique, the yield criteria of the rock model uses Drucker-Prager. Table (II. 2) lists the mechanical characteristics of the rock that was used in this study.

Table II. 2 : Mechanical parameters of rock sample.

Elasticity Modulus (MPa)	Poisson's ratio	Density (Kg/m^3)	Internal Friction Angle (°)	Uniaxial Compressive Strength (MPa)
3.14×10^4	0.3	2750	27.61	139.5

3.3.2. The numerical simulation model verification

The simulation findings, as well as the plots in Figures (II. 11) and (II. 12), are compared with the field measured data in the NP12-X168 well, including the rotational torque and WOB, in order to calibrate the simulation model. The average value of these data is represented by the red line in Figures (II. 11) and (II. 12).

Figure. (II. 11) shows a comparison of Wellbore WOB measurements and simulations. The actual WOB is 41.5 kN, while the simulation results are 39.4 kN, with a relative error of 5.22%. The on-site WOB fluctuation amplitude is 15.57 kN, indicating the simulation model's reliability.

Figure. (II. 12) compares torque between field measured data and simulation results, contrasting the predicted drilling time with the intercepted experimental well depth. The modeling findings how an average torque of 18.64 kNm, which satisfies the dependability criteria. The average torque recorded during on-site drilling is 20.43 kNm.

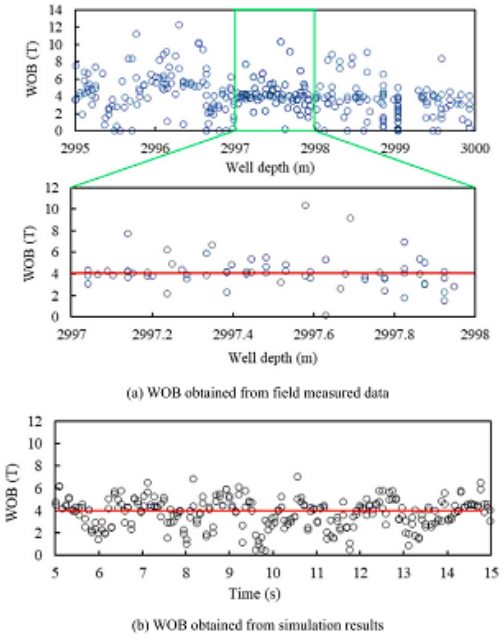

Figure II. 11. The WOB comparison between field measured data and simulation results.

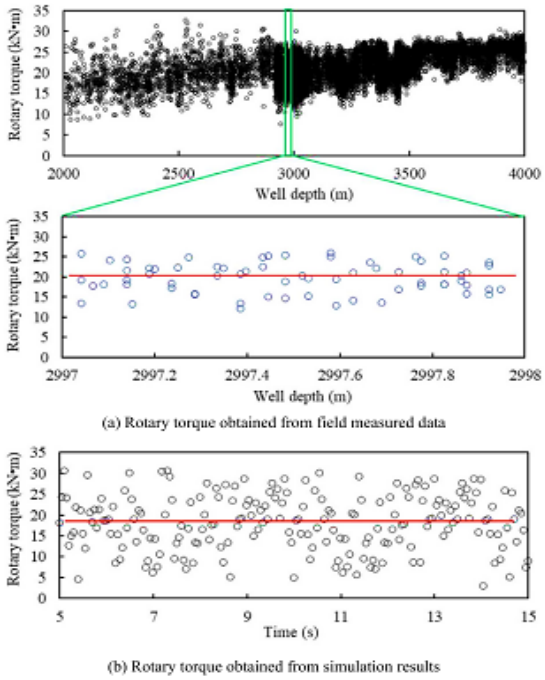

Figure II. 12. The rotary torque comparison between field measured data and simulation results.

3.4. Results and discussion

3.4.1. The stick-slip vibration responses of drill bit

Figure. (II. 13) shows drill bit rotation speed variation over simulation time, stick-slip vibration is shown. The drill bit is in the slip state when the speed is less than zero, and the accumulated energy causes a severe impact stress on the PDC cutter.

Figure. (II. 14) shows the absolute angular displacement variation of a drill bit and rotary table over simulation time. The displacement of the drill bit climbs continuously, whereas the displacement of the rotary table increases linearly. The angular displacement of the drill bit stays constant throughout the interval between locations B and C.

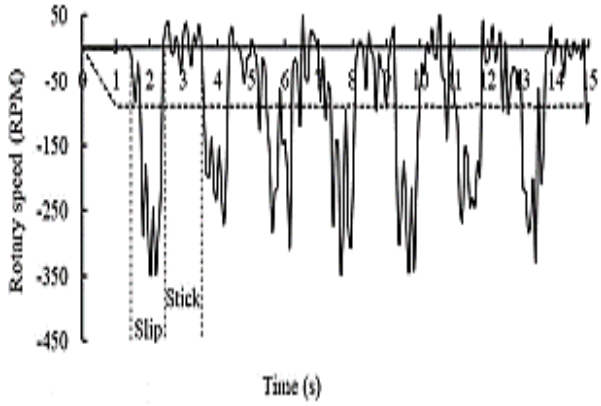

Figure II. 13. The rotary speed of drill bit with respect to time.

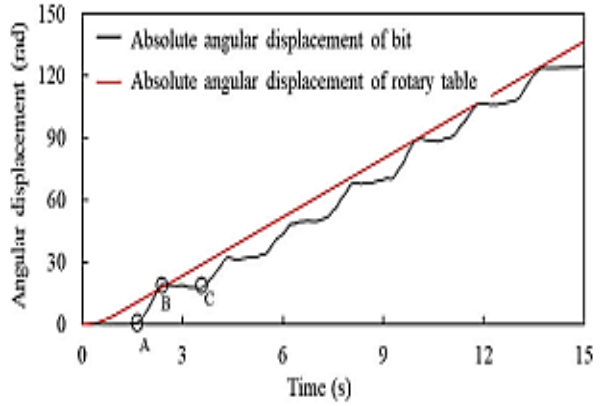

Figure II. 14. The absolute angular displacement variation of drill bit and rotary table versus time.

Figure. (II. 15) shows drill string deformation during simulation, with small deformation at start and large in subsequent rotations. The drill string system's stored energy is primarily responsible for the deformation, which results in stick-slip vibration of the BHA. A drill bit in stick condition makes deformation easier to see.

Figure. (II. 16) shows the variation in lateral acceleration of a drill bit over simulation time, displaying the BHA's intricate vibration, which includes torsional, axial, lateral, and spinning motion. Stick-slip vibration affects the vibration strength; in stick states, vibration is less and in slide situations, it is more powerful.

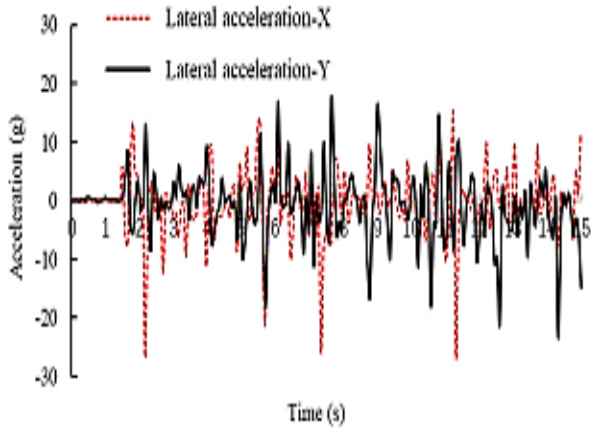

Figure II. 15. The lateral acceleration variation of bit with respect to simulation.

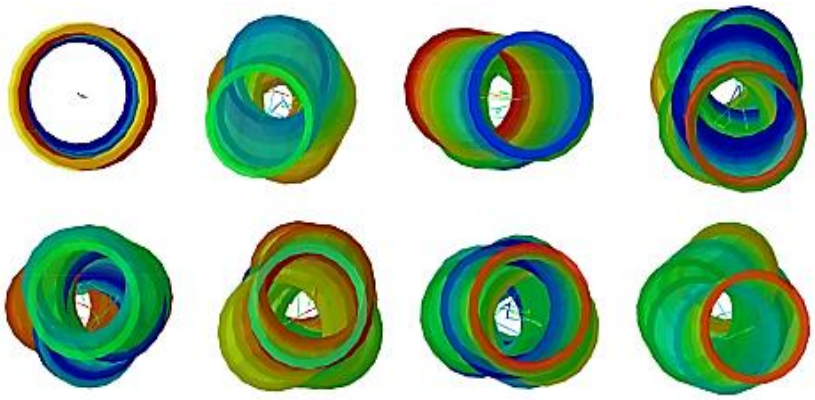

Figure II. 16. The deformation of drill string at different moments.

Figure. (II. 17) shows the penetration depth of a drill bit with respect to simulation time, showing a continuous rise. Drilling efficiency decreases when slip state penetration depth dramatically increases but stick state penetration depth stays constant.

Figure. (II. 18) depicts six periods of bottomhole rock drilling, during which the drill bit's torque and work of breakage WOB are transmitted to create grooving and eventually a breaking pit.

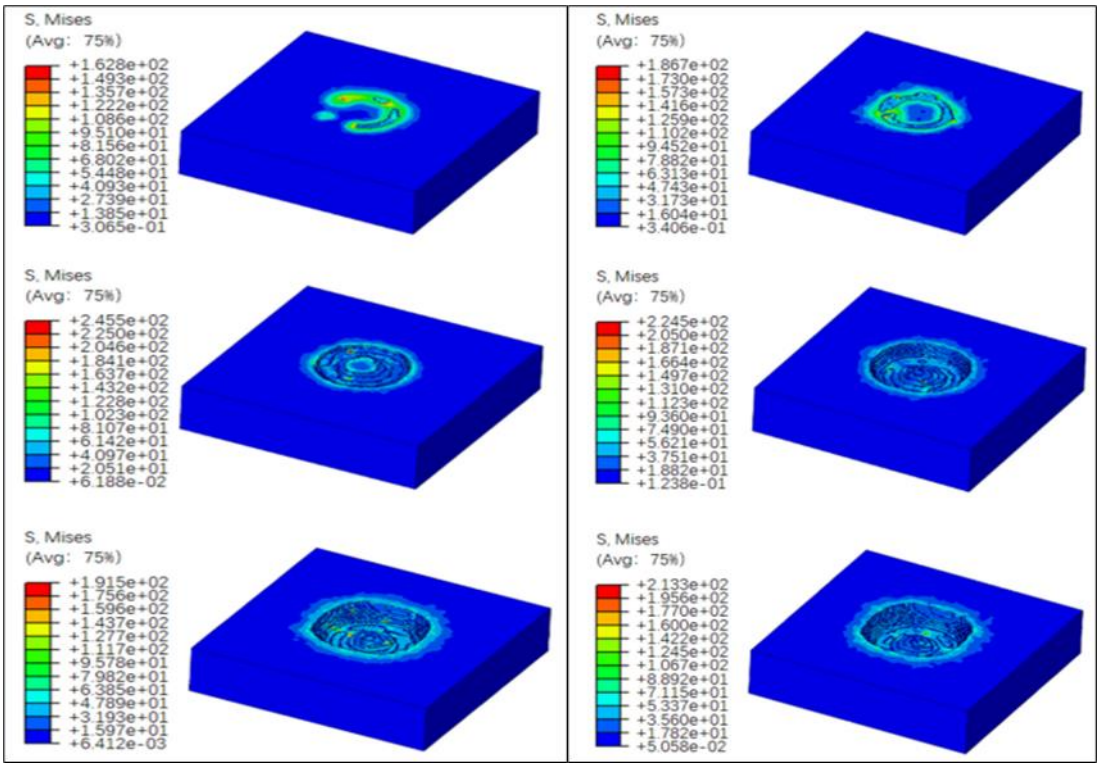

Figure II. 17, 18. The drilled bottom-hole rock at six different moments.

3.4.2. The stick-slip vibration responses of BHA

This section examines drill string vibration regulations, provides references for vibration control techniques, and evaluates BHA's stick-slip vibration response while drilling in highly-deviated wells.

Figure. (II. 19) displays the BHA's rotation speed fluctuation at various drill bit distances. There is no vibration at the rotary table, and stick-slip vibration is more obvious at distances of 30 meters than 800 meters.

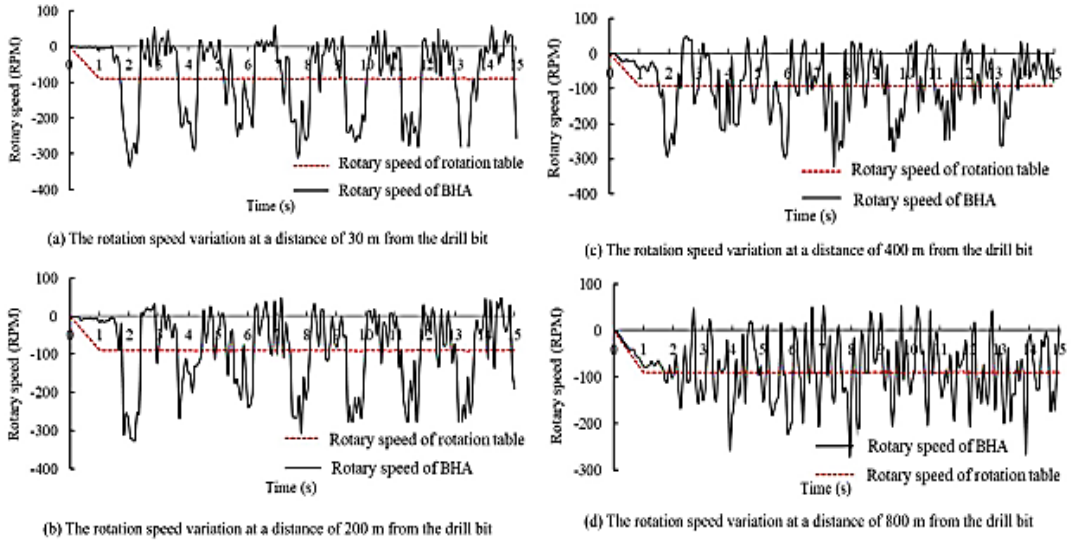

Figure II. 19. The rotation speed variation of BHA at different distance from the drill

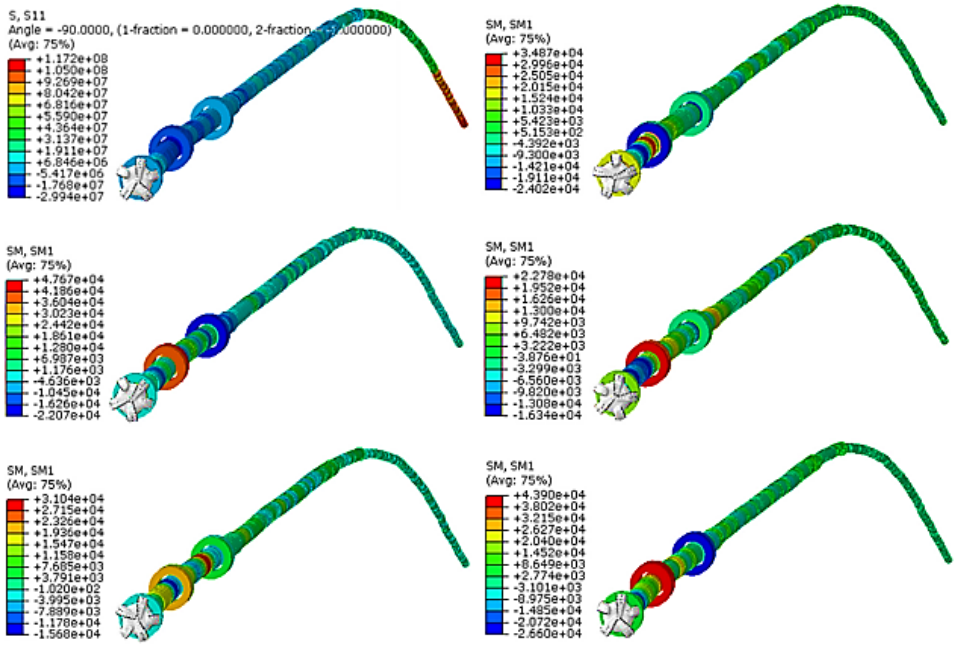

Figure II. 20. The Mises stress and flexural moment nephogram of BHA.

Figure. (II. 20) shows BHA's mises stress and flexural moment nephograms, which display the compressive load on the BHA and the tensile load on the top drill string, suggesting fracture susceptibility.

3.4.3. Stick-slip vibration control method

Stick-slip vibration of the BHA raises the danger of fracture, deforms the drill string system, and reduces the effectiveness of breaking rock. Numerical simulation models are used to explore the torsional impact approach, which reduces it. High frequency torsional impact torque, with a frequency of 1200 times/sec and an impact torque of 960 Nm, is imparted to the drill bit during the simulation process.

Figure. (II. 21) shows that torsional impact drilling, which has a maximum rotation speed of 262.2 RPM, makes the BHA more stable throughout the drilling process by reducing stick-slip vibration by 25.09% as compared to conventional drilling.

Figure. (II. 22) demonstrates the angular displacement curve of torsional impact drilling is smoother than that of standard drilling, which lowers stick-slip vibration and raises BHA when drilling.

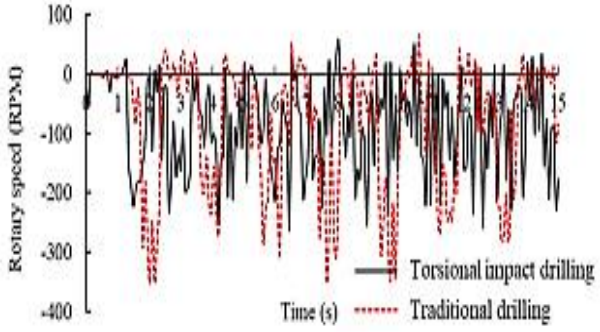

Figure II. 18. The rotation speed variation of drill bit in two drilling method with respect to simulation time.

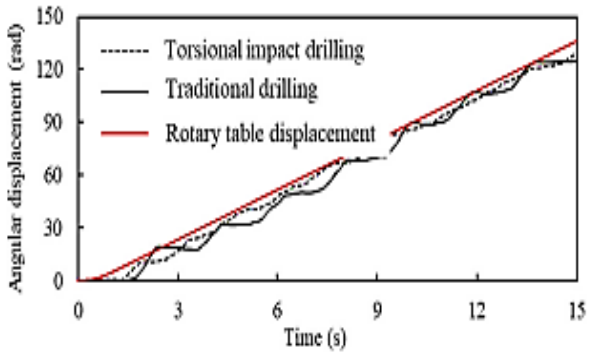

Figure II. 19. The angular displacement variation of drill bit in different drilling method.

Figure. (II. 23) shows that torsional impact drilling, as opposed to conventional drilling techniques, lowers drill bit resistance torque by 34.71%. Because stick-slip vibration is one of the primary sources of vibration during the drilling process, this reduction in resistance torque stabilizes the drill bit rotation.

Figure. (II. 24) compares the drill bit's penetration depth in both conventional and torsional impact drilling. The usefulness of torsional impact drilling in increasing drilling efficiency is demonstrated by its linear growth rate and 58.28% increase in drilling depth.

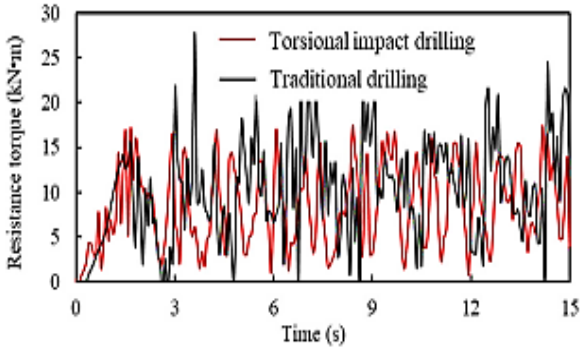

Figure II. 20. The resistance torque of drill bit in torsional impact drilling and traditional drill.

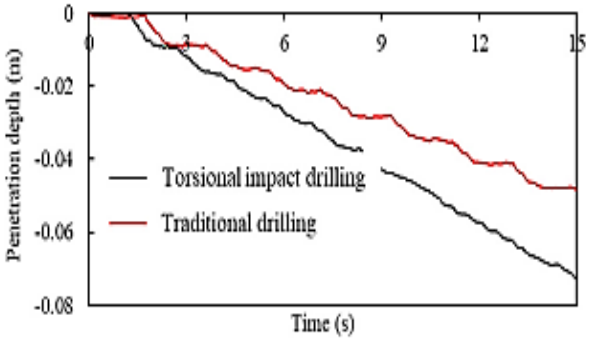

Figure II. 21. The penetration depth of drill bit in torsional impact drilling and traditional drill.

3.5. Conclusion

This work examines the stick-slip vibration behaviors of the drill bit and BHA, as well as the control strategy for these phenomena, using a finite element model of a highly-deviated well. It may be summed up:

- The drill bit exhibits a reduplicative stick-slip condition with low or zero rotation speed and a swiftly growing slip state. Stick-slip vibration is common in highly-deviated well drilling.
- The energy stored by the drill string system causes the BHA to vibrate stick-slip, which results in deformation in both the stick and slip states.
- The stick-slip condition of the drill bit affects the lateral vibration intensity of BHA, with smaller vibrations in stick states and stronger vibrations in slip situations.
- Stick-slip drill bit state decreases drilling efficiency, hence effective drilling time should be increased by reducing bit sticking period in drilling process.
- When BHA comes closer to the drill bit, stick-slip vibration of the BHA reduces and reaches its maximum flexural moment.
- By increasing drilling depth by 58.28% and decreasing bit resistance torque by 34.71%, high frequency torsional impact drilling enhances bit stability, efficiency, and lowers stick-slip vibration.

4. Stick-slip vibration as source of seismic registration

One method utilized in the discovery and extraction of oil and gas resources is seismic-while-drilling, or SWD. It is well known that significant fluctuations in impedance and powerful resonances are caused by the BHA components in both the pilot and seismic data.

The vibrations generated during drilling and the signal used for SWD purposes are characterized by the actions of the various bit types. Their operation, which includes stick-slip, spin, and bouncing conditions.

Seismic waves are produced by these vibrations, which travel through the rock and are detected by surface sensors. Subsurface geology can thus be ascertained and real-time drilling guidance can be provided by the seismic data.

It is noteworthy that one possible source of seismic registration is the stick-slip vibration phenomena. Because of the stick-slip signals, geologists and drillers may make better judgments by learning more about the underlying formation, including its fluid content, stress condition, and kind of rock. Nonetheless, this type of vibration mode can offer current information on the drilling environment, assisting in the optimization of drilling parameters and preventing problems with stopped pipes (Figure II. 25).

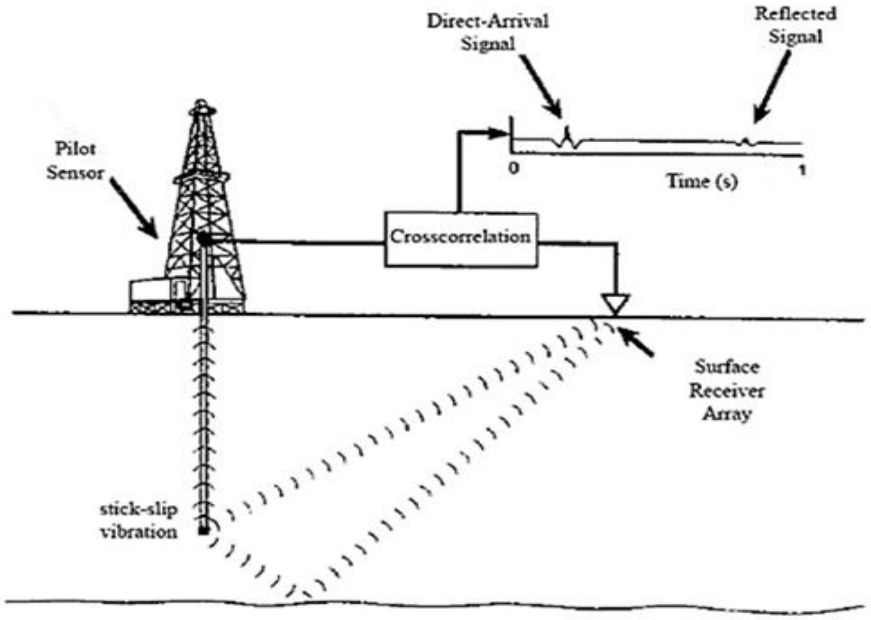

Figure II. 22. Acquisition geometry of SWD using stick-slip vibrations technique.

As a result, the information acquired is so important that it may be used to spot possible drilling dangers like overpressure zones or cracks before they become issues. Furthermore, no downhole instrumentation is used to obtain the stick-slip vibration studies, thus drilling is not halted, and no rig time is lost.

Because of its potential to enhance hydrocarbon production and maximize reservoir characterization, this type of vibration motion offers significant advantages that ought to have been utilized in both the drilling and production domains. They are also used to direct the placement of wells, guarantee that they are drilled in the best possible position, and provide the mechanical characteristics of the underlying formation that maximize well stability and prevent collapse or failure.

5. Conclusion

Drilling expenses may rise as a result of early failure of drill rig parts, especially the drill-string. Unwanted vibration waves along the drill-string are one of the primary causes of drill-string failures. Vibration modeling of the drill string is required to solve this problem since it allows one to predict troublesome vibration patterns and create practical mitigation strategies.

Drill-string vibration models have developed over time from simple static models to complex dynamic models that can precisely forecast drill-string movements down the hole. All models must include certain assumptions and simplifications due to the complex nature of the drill-string and its interactions with the environment.

For useful field applications, more accurate downhole vibration forecasting may require enhanced models. Moreover, new techniques for drilling, such directional and vibration-assisted rotary drilling, add new layers of complexity to vibration modeling.

Drill-string vibration was covered in this chapter, with a focus on stick-slip motion. We examined the difficulties in studying stick-slip vibration in a high-deviated well. In addition to the theoretical techniques for reducing this vibration mode and its potential application as a seismic registration source in petroleum reservoirs and wells were examined.

CHAPTER III

Drill bit stick-slip vibration and SWD

1. Introduction

The complex dynamics of drill bit behavior during the drilling process have long been a subject of extensive research in the oil and gas industry. One of the key challenges in this field is the phenomenon of drill bit stick-slip vibration, which can lead to significant consequences, including premature wear and damage to drilling equipment, increased drilling time, and failures of measurement-while-drilling (MWD) tools. [20]

Stick-slip vibration is characterized by an alternating sequence of stick and slip phases, where the drill bit experiences a period of no motion followed by a rapid slip. Starting from the understanding stick slip vibration as the crucial source of data to optimizing drilling operations, the seize of this phenomenon enabling better decision-making regarding well placement, steering, and overall reservoir characterization.

One approach to mitigate SSV is through "sweeping," which involves applying controlled lateral movements to the drill bit [21]. Sweeping is believed to help break the stick-slip cycle and improve drilling efficiency. This chapter describe in-depth the sweeping techniques for SSV mitigation, including their mechanisms, applications, and effectiveness.

2. Sweep from Stick-Slip vibrations

2.1. Causes and Impacts of Stick-Slip Vibrations

The principal causes of the stick slip are difference in torque input to overcome the static friction in the string resulting from attempts to control the downhole incidents such as **tight hole**, **severe doglegs**, **keyseatings** or **significant drag**. In addition to the coupling between axial and torsional vibration of the bit are also cause of SSV. Despite differences in root cause analysis of stick-slip vibrations, it is collectively agreed upon by researchers that stick-slip can be either bit-induced or friction drillstring-induced. [22]

If we highlighted that, in the "slip" phase, the bit rotation speed will decrease until the bit eventually comes to a standstill or is even displaced beyond the neutral point [23]. We see a small periods of backward rotation as shown in the Figure (III.1), where field measurements of stick-slip show how the RPM reaches negative values before a new stick-phase is initiated.

Moreover, like any friction specially the induced from vibration are a complex problem to the mechanicals engineers. This particularly applicable for stick-slip vibration which can cause undesirable consequences chatter, high energy losses, the abnormal wear and rupture of the friction block...etc.

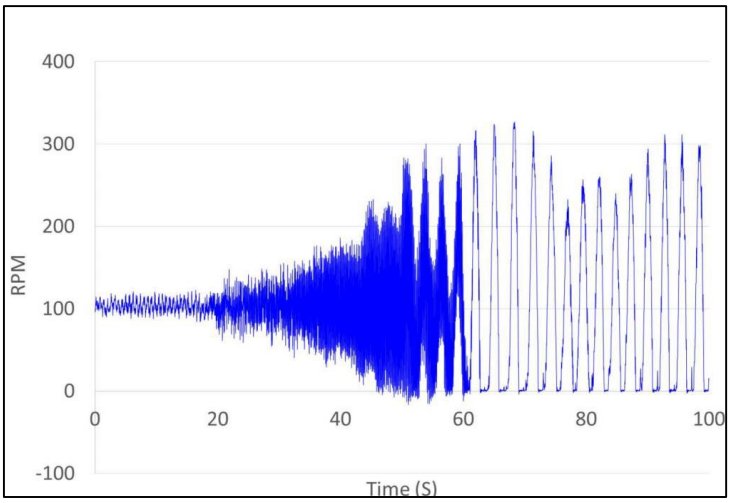

Figure III. 1. Stick-slip manifestation Downhole measurements of RPM variation during drilling.[23]

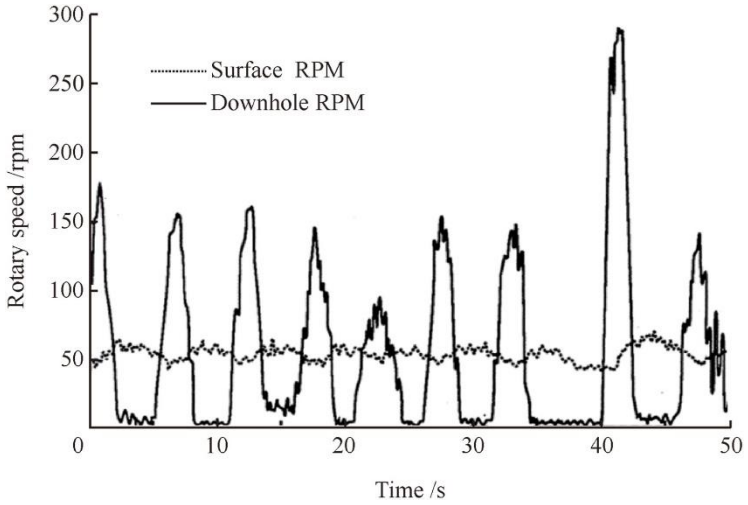

Figure III.2. The difference between RPM in surface and downhole due to the Stick Slip oscillation. [24]

2.2. Mitigation of Torsional Stick-Slip Vibrations

The Sweep from Stick-Slip Vibrations technique is designed to mitigate SSV by applying controlled lateral movements to the drill bit. The principle behind this technique is to disrupt the

stick-slip cycle by introducing additional forces that counteract the frictional forces between the drill bit and the formation, thereby reducing the tendency of the drill string to stick and slip.

Targeting this objective, Stick-slip control techniques classified into two categories [24]:

2.2.1. Passive methods

The physical manipulation of downhole tools by changing\addition of the BHA components can delay the process of stick-slip vibration but cannot eliminate it. Such as the installation of the anti-whirl technology or combine, the PDC bit with the stabilized steerable motor. In addition to tools technologies mentioning:

A. Target torsional vibrations and drilling dysfunctions with PosiTrack

The new technology TVM from NOV specifically designed to manage unwanted torsional, uses a proprietary pressure-compensated telescoping mechanism to absorb vibrations and torsional oscillations caused by stick-slip, drill bit overengagement, and uneven weight transfer and minimizes drill bit instability, safeguards priceless BHA components, and facilitates drilling parameter adjustment.[25]

B. Antiwhirl bit

An instrument for drilling that is made to provide a net imbalance force between its various cutting elements; these bits are often polycrystalline diamond compact bits (PDC type). The bit is forced against the borehole's side by this imbalance force, which produces a stable rotating situation that prevents downhole vibration, whirling, and wobbling in reverse. Compared to more typical bits, which are not dynamically biased to operate smoothly, are intrinsically unstable, are vibration-prone, and have shorter lifespan, antiwhirl bits enable quicker rates of penetration while achieving longer bit lives. But no bit is immune to whirls.[26]

C. Steady scout stick-slip management tool

Steady Scout lowers the peak RPMs encountered during stick-slip, which enhances drilling performance and prolongs bit life. By retracting when differential pressure rises and expanding when pressure falls, the Steady Scout absorbs variations in motor differential pressure. This

leads to a smoother wellbore through stable weight-on-bit, consistent depth of cut, and steady drill string pressure [27]

2.2.2. Active Methods

Controlling parameters like the WOB and RPM can keep the drilling process in an optimal zone and maximize the ROP as shown in the Figure (III.2). Involving the use of real-time drilling parameters as feedback to control the drilling process.

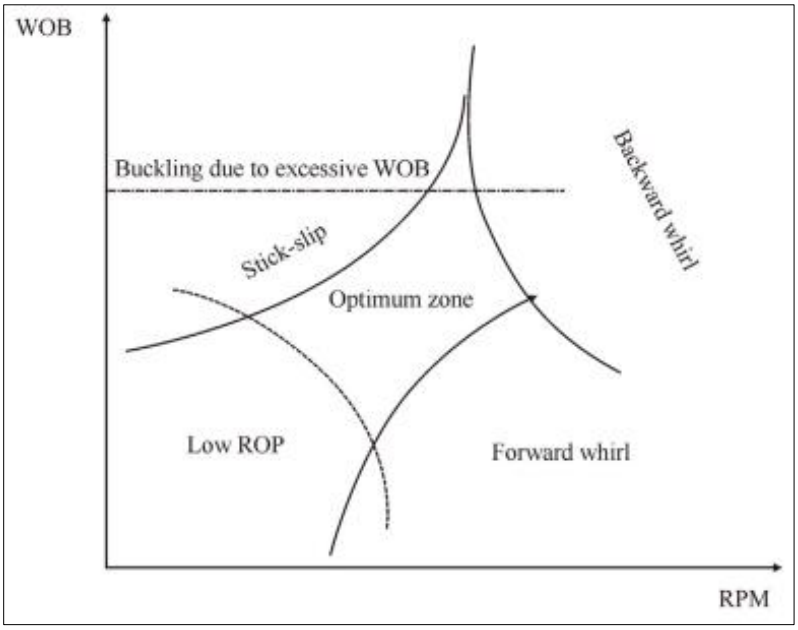

Figure III. 2. Optimal drilling zone [28]

3. Principle of SWD as proposed technique

The SWD technique has been developed as an aid to use the stick slip vibrations. By providing check shot information, in real-time by the placement of the bit on the surface seismic section as the well progresses. By generating look ahead VSP images, the approach to critical horizons can be monitored. Such information, available in real-time at the well site, can have considerable value. It can help in the optimization of the drilling operation and has obvious implications for safety [29].

The SWD involves using selections of surface seismic sensors to record the seismic noise produced by a drill bit during effective drilling as shown in the Figure (III.3). This technique

offers significant advantages, including real-time imaging, reduced drilling risk, cost savings, and increased efficiency.

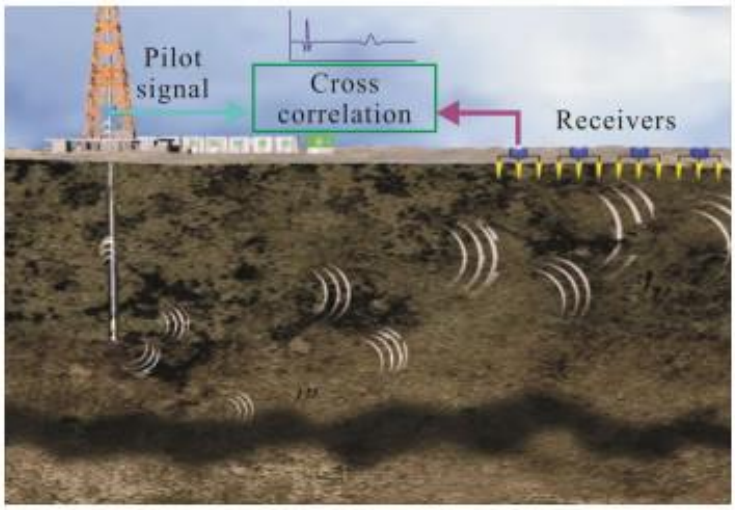

Figure III. 3. Schematic illustration of the seismic while drilling method. [30]

3.1. SWD challenges and methodology

Using SWD technology, IoT-enabled sensors listen to differences in the sound generated by drill-bit penetrating the rock formations ahead of the bit, measuring and recording its vibration properties. The sensors can clearly differentiate layers on changes in the acoustic signals it measures. This data communicated wirelessly to an edge-computing device in the driller's cab. The data is processed and streamed to the cloud. [31]

This method, though challenging due to the continuous and chaotic nature of drill-bit signals. The reliability of SWD data is paramount, as any loss of data is unrecoverable. By continuously recording drill-bit signals with surface receivers.

3.2. Acquisition and Recovery of Noise

During SWD surveys, the seismic source is the vibrations from the drill-bit penetrating rock formations. These vibrations are non-stationary and random due to the variations in the formations and drilling operations. The drill-bit noises are produced at depth, making the signal different from conventional seismic sources. The energy of the drill-bit signal is weaker than other source signals. Acquiring continuous and accurate measurements of the drill-bit signal is

a challenge. Using portable seismometers with greater sensitivity and burying them at a certain depth can help reduce attenuation and ambient noises [32]. Pulse-compression methods can then be used to extract a coherent and interpretable signal.

3.3. Complex Wavefield of SWD

The complexity of Surface Wave Drilling (SWD) is a major challenge. The SWD wavefield can be divided into three components: **drill-bit wavefield**, **drill-string wavefield**, and **surface noise wavefield (**Figure III.4).

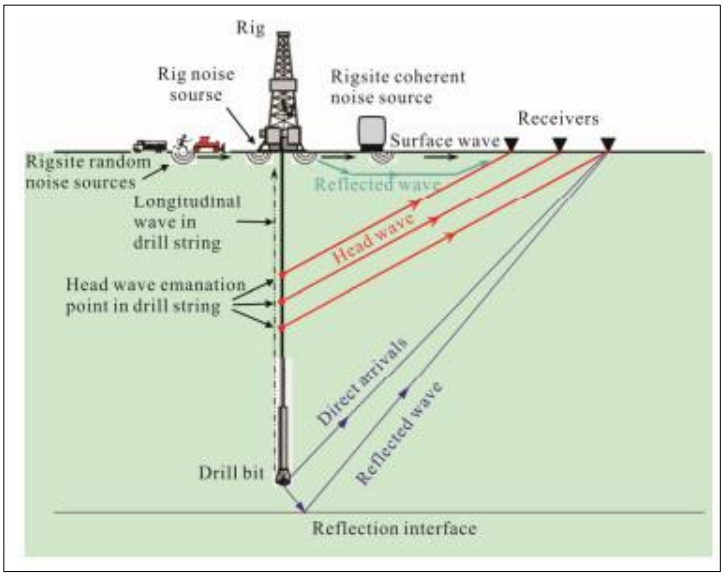

Figure III. 4 Sketch maps of raypaths for the wavefields used in SWD. [30]

A. Drill-bit wavefield

Consists of two wavefields: the direct arrival of drill-bit signals from the bit to the surface, and drill-bit reflections from the impedance interface ahead of the bit. The drill-bit reflection is weaker than the direct arrival but still has a weak hyperbolic moveout.

B. Drill-string wavefield

Travel through the drill string and undergo reflections from discontinuities within it. These reflections can be observed on autocorrelograms and are classified as short period multiples and long period multiples. Short period multiples reverberate between discontinuities in the drill

string while long period multiples travel up and down the entire length repeatedly. The period of the long period multiples can be used as a reference time.

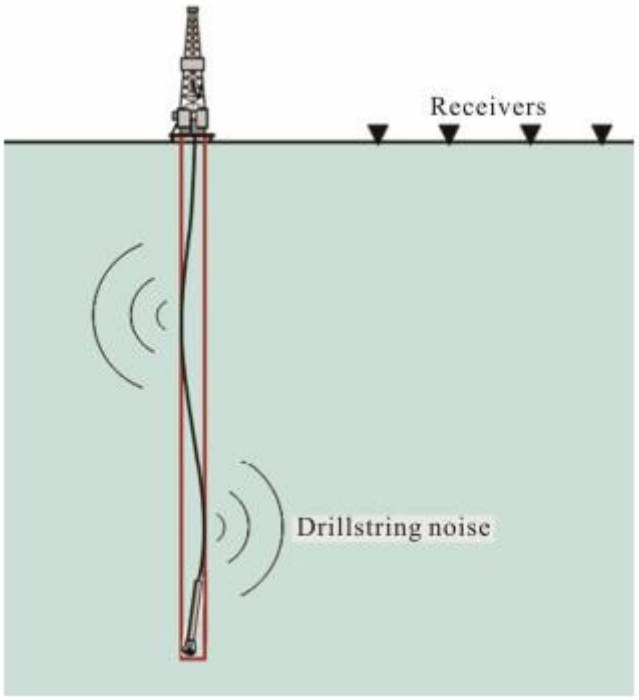

Figure III. 5. Sketch map of producing drill string noise. [30]

The drill string itself generates strong coherent noise due to bending, buckling, and unbalanced vibrations. This noise propagates in the formation similarly to the drill-bit direct arrivals. Additionally, there are drill-bit mud waves and head waves in the drill-string wavefield.

C. Surface noise wavefield

It is the heaviest source of noise in SWD recordings. Various coherent and random noises are produced at the rig and yard, such as those from supply trucks, cranes, equipment movement, diesel rig-power engines, mud shakers, and pumps. These noises significantly decrease the Signal-to-Noise Ratio (SNR) in SWD surface data. The rig derrick also acts as a noise source, producing rig-generated direct arrivals and refractions that interfere with drill-bit signals.

3.4. Separation of Signal and Noise Wavefields

The separation of signal and noise wavefields is crucial in seismic data analysis, particularly in the presence of surface noises that contaminate the acquired seismic traces near drilling wells.

To address this issue, receiver arrays are selectively used to suppress ambient noise and provide better time-offset information for wavefield propagation analysis. Coherent noise wavefields can be identified and removed using corresponding techniques.

The primary ambient noise in surface drill-bit noise data is surface waves generated by noise sources in the wellsite, characterized by low frequency, low group velocity, and large amplitudes [33]. These can be easily removed using filters without causing significant damage to the bit signal. Head waves, which exhibit linear moveout with wellhead offset, can be separated using curvelet transform, but attenuating high velocity components can be challenging. Rig-generated direct arrivals and refractions can be separated using curvelet transform with good spatial and frequency localization. Bottom-hole-assemble multiple and drill-string multiple with hyperbolic moveout can be suppressed using multichannel predictive deconvolution filters.

The lateral vibrations and shock noise caused by contact between the drill string and the well walls can be attenuated using statistical correlation. Noise from cars and human activities can also be filtered using statistical correlation.

Mudlogging data can assist in the separation of signal and noise wavefields by providing information on average velocity, bit depth, and geological information around the well. [34]

3.5. Cross-Coherence Interferometry of Direct Arrivals and Reflections

Cross-coherence used in seismology and engineering, successfully retrieves the seismic response of receivers located at different positions on the surface. This method effectively removes the source signature from the retrieved response, by using only the phase information and ignoring amplitude information, even in the presence of strong noise. Without the need for an independent estimate of the drill-bit seismic source signature, it is convenient to retrieve the subsurface impulse response from drill-bit signals recorded by surface receivers. A critical point is that we should suppress the strong coherent noises that are not generated by the drill-bit source. [35]

A. The Geophone Measurement

The SWD technique utilizes a small array of geophones. On land this would usually be between 12 and 20 geophones. The geophones are usually placed between 6 and 13 ft apart in a

line pointing towards the rig, with the first sensor typically 300 to 600 ft from the wellhead. the amplitude of the surface waves generated by a working rig can be several orders of magnitude greater than the signal radiated from the bit. Simply summing the geophone channels together may not provide sufficient attenuation of the ground roll. To overcome this problem each geophone channel is recorded separately with a high dynamic range. Digital grouping techniques can then be used to separate the bit generated signal from the groundroll. Such techniques are very versatile and may be applied in real time. Because individual sensor outputs are available, corrections for statics and normal moveout can be performed. This is particularly important when the bit is relatively shallow since the normal moveout across the array can be significant. [35]

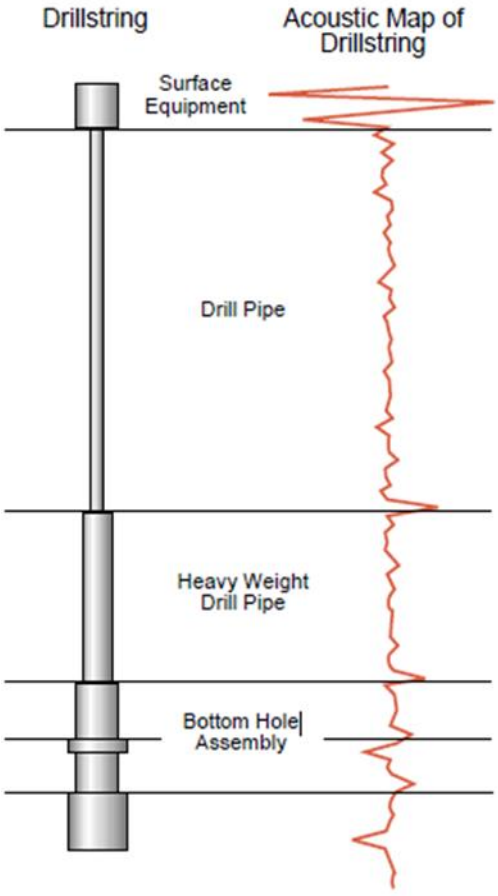

Figure III. 6. Synthetic example of a drillstring image, large reflection coefficients correspond to changes in cross-sectional area of the drillstring. [35]

B. The Drillstring Measurement

Determining the travel time from the bit to the accelerometer along the drillstring is pivotal for calculating the checkshot time, yet it's complicated by factors like tooljoints altering the effective acoustic velocity. Despite the ability to theoretically calculate the velocity using material properties and dimensions, practical constraints often necessitate estimating travel time from available data. Viewing the drillstring as a layered impedance system, reflection coefficients at layer transitions can be derived from accelerometer signal processing, facilitating the creation of an impedance map, as illustrated in Figure (III. 6). However, complications arise from the accelerometer's placement on the swivel rather than at the drillstring's end, necessitating ARMA modeling for signal processing to account for noise pickup from mud pumps [30].

In practice, noise interference from mud pumps can degrade the drillstring image quality, making it challenging to identify specific components accurately. To address this, analyzing the moveout of reflection coefficients across depths aids in determining the drillstring signal's velocity. While this method offers accurate estimates for the drillpipe section, velocity estimations for the bottom hole assembly (BHA) and heavyweight pipe sections are required due to their shorter lengths compared to the entire drillstring. Despite potential discrepancies, this approach ensures precise travel time calculations crucial for effective drilling operations, depicted in Figure (III. 6).

C. The Cross Correlation

Cross-correlating the accelerometer and geophone signals provides insight into the relative travel time between the drillstring and formation paths. However, both signals are plagued by multiples originating from the drillstring, complicating time picking due to multiple peaks in the cross-correlation. While the accelerometer signal follows an ARMA process, with AR and MA orders determined by drillstring length and accelerometer position respectively, estimating parameters for the formation signal's ARMA process, particularly the large-order MA component, proves challenging. Consequently, drillstring multiples from the bit are retained in the cross-correlation, treated as part of the source. Additionally, compensating for differing

transfer functions between sensors necessitates a phase compensation technique to ensure accurate analysis [30].

4. Examples of the Applications in the world

Seismic while drilling (SWD) measurements are an efficient way to obtain accurate time-to-depth information around the wellbore. Additionally, it can provide a detailed seismic image of the structures of reflecting horizons below the trajectory, and the information can be used to support drilling decisions. In terms of operations, the data is acquired while the well is being drilled without use of additional rig time, as shots are acquired during natural stops at connections. It does however require a boat operation for positioning of the seismic source**.**

This technology has been applied in various regions around the world with notable success, particularly in the **North Sea** and the **Gulf of Mexico**, [36] to enhance drilling operations. It provides real-time imaging of subsurface structures for better geological understanding and improved well placement. In the **Middle East**, [35] SWD helps mitigate drilling risks and optimize well placement, while in high-cost areas like offshore **Brazil**, [37] it reduces uncertainties and improves drilling efficiency. SWD is a valuable tool for the oil and gas industry, offering significant benefits in terms of drilling efficiency, cost savings, and risk reduction. Its applications are expected to expand as technology advances.

4.1. Real data example

Two vertical development wells, (A) and (B), were drilled in the Raudhata in field in North Kuwait and were approximately 3 miles apart [35].

A. Well (A):

Table III. 1 : Data of Well (A) [35]

Parameter	Value
Depth Range	1,000 ft - 8,700 ft
Geophone Array	Initially: 12 geophones spaced 13 ft apart
	Eventually: 27 geophones spaced 13 ft apart
Initial Geophone Distance	250 ft from wellhead
Final Geophone Distance	530 ft from wellhead
Accelerometers	Two vertically oriented accelerometers on swivel
Drill Bit Section	Tertiary and Cretaceous systems, Barremian age
Key Observations	Clear structure movement with depth
	Identifiable reflections at the bit for travel time determination
	Slight decrease in signal-to-noise ratio in deeper section, but key reflections remain discernible
Time Difference	Approximately 11 milliseconds one-way time compared to wireline VSP in well A
Key Observations	Clear structure movement with depth

B. Well (B):

Table III. 2 : Data of Well (B) [35]

Parameter	Value
Depth Range	Start: Approximately 1,000 ft
	End: Start of PDC bit section at 8,700 ft
Geophone Array	Initially: 12 geophones spaced 13 ft apart
	Eventually: 27 geophones spaced 13 ft apart
Initial Geophone Distance	250 ft from wellhead
Final Geophone Distance	530 ft from wellhead
Accelerometers	Two vertically oriented accelerometers on swivel
Drill Bit Section	Tertiary and Cretaceous systems, Barremian age
Data Quality	Consistently good throughout depth range
Key Observations	Clear structure movement with depth
Accelerometers	Two vertically oriented accelerometers on swivel
	Identifiable reflections at the bit for travel time determination
	Slight decrease in signal-to-noise ratio in deeper section, but key reflections remain discernible
	Identifiable reflections at the bit for travel time determination
Time Difference	Approximately 11 milliseconds one-way time compared to wireline VSP in well A

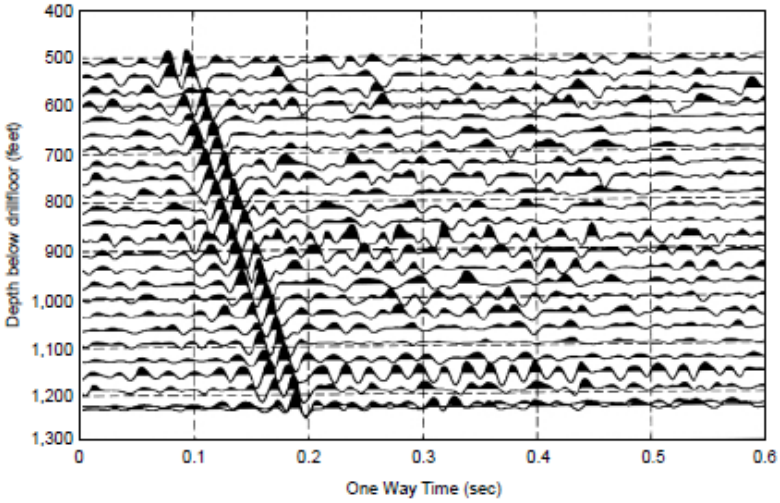

Figure III. 7. Cross correlations from shallow section of well A. The direct arrival from the bit can be clearly seen. [35]

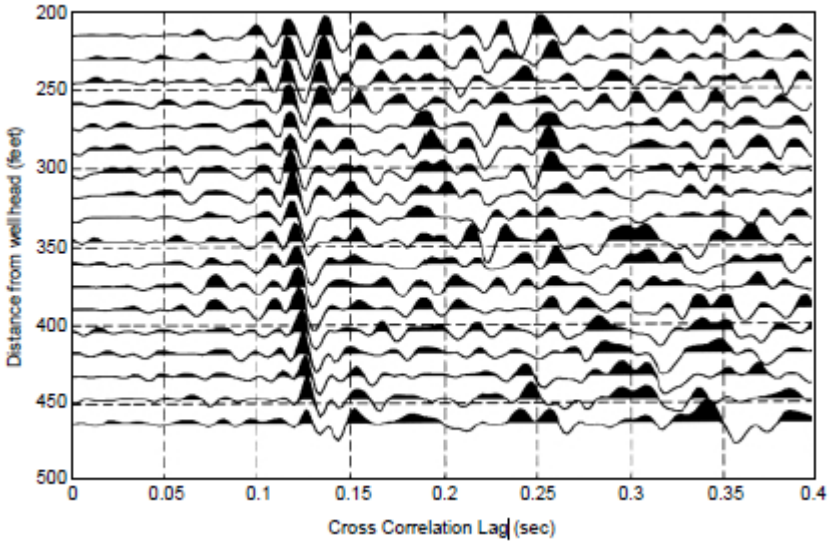

Figure III. 8. Individual geophone cross correlations from one depth level (1,225 ft) of well A. The hyperbolic moveout of the direct arrival is visible from 0.115 sec to 0.127 sec. [35]

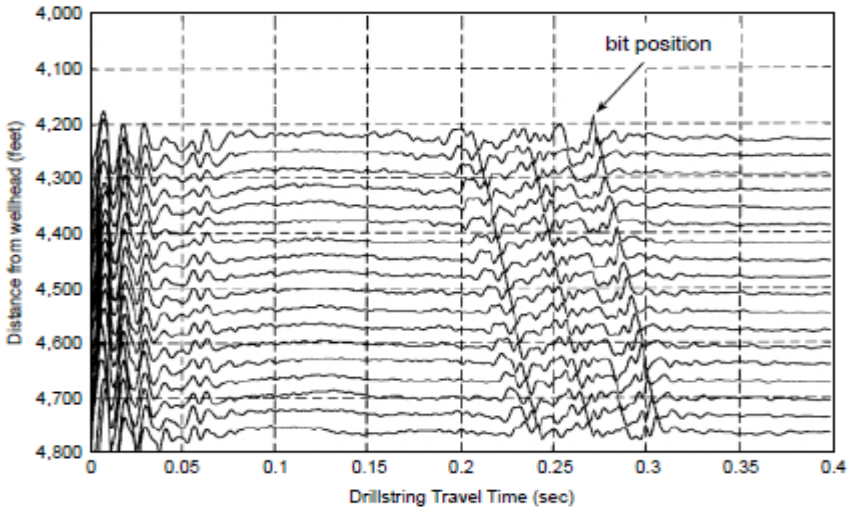

Figure III. 9. Close up of part of Figure (III.7) The reflection coefficient due to the bit/rockinterface is indicated. Identifying this interface gives the drillstring travel time. [35]

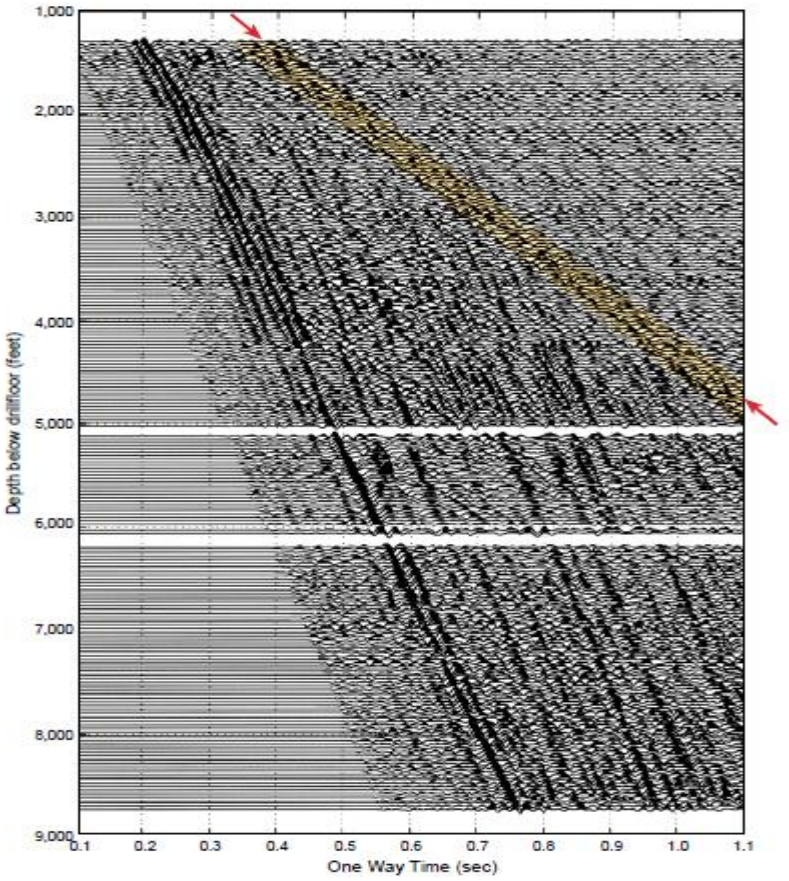

Figure III. 10. Cross correlations for well B. The drillstring multiples have been removed and the data have been corrected to zero offset and one way time. Note tube wave indicated by arrows. [35]

Figure (III. 10) shows the cross correlations between the accelerometer and the geophones after drillstring multiple removal, beamforming to remove the surface waves and application of the phase operator. The data have been corrected for the drillstring travel time and are plotted in one way time. The direct arrival can be seen over the whole depth range. In addition there are several other features, notably tube waves, and some faint evidence of reflected energy.

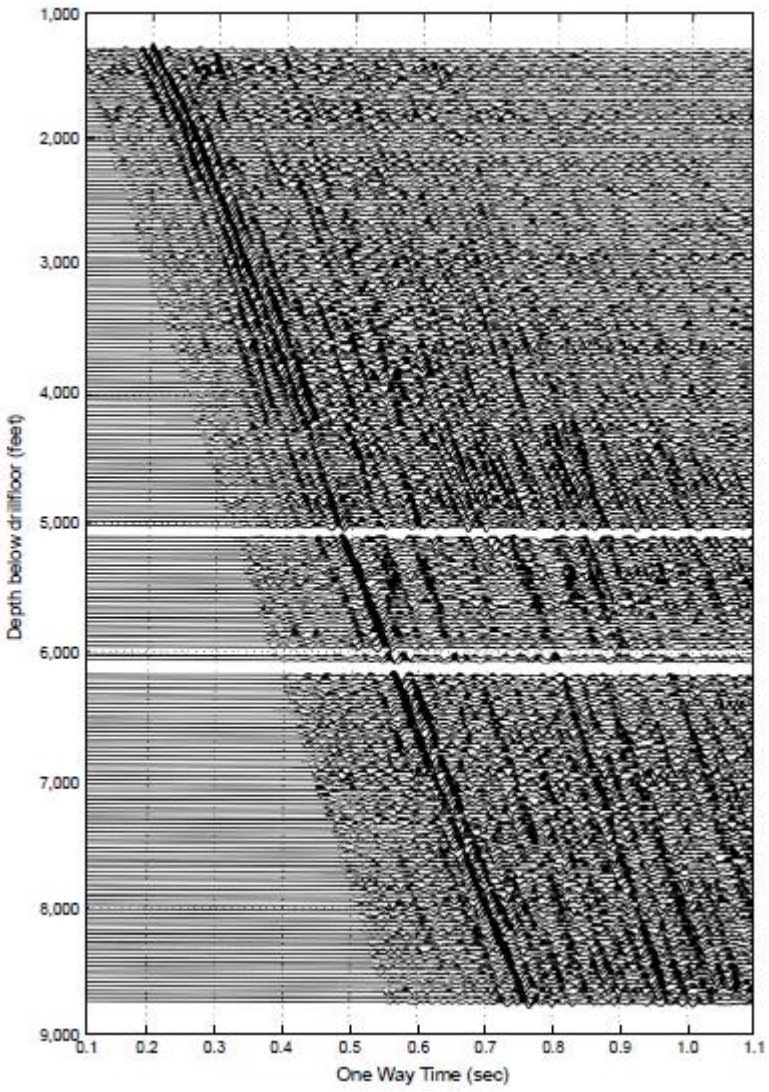

Figure III. 11. The data of Figure (III.10) after tube wave removal. [35]

Figure (III. 11) shows the same data after tube wave removal. It is obvious that the character of the direct wavefield changes with depth. The signal generated by the bit depends on a variety of factors such as weight on bit, rotation speed, lithology, bit wear, mud weight, etc. Since the

amplitude of the direct signal can vary widely with different drilling conditions it is instructive to look at how the energy is distributed over the frequency range.

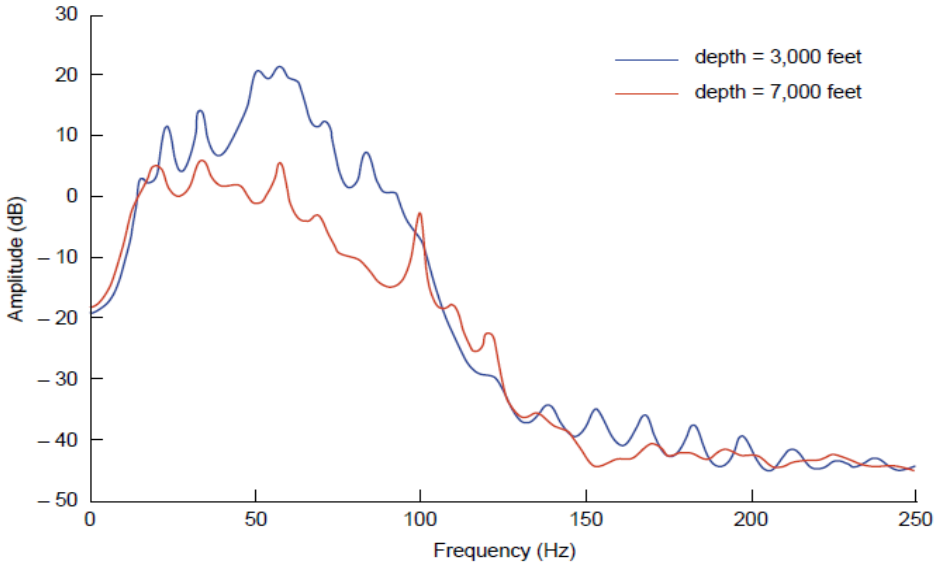

Figure III. 12. Smoothed source spectra for two different depths. Bandwidth decreases with depth.

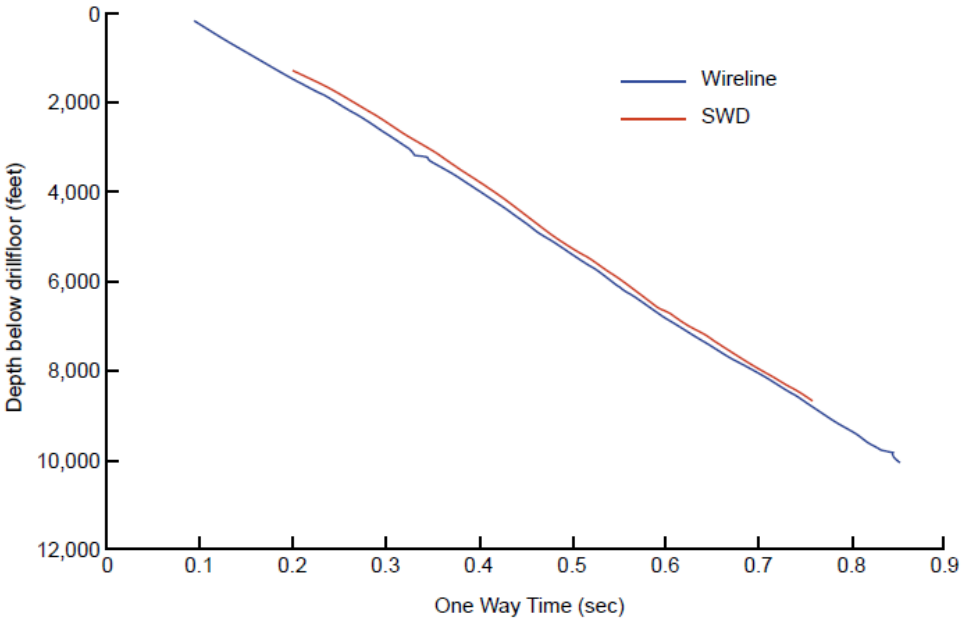

Figure III. 13. Comparison between Seismic-While-Drilling (SWD) time to depth data from well B and wireline checkshot data from well A. There is a difference of approximately 11 milliseconds one way time. [35]

Figure (III. 12) shows the smoothed source spectra for two depths. The data from the shallower depth has a wider bandwidth. This is to be expected, since the effect of attenuation increases as the well gets deeper. It hould also be remembered that the geophone array was lengthened and moved periodically during acquisition in an attempt to improve the signal to noise ratio. Changing the position and coupling of the sensors has an effect on the recorded wavefield.

Figure (III. 13) shows the comparison between the time to depth resulting from the SWD data, and those from a conventional wireline VSP that was acquired in well A. There is a time difference of approximately 11 milliseconds one way time. There could be several reasons for this discrepancy. The data are from different wells, although the wells are close and should have similar time to depth curves. There may be errors in the offset correction applied to the SWD data (straight raypaths were assumed). The wireline data were acquired with an airgun source in the mudpit, which was some 20ft below the surface, while the SWD geophones were placed on the surface. In addition, we would normally expect to see some difference in travel time between an impulsive type source such as an airgun, and a correlation technique, such as SWD. The data from Figure (III. 12) were processed using the optimal deconvolution technique and a 17 trace (approximately 500 ft depth aperture) median filter was applied to the reflected wavefield. The resulting VSP is shown in Figure (III. 14).

C. Comparison

Figure (III. 15) shows part of a surface seismic line that passes close to both wells. Well A is approximately 1,200 ft from the line, while well B is about 2,500 ft away. The two well locations are marked. At the well A position a corridor stack produced from the wireline VSP data has been inset into the surface seismic section. At the well B position a corridor stack produced from the SWD data has been inset. There is a good match to the region below 0.9 sec two way time. The region between 0.5 and 0.9 sec two way time is poorly resolved in the surface section.

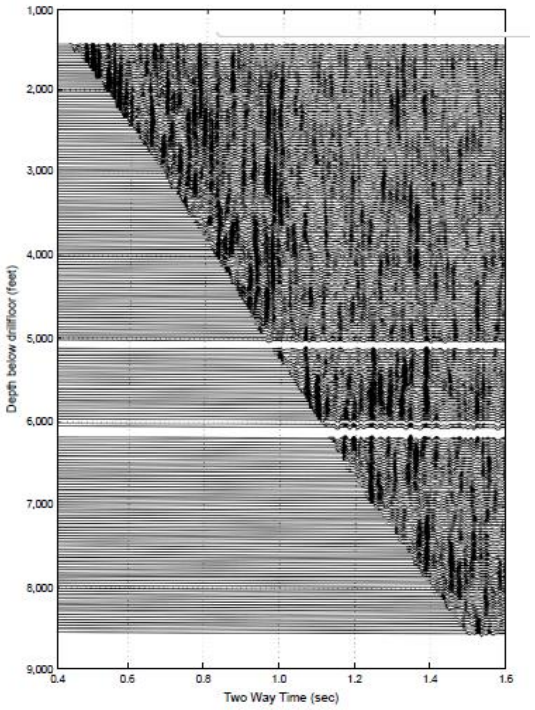

Figure III. 14 VSP image produced from the Seismic-While-Drilling data in well B. [35]

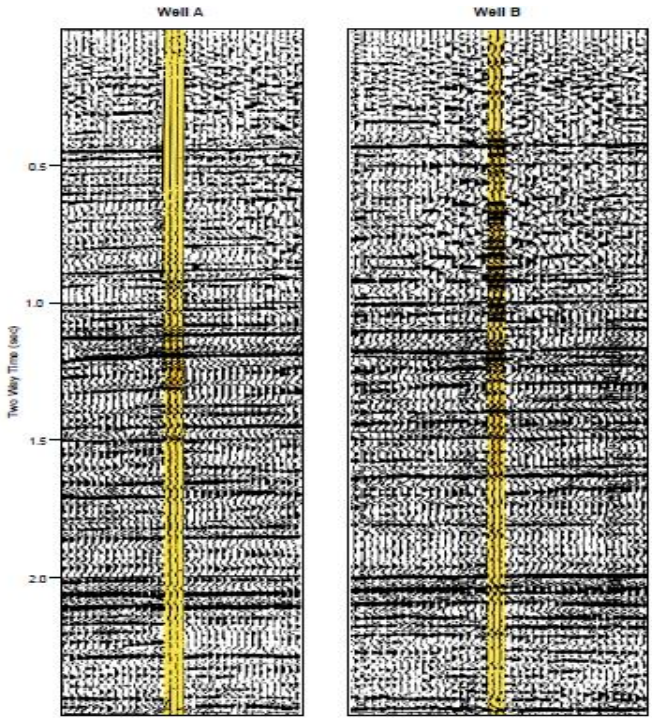

Figure III. 15. Parts of a surface seismic line passing close to both wells. A corridor stack from the wireline data has been inset at the location of well A, while a corridor stack from the Seismic- While-Drilling data has been inset at the location of well B (shown in yellow). [35]

D. Discussion and conclusions

The SWD (Seismic While Drilling) technique has seen limited use in the Middle East due to three primary factors:

- Lower Value in Development Drilling: The real-time benefits of SWD are less significant in well-known development drilling campaigns where horizons and targets are already well established.
- High Quality Surface Seismic Data: In regions like the Gulf, high-quality surface seismic data is readily available, reducing the need for SWD.
- Technical Limitations: Issues such as bit type, deviated wells, and rig noise present challenges to the effective implementation of SWD.

Despite these challenges, the SWD technique has shown potential in North Kuwait wells:

- In well A, hardware problems limited the amount of usable data, but the results from the shallow section confirmed the technique's viability. However, the quality of SWD results is unlikely to match that of wireline VSP data.
- In well B, SWD provided a "real-time" look-ahead image at the rig-site, allowing formations to be identified before drilling through them, which offers operational advantages such as selecting casing points.

E. Applicability in Algeria

Considering the factors and results mentioned, the applicability of SWD technology in Algeria would depend on similar conditions:

- Development Drilling Campaigns: If Algeria's drilling campaigns involve well-known horizons and targets, the real-time benefits of SWD might be less valuable.
- Availability of High-Quality Seismic Data: If high-quality surface seismic data is readily available in Algeria, this might reduce the necessity for SWD.
- Technical Challenges: The same technical limitations (bit type, deviated wells, and rig noise) would need to be addressed.

If these conditions in Algeria mirror those of North Kuwait, the SWD technique might face similar challenges and limitations. However, if there are scenarios where real-time formation

identification and operational advantages (like casing point selection) are critical, SWD could offer significant benefits.

5. Advantages and Utilities in Saudi Arabia

Saudi Aramco faces more challenges, not only does it need to replenish reserves and maintain production output, but whereas other oil companies can acquire reserves through stocks, for Saudi Aramco the only way to add reserves and production is through the "bit." [38]

Due to the last technology SWD, it has been recognized that 3-D seismic data have the potential of providing highly detailed subsurface images that can substantially enhance the understanding of reservoir complexity, leading to improved reserves estimates, reduced drilling risks, and enhanced reservoir development strategies. [39]

For instance, the Partitioned Zone is a joint prospecting area for hydrocarbon exploration and production that the Kingdom of Saudi Arabia (KSA) and the State of Kuwait share. Its almost 4612 sq. km surface area inundated with various challenges and possibilities. This surface area is split into two sections: the eastern exploration side, which recently finished one of the biggest onshore 3D seismic acquisition operations, and the western development side.[40]

In addition to its utilizing advanced seismic technology to re-explore the Empty Quarter in the Arabian desert in a bid to boost its oil and gas reserves. A team of 900 people is currently exploring 15,400 square kilometers of the area. This new exploration effort comes after previous joint ventures with foreign companies failed to find recoverable quantities of oil and gas. While the seismic technology being used provides a detailed three-dimensional picture of rock structures and physical characteristics. Aramco's exploration efforts could potentially impact the company's estimate of its oil and condensate reserves, which currently stand at 261 billion barrels. This could affect the planned international offer of a 5% stake in Aramco, with some analysts predicting a valuation of $1 trillion or more for the company. However, these exploration efforts are expected to help Aramco maintain its reserves estimate for the foreseeable future. [41]

6. Promising SWD in Algerian Industry

Algeria's geological landscape, characterized by hard rock formations and vast surface areas, presents unique challenges for traditional drilling and exploration methods. The lack of comprehensive structural seismic data further complicates exploration and production efforts in the region. SWD technology offers a solution by providing real-time seismic data while drilling, enabling operators to make informed decisions and optimize well placement and production strategies. This technology not only reduces exploration risks and costs but also enhances the overall efficiency and success rates of drilling operations in Algeria's challenging geological environments. It can be defined up include the following:

- SWD provides real-time imaging of subsurface structures, enhancing reservoir characterization and optimizing well placement.
- Early detection of drilling hazards allows for safer and more efficient operations in Algeria's challenging geological environments.
- Real-time data on reservoir properties and structures optimize drilling trajectories, leading to increased hydrocarbon recovery rates.
- SWD improves drilling efficiency, optimizes well placement, and minimizes risks, resulting in significant cost savings for operators.
- SWD reduces the environmental impact of drilling by enabling operations that are more precise and minimizing surface disturbance.
- SWD contributes to the creation of a comprehensive seismic big data repository, providing valuable insights for future exploration and drilling activities in Algeria. [42]

In addition to its direct benefits for offshore exploration, Seismic imaging of the eastern [43] SWD can also complement other technologies used in offshore operations in Algeria. For example, integrating SWD data with existing 3D seismic surveys can provide a more comprehensive understanding of the subsurface geology. This integrated approach can help identify subtle geological features that may not be apparent from seismic data alone, leading to more accurate reservoir characterization and improved well placement offshore. Furthermore, SWD can be combined with other advanced technologies, such as electromagnetic surveys and microseismic monitoring, [44] to further enhance offshore exploration efforts. By leveraging

SWD in conjunction with other technologies, operators can maximize their chances of success in offshore exploration in Algeria.

7. Conclusion

Seismic while drilling (SWD) technology is a significant advancement in the oil and gas industry, providing real-time insights into underground formations to improve drilling operations. By combining seismic data acquisition tools with drilling, SWD enhances decision-making for well placement, steering, and reservoir characterization. Despite challenges such as stick-slip vibrations, SWD offers benefits like reduced risks, cost savings, and increased efficiency. It has already proven effective in regions like the North Sea and the Gulf of Mexico, and as technology progresses, SWD will continue to play a vital role in navigating complex geological environments and improving resource extraction.

CHAPTER IV

Simulation using Python and MatLab

1. Introduction

The key to realizing an idea's potential is to simulate it. This is especially crucial for intricate procedures like the interpretation of seismic data. This chapter will cover how to simulate seismic data and well log curves using MATLAB and Python routines. We will be able to enter, export, and modify seismic data with these functions, which will enable thorough analysis. At the end, we will have a firm grasp on how these instruments can be used to enhance our comprehension of seismic data and its possible uses. We will also be able to compare the Seismic While Drilling technique, which uses drill bit stick-slip vibrations with the Vertical Seismic Profile, and determine which method is more effective.[45]

2. Python toolbx

2.1 SeisPy Python toolbox

SeisPy is a Python package designed for seismic data processing and analysis, similar to SeisLab for MATLAB. It offers a comprehensive suite of tools and functions aimed at facilitating the handling and interpretation of seismic data. Here are some key features of SeisPy:

- **Support for Various Seismic Data Formats**: SeisPy can handle different seismic data formats, including SEG-Y and SAC.
- **Seismic Data Processing Functions**: It includes both basic and advanced processing functions, such as filtering, deconvolution, spectral analysis, and wavelet analysis.
- **Visualization Tools**: SeisPy provides tools for creating time series plots, spectrograms, and seismograms.
- **Seismic Data Inversion and Imaging**: The toolbox supports various inversion and imaging techniques used in seismic analysis.

2.2 Initialization

SeisPy, being based on Python, offers flexibility to define and manage parameters using configuration files or environment variables.

Create a Python script or module **system_defaults.py** that sets the default parameters which do not depend on the user's environment. After that we create another Python script or module **user_defaults.py** that sets the user-specific parameters. Then Create a script

(**initialize_seispy.py**) that combines the system and user defaults and initializes SeisPy with these settings. In the main script or Jupyter notebook, call the initialization function before using SeisPy functions.[45]

A Python package for handling headers, Kirchhoff migration, and other tasks while visualizing seismic data. includes the following features:

- load_header: load mat file header
- load_segy: load segy dataset
- sorthdr: sort seismic header
- sortdata: sort seismic data
- selectCMP: select a CMP gather with respect to its midpoint position
- analysefold: Positions of gathers and their folds
- imageseis: Interactive seismic image
- wiggle: Seismic wiggle plot
- plothdr: Plots header data
- semblanceWiggle: Interactive semblance plot for velocity analysis
- apply_nmo: Applies nmo correction
- nmo_v: Applies nmo to single CMP gather for constant velocity
- nmo_vlog: Applied nmo to single CMP gather for a 1D time-velocity log
- nmo_stack: Generates a stacked zero-offset section
- stackplot: Stacks all traces in a gather and plots the stacked trace
- generatevmodel2: Generates a 2D velocity model
- kirk_mig: Kirkhoff migration
- time2depth_trace: time-to-depth conversion for a single trace in time domain
- time2depth_section: time-to-depth conversion for a seismic section in time domain
- agc: applies automatic gain control for a given dataset.

2.3 Command-line help

To create a similar command-line interface for SeisPy that lists functions dealing with specific data structures and provides a brief description of their purpose, you can use a

combination of Python's introspection capabilities and a predefined dictionary of function descriptions.

- **Create a Dictionary of Function Descriptions**: Define a dictionary where keys are the function names and values are their descriptions. This dictionary can be organized based on data types, similar to how **s_tools**, **l_tools**, **pw_tools**, and **t_tools** work in SeisLab.
- **Define Functions to List Tools**: Create functions to list and filter these tools based on the search term provided.
- **Implement the Command-Line Interface**: Use argument parsing to create a command-line tool that users can interact with.

3. MATLab toolbox

3.1 SeisLab MATLAB toolbox

A MATLAB package called SeisLab is intended to make processing and analyzing seismic data easier. Seismic data may be read, written, manipulated, and shown in a variety of forms using the toolbox's numerous functions and capabilities.[46]

Among SeisLab's primary characteristics are:

- SEG-Y, SAC, and SEGY are among the seismic data formats that are supported.
- Filtering, gain modification, and time shifting are examples of fundamental seismic data processing operations.
- Advanced seismic data processing features, such wavelet analysis, spectrum analysis, and deconvolution;
- Tools for visualizing data, like spectrogram, time series plotting, and seismogram creation.
- Support for imaging and inversion of seismic data.

3.2 Initialization

Certain settings are required for SeisLab to operate correctly. The function presets, which invokes the systemDefaults4Seislab and userDefaults4Seislab routines, sets these settings. The latter defines settings (such the folders where data files, like Seg-Y files or LAS files with well data, are placed) that the user is likely to alter. In contrast, the function systemDefaults4Seislab

sets the settings that are independent of the user's surroundings. In any event, userDefaults4Seislab allows you to modify any parameter that is defined in systemDefaults4Seislab. Presets should come before a session utilizing SeisLab functions because these parameters are needed in many of the functions. The first three sentences are a basic illustration of a SeisLab session.[46]

- presets % Initialize parameters
- seismic=s_data % Create a synthetic seismic dataset
- s_wplot (seismic) % Plot the seismic dataset

Naturally, SeisLab functions also make use of Matlab's normal help facilities, help and lookfor. Furthermore, the following functions are designed to find functions for a certain type of data structure that do specified jobs rapidly.

- l_tools List functions that deal with well logs.
- s_tools List functions that deal with seismic data.
- pw_tools List functions that deal with pseudo-well structures.
- t_tools List functions that deal with tables.

Each of these functions, when used without an argument, shows the whole collection of functions that are available for that particular type of dataset along with a brief description of what each one does. An extra search word can be added to limit the outcome. Consequently:
>> s_tools plot

- s_2d_spliced_synthetic: Plot synthetic spliced into seismic line
- s_3d_header_plot: Make contour plot of one header as function of...
- s_3d_spliced synthetic: Plot synthetic spliced into inline and cross-line...
- s_compare: Plot one seismic data set on top of another for...
- s_cplot: Plot seismic data in form of color-coded pixels...
- s_header_plot: Plot header values of a seismic data set
- s_ispectrum: Interactively pick windows on seismic plot and...
- s_plot: "Quick-look" plot of seismic data (color if more
- s_spectrum: Plot amplitude and/or phase spectra of one or...

- s_spick1: Interactively pick time/trace pairs from a plot...
- s_spicks: Interactively pick time/trace pairs from a plot....
- s_volume_browser: Interactive display/plot of a 3D seismic data set...
- s_wedge_model: Compute/plot synthetic from wedge model and...
- s_wplot: Plot seismic data in wiggle-trace format

Shows only functions relevant to the display of seismic data sets; shortened lines are indicated by ellipses.

3.3 Input arguments of functions

There are mandatory and optional input arguments for most SeisLab functions. Required arguments are ―positional‖; that is, they are listed in a certain order (e.g., first, second, etc.) and come before optional arguments. If there are any more optional input parameters, they are arranged arbitrarily. They are made up of a keyword, one or more values, and a cell array containing them all. Strings are used as keywords. [46]

This is demonstrated by the SeisLab function call that follows, which depicts the seismic dataset in wiggle-trace format.

s_wplot (seismic, {`trough fill', [0.6 0.6 0.6]}, {`annotation', `cdp'})

It is necessary to provide the first input parameter, seismic, which is the name of the seismic dataset to plot. The two possible additional input parameters are denoted by curly brackets.

It is necessary to provide the first input parameter, seismic, which is the name of the seismic dataset to plot. The two possible additional input parameters are denoted by curly brackets.

Shortening or abbreviating a term is permissible as long as the result is distinct, meaning that it cannot be used to refer to another keyword. *Linestyle* and linewidth, for instance, are two keywords that begin with the word "line." They may be shortened to linest and linewi, respectively, or even to lines and *linew*. If either term were to lose one character, the acronyms would no longer be distinctive. You can prohibit keyword abbreviations by setting the global variable S4M's "keyword expansion" value to false.

3.4 Test datasets

Fast access to test data is often desirable for testing and demonstration purposes. As a result, many functions are available to generate diverse test datasets. These functions all share the trait of having the dataset as their only output parameter and no input arguments. They often use the naming pattern x_data and x_datann, where x represents the letters l, pw, s, and t, and nn is a number with one or two digits, or a digit and a letter, as in the example below.

3.5 Test datasets for seismic data

As seen in Figure (IV. 1), s_data produces a seismic dataset made up of 12 traces, each lasting 1000 ms and filtering random noise. It has just the CDP heading. A 3-D seismic dataset is created using s_data3d; the only distinction between a 2-D and a 3-D dataset is that the latter needs headers containing position information, ideally in the form of cross-line and inline numbers. The dataset produced by s_data3d therefore has two headers: xline_no and iline_no. [46]

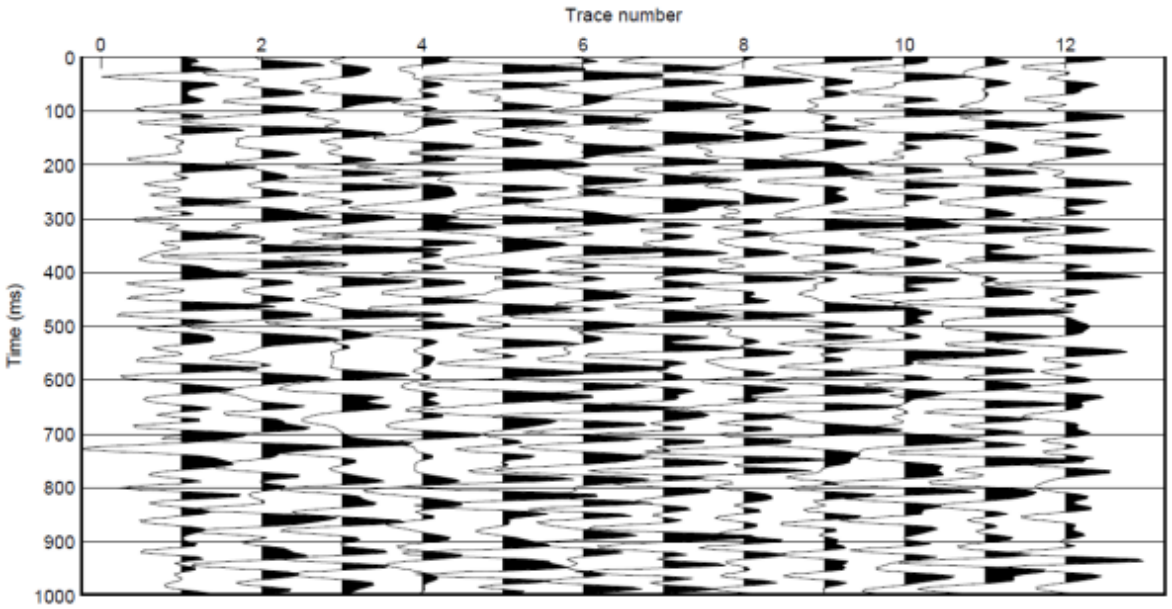

Figure IV. 1. Gaussian noise with filters, produced by s_plot (s_data).

4. CREWES MATLAB toolbox

A set of software tools created by the University of Calgary's Consortium for Research in Elastic Wave Exploration Seismology (CREWES) is called the CREWES Matlab toolbox. With

an emphasis on exploratory seismology, the toolbox offers a collection of functions and scripts for processing and interpreting seismic data. A variety of methods for analyzing seismic data are included in the toolbox, including seismic imaging, velocity analysis, wavelet analysis, and seismic signal processing. It also has modules for well log analysis, seismic data display, and synthetic seismogram synthesis.[47]

Many new seismic modeling tools have been developed using Matlab. Among these are acoustic finite difference modeling, complete waveform modeling using diffraction summation, raytracing for v (z), and raytracing for v (x, z). The first and final of these are much improved versions of earlier models. Both the diffraction summation modeling and the v (x, z) raytracer are unique.

A quick and adaptable raytracer for calculating travel times in isotropic, horizontally stratified media is the v (z) raytracing facility. It is capable of twopoint raytracing and shooting fans of rays. (Two-point raytracing involves tracing a ray through predetermined starting and finishing locations. Ray shooting denotes a situation in which the ray's takeoff angle and beginning position are specified, but its destination is not.) For P-P, S-S, P-S, and S-P modes, functions for automatically calculating the traveltimes of main reflections in shot-record geometry are offered. Other geometries (like VSP) may be modeled and an arbitrary multimode traced with a little additional work.

Travel durations may be calculated by shooting rays across a 2D, arbitrarily variable velocity field using the v (x, z) raytracer. It functions by resolving the rays on a spatial grid differential equation. A fourth-order Runge-Kutta solver is used to step rays over the grid at constant time increments. Modeling and migration tools for normal incidence are included.

The event facility includes full-waveform, zero-offset modeling. This superimposes zero-offset diffraction responses to create high-resolution synthetics. In addition to basic geometric correction factors, diffraction hyperbolae can be overlaid along any track in (x, z). This is helpful for recording the reaction of basic geologic features and for analyzing how well migration algorithms function.

Lastly, there has been an update and improvement to the acoustic finite difference facility. Performance has been enhanced, several problems have been fixed, and function interfaces have

been simplified. This is a very adaptable facility that can simulate the propagation of sound waves in isotropic, heterogeneous media. It is easy to manage source records, VSPs, and cross-well geometries when sources and receivers are positioned arbitrarily. Additionally, a code for an exploding reflector is included for fast seismic section stacking modeling.

We can replicate much of the functionality provided by the CREWES MATLAB toolbox. ObsPy, Segyio, SciPy, NumPy, and Matplotlib together offer powerful tools for seismic data processing, analysis, and visualization. Each package brings its strengths, and together they form a robust ecosystem for geophysical and seismic analysis in Python.

4.1 The V(Z) raytracing facility

Technical details

Analytical formulas, such as those found in Slotnick 1959, can be used to do raytracing in media with linear gradients and constant velocity. When a ray is recognized by its horizontal slowness, or ray parameter, p, the formula for the transit time between depths z1 and z2 is:

$$t(p) = \int_{z1}^{z2} \frac{1}{v(z)\sqrt{1 - p^2 v^2(z)}} dz \qquad (\mathbf{1})$$

and the horizontal distance travelled is:

$$x(p) = \int_{z1}^{z2} \frac{pv(z)}{\sqrt{1 - p^2 v^2(z)}}\, dz \qquad (\mathbf{2})$$

These equations can be implemented computationally by approximating v (z) using a set of N discrete layers v_k, where k = 1, 2 N. The traveltime expression for a ray that goes from layer 1 at the top to layer N at the bottom (layer number rises with z) is:

$$t(p) = \sum_{k=1}^{N} \frac{\Delta Z_k}{v_k\sqrt{1 - p^2 v_k^2}} \qquad (\mathbf{3})$$

and the distance formula changes to:

$$x(p) = \sum_{k=1}^{N} \frac{p v_k \Delta Z_k}{\sqrt{1 - p^2 v_k^2}} \qquad (\mathbf{4})$$

These expressions can be vectorized and implemented very efficiently in Matlab. This is done in the function shootray (italics will be used to denote Matlab function names). The quantity

ρv_k is easily shown to be $\sin\theta_k$ where θ_k is the angle the ray makes with the vertical in the K^{th} layer (Figure IV. 2). For a single p value, let **sn** denote a column vector of θ_k, **cs** a similar vector of $\cos\theta_k$, and **dz** a similar vector of layer thicknesses. Then equation (4) is implemented with the single line of Matlab code as: **x=sum ((sn.*dz)./cs)**. This expression uses the array multiplication and division operators (.* and ./) that perform element-by-element operations on matrices.[47]

The sum operator does the obvious summation. The same single line of code can trace M rays simultaneously if **sn**, **cs**, and **dz** are extended to matrices with one ray per column. Then, the resulting x is a row vector with one entry per ray. This operation is extremely fast and, for traveltimes, equation (3) can be implemented with similar efficiency. These ideas are implemented in shootray and form the basic computation module for v (z) raytracing.[47]

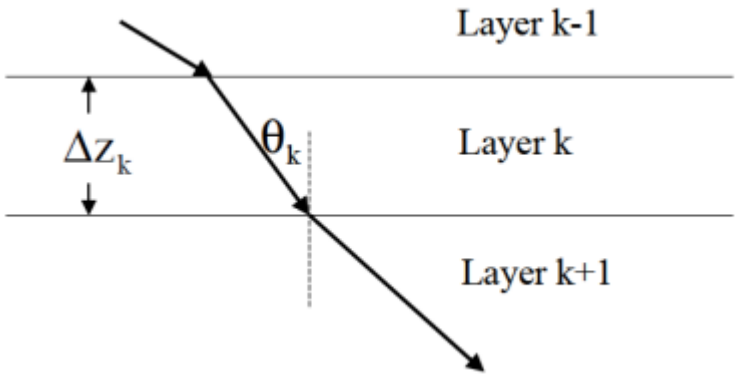

Figure IV. 2. Tracing a ray through a series of horizontal layers.

The procedure just described is known as .ray shooting. Because the starting point and direction of the ray are specified but the final position is not known until the calculation is completed. Often, it is desired to trace rays between two specific points such as a source and receiver, perhaps via a reflection at a specific depth. For general v (z), there is no known solution technique that solves this two-point raytracing problem in one step. Instead, an iterative procedure must be used. Suppose it is desired to trace a fan of rays from some fixed point x_1 at the top of layer 1 to a point x_2 at the bottom of layer N. The shootray procedure can be used to shoot a fan of M rays from x_1 that is estimated to bracket the point x_2. Assuming that $x_1 > x_2$, the fan can have extremal p values of $p_1 = 0$ and $p_M = v_{max}^{-1}$ = that, if it is indeed possible to trace a ray to x_2, will bracket x_2. Suppose it is found that rays p_k and p_{k+1} (of the fan of M rays,

kϵ ({1,2,.M-1}) bracket the point x_2 , then a new fan of M rays can be shot with p_k and p_{k+1} as the extremal ray parameters. This procedure can then be repeated as often as desired until a ray is found that comes within an arbitrary "capture radius" of x_2.

Thus the two-point problem of shooting a ray across of stack of layers can be solved to any desired precision. However, a solution is not guaranteed because there can be "shadow zones" where classical rays cannot penetrate. Matlab function traceray_pp uses the procedure just described to trace a reflection from a source at x_1 via a reflector at an arbitrary depth z_r to a receiver at x_2. The reflector depth need not be a layer boundary. Rather than trace a ray down to the bottom of a stack of N layers and then back up, an equivalent problem using 2N layers and one-way raytracing is formulated and solved (Figure IV. 3). If the reflector depth occurs within layer N, then that layer is reshaped to terminate at z_r. A stack of 2N layers is then formed by reversing the order of layers 1→N and placing them beneath layer N. That is, the new stack has the layer sequence numbers: 1,2, . N-1, N, N, N-1, . 2, 1. Then, the two-point procedure described in the preceding paragraph is performed to trace a ray from x_1 at the top of layer 1 to x_2 at the bottom of layer 2N. This ray will have the same traveltime and ray parameter as that which solves the original problem.[47]

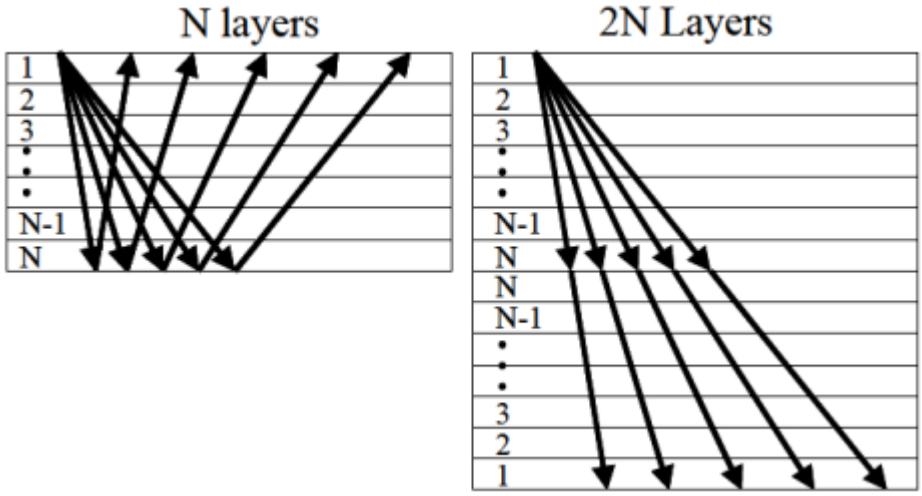

Figure IV. 3. Tracing a fan of rays down to a reflector and back up to receivers through N layers is a two-point issue. Tracing the rays straight through a stack of 2N layers is the equivalent solution.

A similar procedure is used by function traceray_ps to resolve the trace-a P-S reflection problem. The assignment of S-wave velocities to the second (inverted) stack of N layers in the

2N layer stack is the sole distinction. As a result, two velocity models—one each for P and S waves—must be provided. These models may have entirely distinct layer borders. The required P-S reflection problem may be solved by solving the two-point problem across the constructed 2N layer stack. By simply flipping the meaning of the P and S wave velocities, the same function may also trace an S-P reflection.

By simply changing the layer stack to only contain those layers that are actually traveled on the down and up legs, the functions traceray_pp and traceray_ps can both support sources and receivers at varying depths.

Function traceray uses this process to trace a general multimode through a layered medium. The multimode is described by a raycode that is a list of ordered pairs, (z_m ,i_m), where the depth at the start of a ray segment i_m is either 1 (for a P-wave) or 2 (for an S-wave). For example, the raycode [0, 1; 1000, 2; 500, 2; 1000, 1; 0, 1] indicates a P-S-S-P mode. It is a P-wave from 0 to 1000 m, an S-wave from 1000 to 500 m, and S-wave from 500 to 1000 m, and finally a P-wave from 1000 to 0 m. (Note that the final value of i_m is meaningless.) This problem is solved with the same stratagem as before by building an equivalent stack of layers and tracing rays through it one-way. In this way, a completely arbitrary multimode can be traced through a v (z) medium.[48]

We will go over several examples for the v (z) raytrace capability in this section. All of them were pulled straight out of the m-file raytrace_demo that came with the CREWES software package. Therefore, demo may thus be used to replicate any of them.

For the velocity model shown in (Figure IV. 4), consider the task of tracing P-P and P-S reflections from a target at z_s=3000 m depth. This velocity model includes a 200m thick water layer at the top so OBC geometry is adopted. Let the source be at z_{src}=50 m and the receivers on the ocean bottom at z_{rec}=200 m. Also let the receivers are at offsets xoff= [1000, 1100 1200….3000] for a total of 21 receivers.[48]

The Matlab code needed to trace the P-P reflection and create Figure (IV. 6) is then displayed in Figure (IV. 5). Because it was chosen to provide all of the code needed to generate the fully annotated plot, the code sample is quite complicated. On the third line, the raytracing is really carried out. The P-wave velocity and layer depths are the first two inputs to traceray_pp. The

recording geometry is specified by the following four inputs, and the next six numerical values are, in order,: The parameters include the capture radius (10 meters), the number of iterations to attempt before assuming nonconvergence (10), the flag indicating that the final times are to be improved by linear interpolation between the captured ray and the next closest ray, the request to plot the raypaths in the current figure window, and the information about failed rays to be printed on the screen. (You may use Matlab to view a detailed explanation of these settings by typing "help traceray_pp‖ at the command line.) A vector of traveltimes (t) and a vector of ray parameters (p) are the variables that traceray_pp returns. In line 12 of this example, the journey times are plotted against offset.

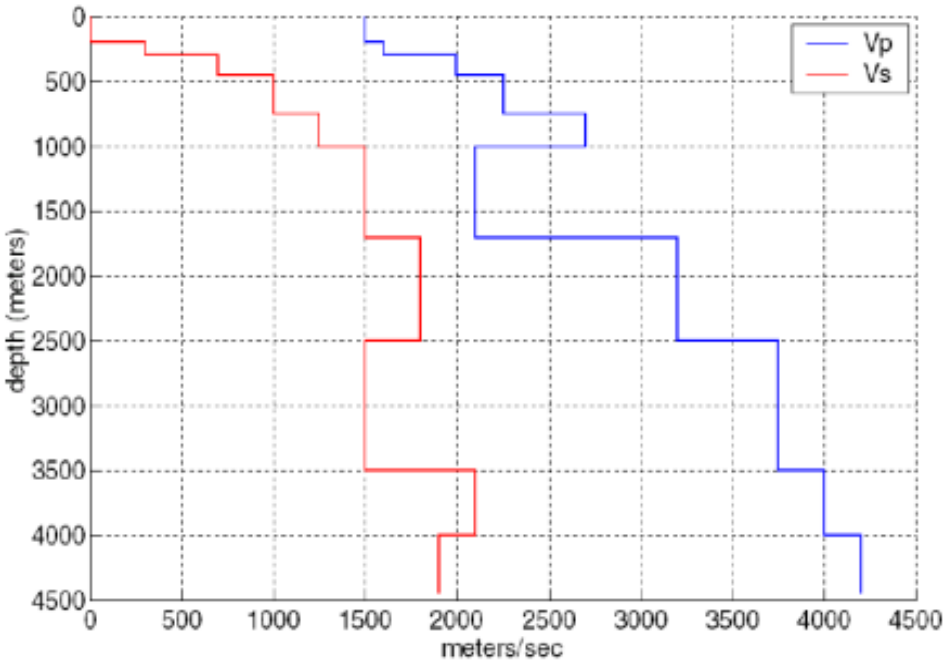

Figure IV. 4. The P-wave velocity curve (right) and S-wave velocity curve (left) of a basic layered medium are depicted. Take note of the upper 200 m water layer.

The Python code

```
import numpy as np
import matplotlib.pyplot as plt
def traceray_pp(vp, zp, zsrc, zrec, zd, xoff, param1, param2, param3, param4,
param5, param6):
    t = np.random.rand(len(xoff))
    p = np.random.rand(len(xoff))
    return t, p
vp = np.array([1, 2, 3])
```

```
zp = np.array([1, 2, 3])
zsrc = 100
zrec = 200
zd = 300
xoff = np.linspace(0, 3000, 100)
t, p = traceray_pp(vp, zp, zsrc, zrec, zd, xoff, 10, -1, 10, 1, 1, 2)
fig, (ax1, ax2) = plt.subplots(2, 1, figsize=(10, 8))
ax1.plot(xoff, zrec * np.ones_like(xoff), 'bv', label='Receiver')
ax1.plot(0, zsrc, 'r*', label='Source')
ax1.set_title('OBC simulation, P-P mode, water depth 200 meters')
ax1.set_xlabel('meters')
ax1.set_ylabel('meters')
ax1.grid(True)
ax1.legend()
ax2.plot(xoff, t)
ax2.set_xlabel('meters')
ax2.set_ylabel('seconds')
ax2.grid(True)
ax2.set_xlim([0, 3000])
plt.tight_layout()
plt.show()
```

```
figure;subplot(2,1,1);flipy
%Trace P-P rays and plot in upper subplot
[t,p]=traceray_pp(vp,zp,zsrc,zrec,zd,xoff,10,-1,10,1,1,2);
%put source and receiver markers
line(xoff,zrec*ones(size(xoff)),'color','b','linestyle','none','marker','v')
line(0,zsrc,'color','r','linestyle','none','marker','*')
%annotate plot
title('OBC simulation, P-P mode, water depth 200 meters')
xlabel('meters');ylabel('meters');grid
%plot traveltime versus offset in lower subplot
subplot(2,1,2);flipy;
plot(xoff,t);grid;xlabel('meters');ylabel('seconds')
xlim([0 3000])
```

Figure IV. 5. This Matlab and Python code sequence creates Figure (IV. 6) by tracing P-P rays using the velocity model in Figure (IV. 4).

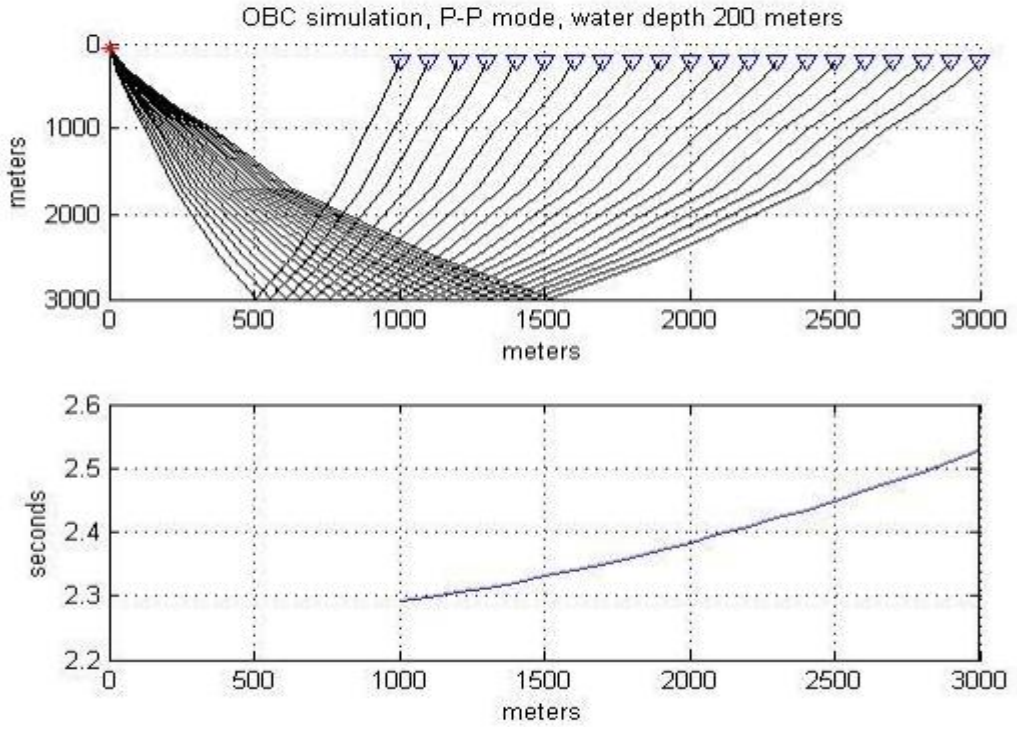

Figure IV. 6. This figure is produced by executing the code of Figure (IV. 5) and utilizing Figure (IV. 4) velocity model. The actual raypaths, as drawn by traceray_pp in line 3, are shown in the top frame. The traveltimes are displayed against offset in the bottom frame.

The usage of traceray_ps to simulate the P-S reflection that corresponds to the P-P reflection that was just covered is shown in the code snippet shown in Figure (IV. 7). Line 3 plots and traces the rays in the upper part of Figure (IV. 8) as it did previously. With two extra input parameters in the third and fourth positions to define the S-wave velocity structure, the syntax for calling traceray_ps is much the same as that of traceray_pp.

The Python code

```
import numpy as np
import matplotlib.pyplot as plt

def traceray_ps(vp, zp, vs, zs, zsrc, zrec, zd, xoff, param1, param2, param3,
param4, param5, param6):
    # Dummy implementation for example purposes
    t = np.random.rand(len(xoff))
    p = np.random.rand(len(xoff))
    return t, p
```

```
vp = np.array([1, 2, 3])  # P-wave velocities
zp = np.array([1, 2, 3])  # Depths for P-wave velocities
vs = np.array([1, 2, 3])  # S-wave velocities
zs = np.array([1, 2, 3])  # Depths for S-wave velocities
zsrc = 100  # Source depth
zrec = 200  # Receiver depth
zd = 300  # Depth difference
xoff = np.linspace(0, 3000, 100)  # Offsets

t, p = traceray_ps(vp, zp, vs, zs, zsrc, zrec, zd, xoff, 10, -1, 10, 1, 1, 2)

fig, (ax1, ax2) = plt.subplots(2, 1, figsize=(10, 8))

ax1.plot(xoff, zrec * np.ones_like(xoff), 'bv', label='Receiver')
ax1.plot(0, zsrc, 'r*', label='Source')
ax1.set_title('OBC simulation, P-S mode, water depth 200 meters')
ax1.set_xlabel('meters')
ax1.set_ylabel('meters')
ax1.grid(True)
ax1.legend()

ax2.plot(xoff, t)
ax2.set_xlabel('meters')
ax2.set_ylabel('seconds')
ax2.grid(True)
ax2.set_xlim([0, 3000])

plt.tight_layout()
plt.show()
```

```
figure;subplot(2,1,1);flipy
%Trace P-S rays and plot in upper subplot
[t,p]=traceray_ps(vp,zp,vs,zs,zsrc,zrec,zd,xoff,10,-1,10,1,1,2);
%put source and receiver markers
line(xoff,zrec*ones(size(xoff)),'color','b','linestyle','none','marker','v')
line(0,zsrc,'color','r','linestyle','none','marker','*')
%annotate plot
title('OBC simulation, P-S mode, water depth 200 meters')
grid;xlabel('meters');ylabel('meters');
%plot traveltime versus offset in lower subplot
subplot(2,1,2);flipy;
plot(xoff,t);grid;xlabel('meters');ylabel('seconds')
xlim([0 3000])
```

Figure IV. 7. This Matlab code sequence creates Figure (IV. 8) by tracing P-S rays using the velocity model from Figure (IV. 4).

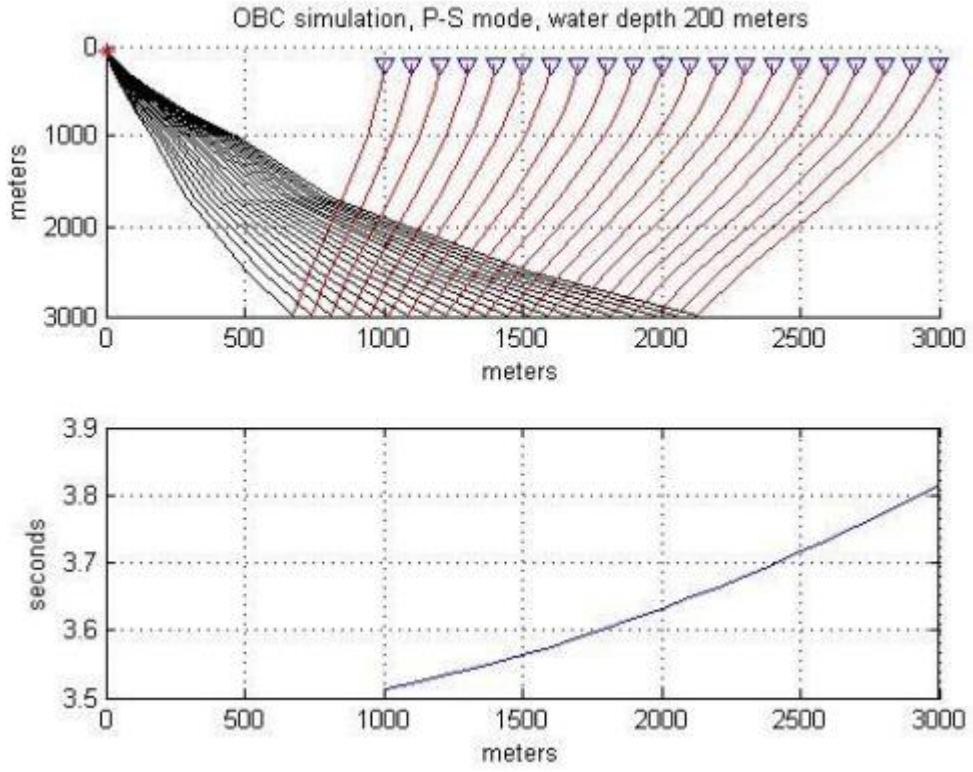

Figure IV. 8. This figure is produced by running the code of Figure (IV. 7) and utilizing Figure (IV. 4) velocity model. The actual raypaths, as drawn by traceray_ps in line 3, are shown in the top frame. The traveltimes are displayed against offset in the bottom frame.

Next, consider the task of calculating P-P and P-S reflections for an offset VSP. Let the source be at the surface and offset 1500 m from the well. The receivers are in the well from 500 to 2500 m at 100 m intervals. Let the P-wave velocity structure be given by vp(z) =1800 + .6z with vp/vs=2. The code to model a P-P arrival from a reflection at zd=3000 m is shown in Figure 09 and the resulting plot is in Figure (IV. 10). Line 2 creates the velocity model for both P and S and line 5 preallocates a vector to hold the traveltimes. Lines 7-9 loop over receiver depth and call traceray_pp for each receiver. As before, traceray_pp draws the raypaths in the upper part of Figure (IV. 10) while the traveltimes are plotted in the lower part of the same Figure by the command on line 18.[49]

The code presented in Figure (IV. 11) draws the P-S reflection for the VSP shape. The sole distinction between this method and the P-P instance is that traceray_ps, rather than traceray_pp, is called in the loop. Writing an appropriate loop may fit the majority of recording geometries.

For instance, all that is needed for a VSP with a non-vertical borehole is a change in both receiver coordinates (x, z) for every iteration. It is possible to conduct Crosswell experiments by varying the depths of the source and receiver at each repetition.

The Python code

```
import numpy as np
import matplotlib.pyplot as plt

# Assuming traceray_pp is a function defined somewhere else
def traceray_pp(vp, zp, zsrc, zrec, zd, xoff, param1, param2, param3, param4,
param5, param6):
    # Dummy implementation for example purposes
    t = np.random.rand()  # Replace with actual travel time calculation
    p = np.random.rand()  # Replace with actual ray parameter calculation
    return t, p

# Build the velocity model
zp = np.arange(0, 4001, 10)
vp = 1800 + 0.6 * zp
vs = 0.5 * vp
zs = zp

# P-P offset VSP
fig, (ax1, ax2) = plt.subplots(2, 1, figsize=(10, 8))

zrec = zp  # Assuming zrec is the same as zp for this example
t = np.zeros(len(zrec))  # Preallocate t
xoff = np.linspace(0, 3000, 100)  # Define xoff
zsrc = 100  # Source depth, assumed value
zd = 300  # Depth difference, assumed value

for kk in range(len(zrec)):
    t[kk], p = traceray_pp(vp, zp, zsrc, zrec[kk], zd, xoff, 10, -2, 30, 1, 1,
2)

ax1.plot(xoff, zrec, 'bv', label='Receiver')
ax1.plot(0, zsrc, 'r*', label='Source')
ax1.set_title('VSP Vertical gradient simulation, P-P mode')
ax1.set_xlabel('meters')
ax1.set_ylabel('meters')
ax1.grid(True)
ax1.legend()
```

```
ax2.plot(t, zrec)
ax2.set_xlabel('seconds')
ax2.set_ylabel('depth (meters)')
ax2.grid(True)
ax2.set_ylim([0, 3000])

plt.tight_layout()
```

```
%build the velocity model
zp=0:10:4000;vp=1800+.6*zp;vs=.5*vp;zs=zp;
%P-P offset VSP
figure;subplot(2,1,1);flipy
t=zeros(size(zrec)); %preallocate t
%loop over receiver depth
for kk=1:length(zrec);
    [t(kk),p]=traceray_pp(vp,zp,zsrc,zrec(kk),zd,xoff,10,-2,30,1,1,2);
end
   %draw source and receiver symbols
   line(xoff,zrec,'color','b','linestyle','none','marker','v')
   line(0,zsrc,'color','r','linestyle','none','marker','*')
   %annotation
   title([' VSP Vertical gradient simulation, P-P mode '])
   grid;xlabel('meters');ylabel('meters');
   %plot traveltime versus depth
   subplot(2,1,2);
   plot(t,zrec);xlabel('seconds');ylabel('depth (meters)')
   grid;flipy;ylim([0 3000])
```

Figure IV. 9. A P-P reflection for offset VSP geometry is modeled by this code.

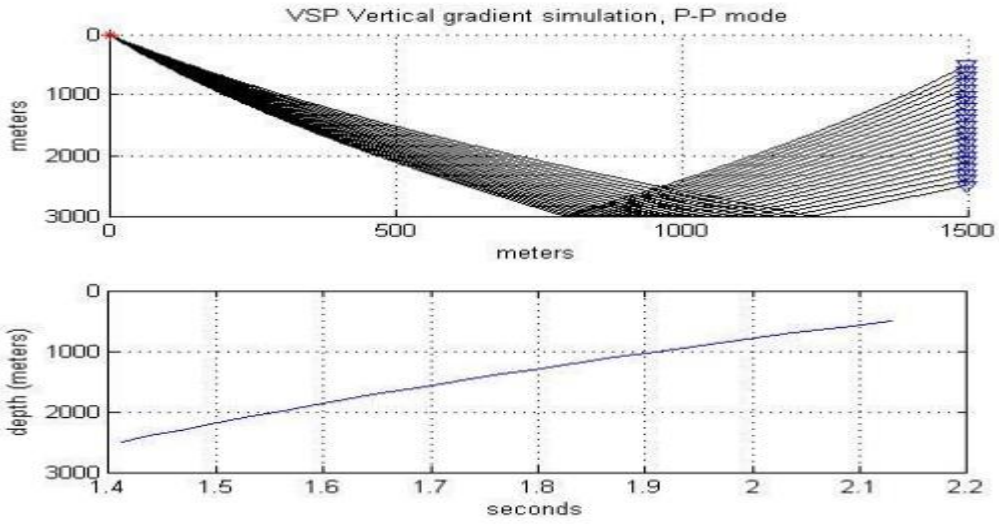

Figure IV. 10. An offset VSP recording's P-P reflection is displayed. The code in Figure (IV. 9) calculated the traveltimes (bottom) and raypaths (top).

The Python code

```
import numpy as np
import matplotlib.pyplot as plt

# Assuming vp, zp, vs, zs, zsrc, zrec, zd, xoff are defined elsewhere in your
code

# Function definition placeholder for traceray_ps
def traceray_ps(vp, zp, vs, zs, zsrc, zrec, zd, xoff, arg1, arg2, arg3, arg4,
arg5, arg6):
    # This is a placeholder function. Replace it with the actual
implementation.
    t = 0  # Example value
    p = 0  # Example value
    return t, p

# P-S offset VSP
plt.figure()

# Subplot 1
plt.subplot(2, 1, 1)
plt.gca().invert_yaxis()  # flipy equivalent

t = np.zeros(len(zrec))

# Preallocate t and compute travel times
for kk in range(len(zrec)):
    t[kk], p = traceray_ps(vp, zp, vs, zs, zsrc, zrec[kk], zd, xoff, 10, -2,
30, 1, 1, 2)

# Draw source and receiver symbols
plt.plot(xoff, zrec, 'bv', label='Receiver')
plt.plot(0, zsrc, 'r*', label='Source')

# Annotation
plt.title('VSP Vertical gradient simulation, P-S mode')
plt.grid(True)
plt.xlabel('meters')
plt.ylabel('meters')
plt.legend()

# Subplot 2
plt.subplot(2, 1, 2)
plt.plot(t, zrec)
```

```
plt.xlabel('seconds')
plt.ylabel('depth (meters)')
plt.grid(True)
plt.gca().invert_yaxis()  # flipy equivalent
plt.ylim([0, 3000])

plt.show()
```

```
%P-S offset VSP
figure;subplot(2,1,1);flipy;
t=zeros(size(zrec)); %preallocate t
for kk=1:length(zrec);
    [t(kk),p]=traceray_ps(vp,zp,vs,zs,zsrc,zrec(kk),zd,xoff,10,-2,30,1,1,2);
end
   %draw source and receiver symbols
   line(xoff,zrec,'color','b','linestyle','none','marker','v')
   line(0,zsrc,'color','r','linestyle','none','marker','*')
   %annotation
   title([' VSP Vertical gradient simulation, P-S mode '])
   grid;xlabel('meters');ylabel('meters');
   %plot traveltime versus depth
   subplot(2,1,2);
   plot(t,zrec);xlabel('seconds');ylabel('depth (meters)')
   grid;flipy;ylim([0 3000])
```

Figure IV. 11. This code simulates an offset VSP's P-S reflection.

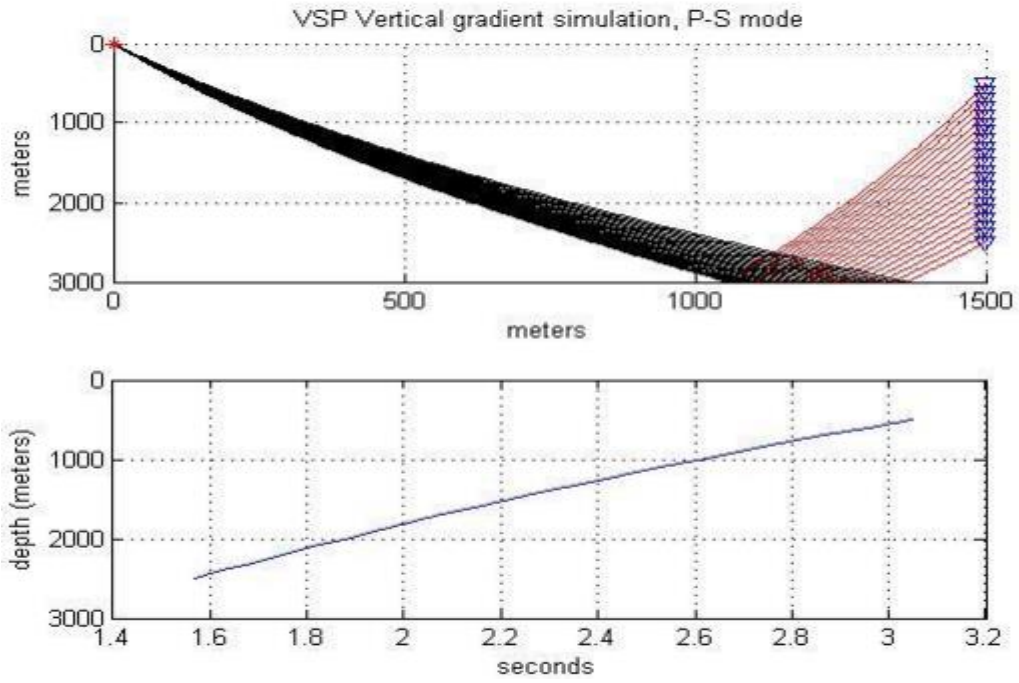

Figure IV. 12. For an offset VSP, a P-S reflection is displayed.

Finally, let's look at the challenge of tracing a complicated multimode. Put another way, let the ray to oscillate between P and S and bounce up and down between different depths. The most versatile of the three trace_ray routines, traceray_pp, makes this feasible. All of them employ the previously mentioned process, which creates an analogous stack of layers and moves the beam through it in a single direction. For the purpose of tracing primary (single bounce) reflections from a single source to a number of receivers, the functions traceray_pp and traceray_ps are optimized. A ray that experiences any number of bounces and mode changes may be traced using function traceray, which is significantly more versatile. As previously mentioned, a ray code describes the ray. The raycode for an M-bounce multiple is a matrix consisting of M+2 rows and 2 columns. For the start and finish depths, there are two more rows.

The list of depths the ray is to travel is in the first column, and the list of flags designating the P or S mode is in the second. The depths in the list match either mode-conversion or reflection points, or both. There is no need that these depth values relate to the velocity model layers. The raycode (lines 2-3) for a complex multi-bounce P wave with zero depth and 300 m depth is seen in Figure (IV. 13). To input the raycode, just insert a series of numbers paired with a semicolon (row separator from Matlab). Tracery_pp is called with a list of receiver offsets ranging from 1000 to 3000 m on line 7. Although the P and S-wave velocity models are not demonstrated, they are created using the same linear gradient medium as the VSP example in Figure (IV. 9). [49]

The majority of the parameters in traceray_ray have previously been covered and are comparable to those in traceray_ps. Nevertheless, since source and receiver depth are included in the raycode, no parameters are available for them.

The Python code

```
import numpy as np
import matplotlib.pyplot as plt

# Define the ray code for a pure P multiple
raycode = np.array([
    [0, 1], [1500, 1], [1300, 1], [2000, 1], [1800, 1],
    [3000, 1], [2000, 1], [2300, 1], [1000, 1], [1500, 1],
    [300, 11]
])
```

```
# Function placeholder for traceray
def traceray(vp, zp, vs, zs, raycode, xoff, arg1, arg2, arg3, arg4, arg5,
arg6):
    # This is a placeholder function. Replace it with the actual
implementation.
    t = np.zeros_like(xoff)  # Example array of zeros
    p = np.zeros_like(xoff)  # Example array of zeros
    return t, p

# Trace the rays
xoff = np.arange(1000, 3100, 100)
t, p = traceray(vp, zp, vs, zs, raycode, xoff, 10, -1, 10, 1, 1, 2)

# Create figure and subplot 1
plt.figure()
plt.subplot(2, 1, 1)
plt.gca().invert_yaxis()  # flipy equivalent

# Source and receiver symbols
plt.plot(xoff, raycode[-1, 0] * np.ones_like(xoff), 'bv', label='Receiver')
plt.plot(0, raycode[0, 0], 'r*', label='Source')

# Annotate
plt.title('A P-P-P-P-P-P-P-P-P-P mode in vertical gradient media')
plt.grid(True)

# Plot traveltimes
plt.subplot(2, 1, 2)
plt.gca().invert_yaxis()  # flipy equivalent
plt.plot(xoff, t)
plt.grid(True)
plt.xlabel('offset')
plt.ylabel('time')
plt.xlim([0, 3000])

plt.show()
```

```
%define the ray code for a pure P multiple
raycode=[0 1;1500 1;1300 1;2000 1;1800 1;3000 1;2000 1;2300 1;1000 1;1500 1; 300 1];
figure;subplot(2,1,1);flipy
%trace the rays
xoff=1000:100:3000;
[t,p]=traceray(vp,zp,vs,zs,raycode,xoff,10,-1,10,1,1,2);
%Source and receiver symbols
line(xoff,raycode(end,1)*ones(size(xoff)),'color','b','linestyle','none','marker','v')
line(0,raycode(1,1),'color','r','linestyle','none','marker','*')
%annotate
title('A P-P-P-P-P-P-P-P-P-P mode in vertical gradient media');grid
%Plot traveltimes
subplot(2,1,2);flipy
plot(xoff,t);grid;xlabel('offset');ylabel('time')
xlim([0 3000])
```

Figure IV. 13. This code sample demonstrates how to use traceray_pp to produce a complex multiple that always stays a P-wave.

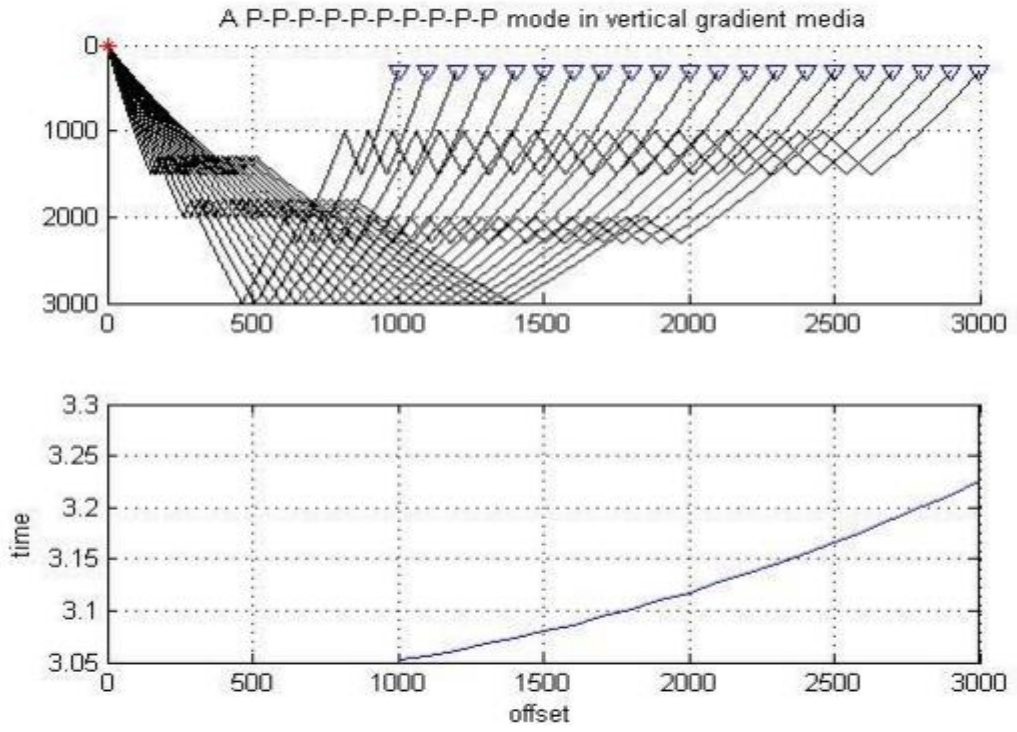

Figure IV. 14. The difficult multiple's raypath, which stays a P-wave on each bounce, is displayed at the top.

The Python code

```
import numpy as np
import matplotlib.pyplot as plt
```

```
# Define the ray code for a P-S multimode
raycode = np.array([
    [0, 1], [1500, 2], [1300, 2], [2000, 2], [1800, 2],
    [3000, 1], [2000, 1], [2300, 1], [1000, 1], [1500, 2],
    [300, 1]
])

# Function placeholder for traceray
def traceray(vp, zp, vs, zs, raycode, xoff, arg1, arg2, arg3, arg4, arg5,
arg6):
    # This is a placeholder function. Replace it with the actual
implementation.
    t = np.zeros_like(xoff)  # Example array of zeros
    p = np.zeros_like(xoff)  # Example array of zeros
    return t, p

# Trace the rays
xoff = np.arange(1000, 3100, 100)
t, p = traceray(vp, zp, vs, zs, raycode, xoff, 10, -1, 10, 1, 1, 2)

# Create figure and subplot 1
plt.figure()
plt.subplot(2, 1, 1)
plt.gca().invert_yaxis()  # flipy equivalent

# Source and receiver symbols
plt.plot(xoff, raycode[-1, 0] * np.ones_like(xoff), 'bv', label='Receiver')
plt.plot(0, raycode[0, 0], 'r*', label='Source')

# Annotate
plt.title('A P-S-S-S-S-P-P-P-P-S mode in vertical gradient media')
plt.grid(True)

# Plot traveltimes
plt.subplot(2, 1, 2)
plt.gca().invert_yaxis()  # flipy equivalent
plt.plot(xoff, t)
plt.grid(True)
plt.xlabel('offset')
plt.ylabel('time')
plt.xlim([0, 3000])

plt.show()
```

```
%define the ray code for a P-S multimode
raycode=[0 1;1500 2;1300 2;2000 2;1800 2;3000 1;2000 1;2300 1;1000 1;1500 2; 300 1];
figure;subplot(2,1,1);flipy
%trace the rays
xoff=1000:100:3000;
[t,p]=traceray(vp,zp,vs,zs,raycode,xoff,10,-1,10,1,1,2);
%Source and receiver symbols
line(xoff,raycode(end,1)*ones(size(xoff)),'color','b','linestyle','none','marker','v')
line(0,raycode(1,1),'color','r','linestyle','none','marker','*')
%annotate
title('A P-S-S-S-S-S-P-P-P-P-P-S mode in vertical gradient media');grid
%Plot traveltimes
subplot(2,1,2);flipy
plot(xoff,t);grid;xlabel('offset');ylabel('time')
xlim([0 3000])
```

Figure IV. 15. With the exception of the raycode's requests for a P-S conversion at 1300 m, an S-P conversion at 3000 m, and another P-S conversion at 1500 m (on the up leg), this code generates a multimode that resembles Figure (IV. 14).

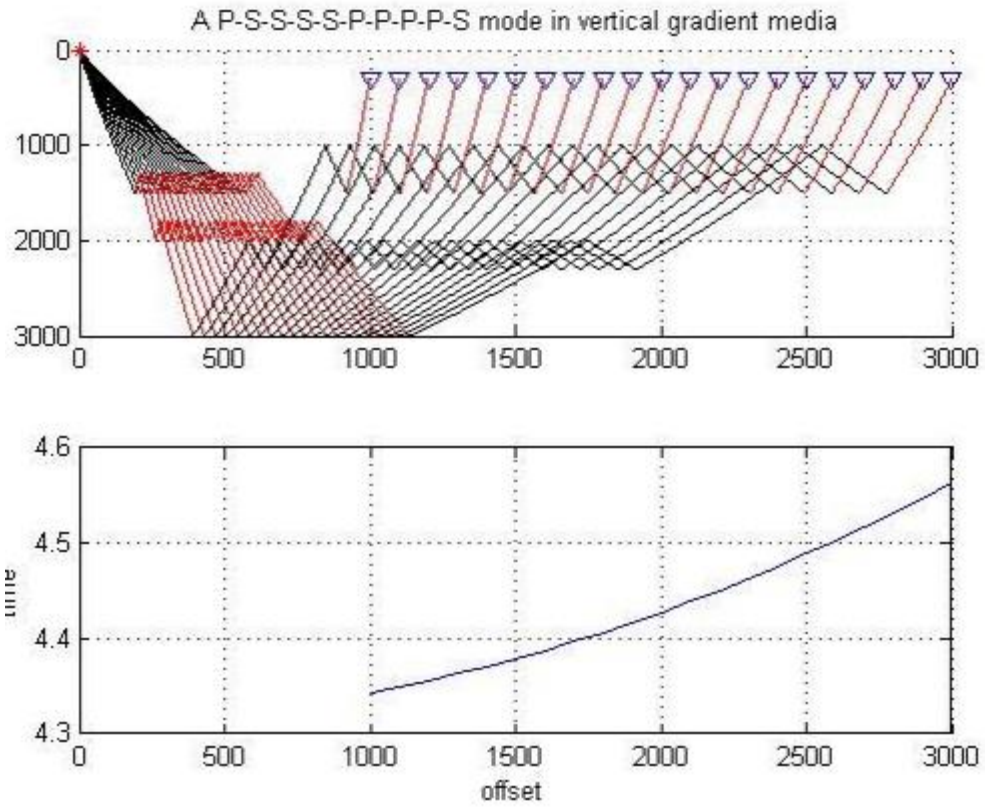

Figure IV. 16. The raypath generated by the code snippet in Figure (IV. 15) for an intricate P-S multimode is displayed (top).

5. GemPy Toolbox

An open-source Python software called GemPy offers a foundation for modeling geology in three dimensions. It is intended to assist earth scientists, such as geologists, in developing geological models that will enable them to investigate the Earth's underlying structure. The package is constructed on top of widely used scientific libraries, including Matplotlib, SciPy, and NumPy. [49]

GemPy models an area's geological characteristics using a combination of mathematical techniques and geological concepts. By specifying the form, direction, and characteristics of various geological units, such as rock layers, faults, and other geological features, users of the program may generate geological models.

The capacity of GemPy to build intricate, multi-layered geological models is one of its primary characteristics. Faults and other geological features that may cut through layers of rock, as well as several layers of rock with different qualities, are all handled by the program. In addition, GemPy offers a number of visualization tools that let users see and work with their models in three dimensions. This includes the capacity to produce isosurfaces, inspect cross-sections, and make accurate geological maps.[49]

5.1 Principles of Geological Modeling using GemPy

Importing GemPy

```
import gempy as gp

# Importing auxiliary libraries
import numpy as np
import pandas as pd
import matplotlib.pyplot as plt
import os

# Setting options
np.random.seed(1515)
pd.set_option('precision', 2)
```

Figure IV. 17. Importing GemPy.

Importing and creating a set of input data

GemPy stores the data needed to create models in Python objects. The main categories of data are:

- Surface_points
- Orientations
- Grid
- Surfaces
- Series
- Additional data
- Faults

The bulk of data may also be produced using CSV (comma-separated values) files, which are files that include raw data. Spreadsheet applications such as Microsoft Excel and OpenOffice Calc, or the simple export of model data from another tool such as GeoModeller, can be used to produce these files.

In this case, all of the input data is created by importing such CSV files. The input_data subdirectory in the GemPy root folder contains these example files. The data includes orientation measurements and the location values of all surface points in x, y, and z. In the latter, polarity, azimuth, and poles are also discussed. Moreover, surface points are given a formation. This may be a lithological unit like "sandstone" or a structural component like a "main fault". It is important to remember that in GemPy, interface position points denote a layer's bottom. Such sites require the definition of a suitable inverted orientation measurement in order to make them resemble the top of a formation (for example, during an intrusion simulation).

```
                                "simple_fault_model_points.csv",
            default_values=True)
```

Out:

```
Active grids: ['regular']

Simple_Exemple  2023-05-02 16:26
```

```
geo_model.surfaces
```

As we construct our Data from CSV-files, we have to provide the real extent of our model in x, y, and z as well as the necessary resolution for each axis. This resolution will dictate how many voxels are used in the modeling process. We employ a medium resolution of 50x50x50, or 125,000 voxels, in this instance.

The scope of the model should be chosen to encompass all relevant data in a typical region. As the voxels in our model are prisms rather than cubes, the resolution and extent may vary. We do not recommend going much higher than 100 cells in each direction (1,000,000 voxels) due to the fact that greater resolutions will demand more processing resources. [49]

```
geo_model = gp.create_model('Simple_Exemple')

data_path = 'https://raw.githubusercontent.com/cgre-aachen/gempy_data/master/'
# Importing the data from CSV-files and setting extent and resolution
gp.init_data(geo_model, [0, 2000., 0, 2000., 0, 750.], [50, 50, 50],
             path_o=data_path + "/data/input_data/getting_started/"
                               "simple_fault_model_orientations.csv",
             path_i=data_path + "/data/input_data/getting_started/"
```

	Surface	Series	Order_surface	Color	Id
0	Shale	Default series	**1**	#13436F	**1**
1	Sandstone_1	Default series	**2**	#71C022	**2**
2	Silstone	Default series	**3**	#9FEAFF	**3**
3	Sandstone_2	Default series	**4**	#1B5F9D	**4**
4	Main_Fault	Default series	**5**	#6A6B8C	**5**
5	Basement	Basement	**1**	#F2B55C	**6**

The command get_data may then be used to list the input data. Keep in mind that the sequence of formations and their corresponding assignment to series remain wholly discretionary. This will be fixed in the next.[49]

```
gp.get_data(geo_model, 'orientations').head()
```

	X	Y	Z	G_x	G_y	G_z	Smooth	Surface
0	1000	1000	300	0.32	$1e^{-12}$	0.95	0.01	Shale
1	400	1000	420	0.32	$1e^{-12}$	0.95	0.01	Sandstone_2
2	500	1000	300	-0.95	$1e^{-12}$	0.32	0.01	Main_Fault

Our goal is to have our geological units arranged according to age. Such order may be provided, for example, by a stratigraphic depositional sequence, unconformities brought about by erosion, or other lithological genesis processes like igneous intrusions. Our model's shortcomings must be disclosed in a comparable age-related order. The GemPy method set_series may be used to assign formations to different sequential series by utilizing a declaration in a Python dictionary.[49]

The sample model consists of one primary normal fault that displaces the four main layers, together with an underlying basement that GemPy automatically generates. These layer formations can be assigned to a single series named Strat_Series‖, assuming a straightforward stratigraphy in which each younger unit was deposited over the underlying older one. As the first key element in the set_series dictionary, we declare a corresponding ―Fault_Series‖ for the defect. These series might have any other names, but the names in the input data must be used to refer to the formations.

```
geo_model.surfaces
```

	Surface	Series	Order_surface	Color	Id
0	Shale	Default series	**1**	#13436F	**1**
1	Sandstone_1	Default series	**2**	#71C022	**2**
2	Silstone	Default series	**3**	#9FEAFF	**3**
3	Sandstone_2	Default series	**4**	#1B5F9D	**4**
4	Main_Fault	Default series	**5**	#6A6B8C	**5**
5	Basement	Basement	**1**	#F2B55C	**6**

```
gp.map_stack_to_surfaces(geo_model,
                         {"Fault_Series": 'Main_Fault',
                          "Strat_Series": ('Sandstone_2', 'Siltstone',
                                           'Shale', 'Sandstone_1', 'basement')},
                         remove_unused_series=True)
```

	Surface	Series	Order_surface	Color	Id
4	Main_Fault	Fault_Series	**1**	#6A6B8C	**1**
0	Shale	Strat_Series	**1**	#13436F	**2**
1	Sandstone_1	Strat_Series	**2**	#71C022	**3**
2	Silstone	Strat_Series	**3**	#9FEAFF	**4**
3	Sandstone_2	Strat_Series	**4**	#1B5F9D	**5**
5	Basement	Strat_Series	**5**	#F2B55C	**6**

```
geo_model.surfaces
```

	Surface	Series	Order_surface	Color	Id
4	Main_Fault	Fault Series	**1**	#6A6B8C	**1**
0	Shale	Strat_Series	**1**	#13436F	**2**
1	Sandstone_1	Strat_Series	**2**	#71C022	**3**
2	Silstone	Strat_Series	**3**	#9FEAFF	**4**
3	Sandstone_2	Strat_Series	**4**	#1B5F9D	**5**
5	Basement	Strat_Series	**5**	#F2B55C	**6**

```
geo_model.stack
```

	Order_series	BottomRelation	isActive	isFault	isFinite
Fault_Series	1	Erosion	True	False	False
Strat_Series	2	Erosion	True	False	False

```
geo_model.set_is_fault(['Fault_Series'])
```

Out:

```
Fault colors changed. If you do not like this behavior, set change_color to False.
```

	Order_series	BottomRelation	isActive	isFault	isFinite
Fault_Series	1	Fault	True	True	False
Strat_Series	2	Erosion	True	False	False

```
geo_model.faults.faults_relations_df
```

	Fault_Series	Strat_Series
Fault_Series	False	True
Strat_Series	False	False

```
geo_model.faults
```

	Order_series	BottomRelation	isActive	isFault	isFinite
Fault_Series	1	Fault	True	True	False
Strat_Series	2	Erosion	True	False	False

```
geo_model.faults.faults_relations_df
```

	Fault_Series	Strat_Series
Fault_Series	False	True
Strat_Series	False	False

Transmission of data depending on data input

The "geo_model" input data we used to develop our model has all the information we need. We may obtain a variety of data kinds by utilizing the APIs or gp.get_data.

For example, we may use the following to get our modeling grid's coordinates:

```
geo_model.grid
```

```
Out:
Grid Object. Values:
array([[  20. ,   20. ,    7.5],
       [  20. ,   20. ,   22.5],
       [  20. ,   20. ,   37.5],
       ...,
       [1980. , 1980. ,  712.5],
       [1980. , 1980. ,  727.5],
       [1980. , 1980. ,  742.5]])
```

As previously stated, the interpolation of two types of data—surface_points and orientation measurements—is the foundation of GemPy's fundamental algorithm. The function get_data was previously added. Additionally, you may declare the string attribute dtype‖ to be either 'orientations' or'surface_points' (interfaces) to indicate the type of data you wish to call.

Interfaces Dataframe

```
gp.get_data(geo_model, 'surface_points').head()
```

	X	Y	Z	Smooth	Surface
52	700	1000	300.0	$2.00e^{-6}$	Main_Fault
53	600	1000	200.0	$2.00e^{-6}$	Main_Fault
54	500	1000	100.0	$2.00e^{-6}$	Main_Fault
55	1000	1000	600.0	$2.00e^{-6}$	Main_Fault
56	1100	1000	700.0	$2.00e^{-6}$	Main_Fault

Orientations Dataframe

```
gp.get_data(geo_model, 'orientations')
```

	X	Y	Z	G_x	G_y	G_z	Smooth	Surface
2	500	1000	300	-0.95	$1.00e^{-12}$	0.32	0.01	Main_Fault
0	1000	1000	300	0.32	$1.00e^{-12}$	0.95	0.01	Shale
1	400	1000	420	0.32	$1.00e^{-12}$	0.95	0.01	Sandstone_2

We notice that now all surfaces have been assigned to a series and are displayed in the correct order (from young to old).

Visualizing input data

It also displays the data that we entered. For example, this may be useful to confirm that all measurements and points are defined as intended. We may project our data points in two dimensions onto a plane in any direction (x, y, or z) by using the plot_data function.

```
plot = gp.plot_2d(geo_model, show_lith=False, show_boundaries=False)
plt.show()
```

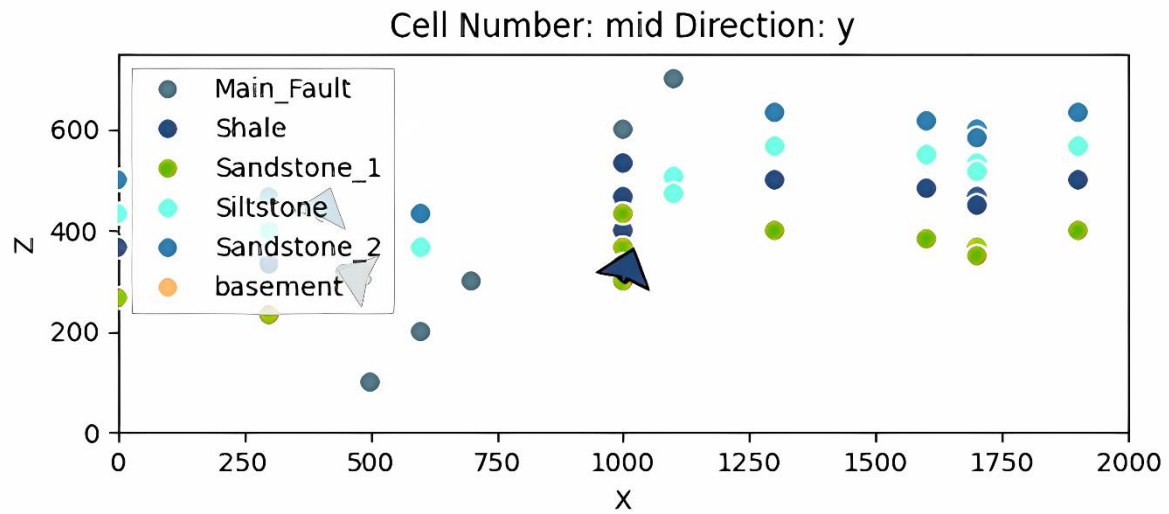

Using plot_data_3D, we can also view this data in three dimensions. For direct 3D visualization in GemPy, the Visualization Toolkit (VTK) has to be installed. GemPy offers interactive 3D charts. We can now drag and drop any measurement or data point thanks to this.

Particularly useful are VTK's perpendicular axis views for moving points solely on a designated 2D plane. After that, any changes made will be permanently stored in the "InputData" dataframe. Then, in order to reset our data points, we have to reload our original input data. A new window with a 3D interactive depiction of our data will appear when you execute the cell below.

```
gpv = gp.plot_3d(geo_model, image=False, plotter_type='basic')
```

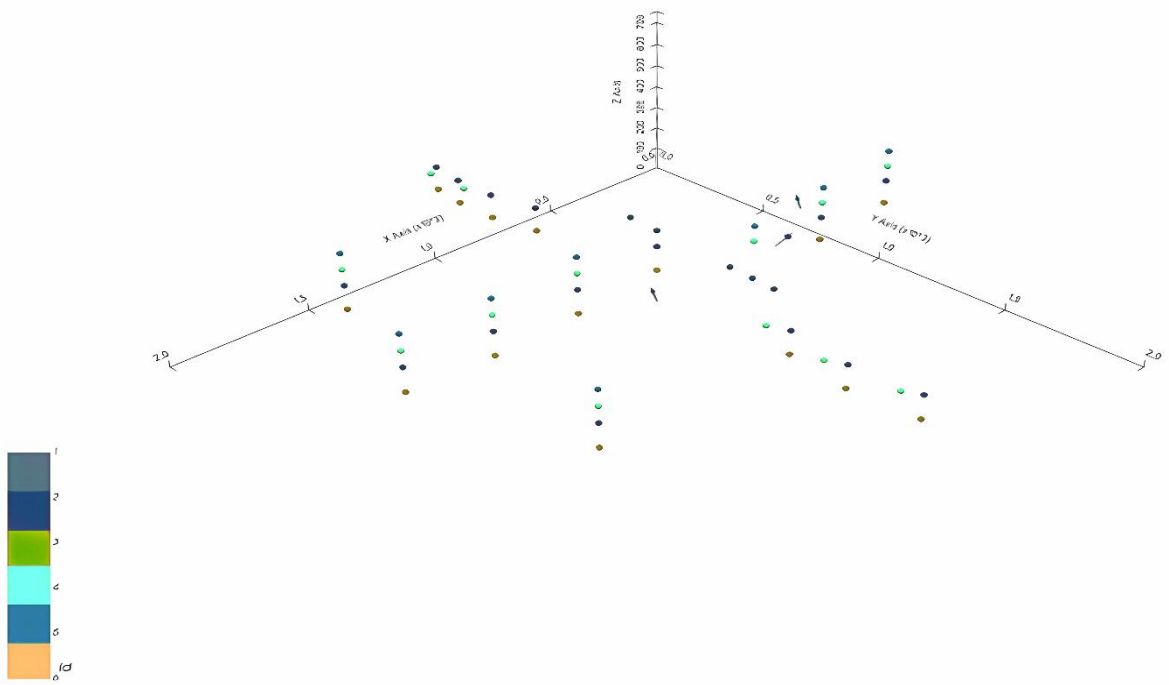

Model generation

After confirming that every main data point in our object DataManagement has been defined as intended. Now that we have the input data ready for interpolation, we can proceed to the next stage of creating our geological model. InputData (in this case, geo_data). To do this, use the code below to create an InterpolatorData object from our InputData object:

```
gp.set_interpolator(geo_model,
                    compile_theano=True,
                    theano_optimizer='fast_compile',
                    )
```

Out:

```
Setting kriging parameters to their default values.
Compiling theano function...
Level of Optimization:  fast_compile
Device:  cpu
Precision:  float64
Number of faults:  1
Compilation Done!
Kriging values:
                     values
range              2926.17
$C_o$            203869.05
drift equations     [3, 3]

<gempy.core.interpolator.InterpolatorModel object at 0x7fcb8ab2c5e0>
```

This function provides mathematical parameters required for carrying out the interpolation in addition to rescaling the extent and coordinates of the original data (storing it in the property geo_data_res, which functions as a typical InputData object). This step's calculation might take some time because it also creates a theano function that is needed to compute the model. If this is not required, we may avoid it by telling the function to compile_theano = False. Right now, we have all we need to use compute_model to compute our whole model. Usually, this will result in two different array solutions. In the first, the lithological formations are described in depth, and in the second, the fault network of the model is discussed. There are two subarrays as entries in each of these arrays: [50]

1. Lithology block model solution:
   - Entry [0]: Each voxel's lithological formation type is given by a corresponding formation_number in this array.
   - Entry [1]: A possible field array that in the block model indicates the orientation of lithological units and layers.

2. Fault network block model solution:
   - Entry [0]: Array where each voxel has a unique integer representing each fault-separated section of the model.
   - Entry [1]: Possible field array connected to the block model's fault network. We demonstrate these various model solutions and their applications below.

```
sol = gp.compute_model(geo_model)

sol
```

Out:

```
Lithology ids
  [6. 6. 6. ... 2. 2. 2.]
```

```
geo_model.solutions
```

Out:

```
Lithology ids
  [6. 6. 6. ... 2. 2. 2.]
```

Direct model visualization in GemPy

Model solutions may be rapidly inspected in 2D sections in GemPy directly. Let's now investigate our lithology block:

```
gp.plot_2d(geo_model, show_data=True)
plt.show()
```

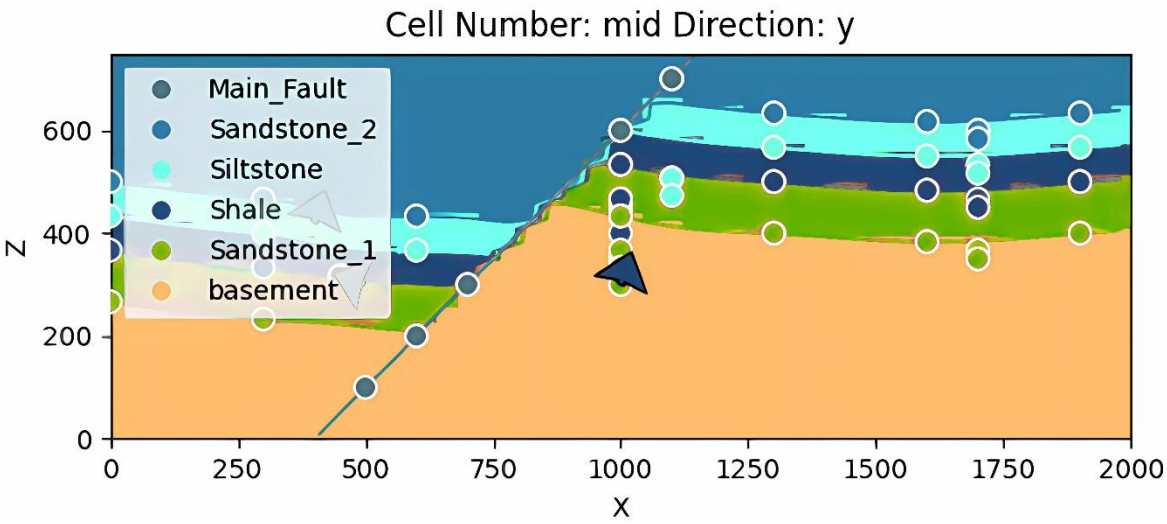

We have selected a section that passes through the center of our block using cell_number=25 and keeping in mind that we specified our resolution to be 50 cells in each direction. Since we moved 25 cells in the direction of "y," a plane parallel to the x and y axes is shown in the plot. By setting plot_data=True, the original data and the outcomes might be plotted simultaneously.

We can travel about and examine our 3D block model by adjusting the parameters for cell_number and orientation and seeing it from various 2D planes. Without lithological scalar-field solution, we may do the same thing:

```
gp.plot_2d(geo_model, show_data=False, show_scalar=True, show_lith=False)
plt.show()
```

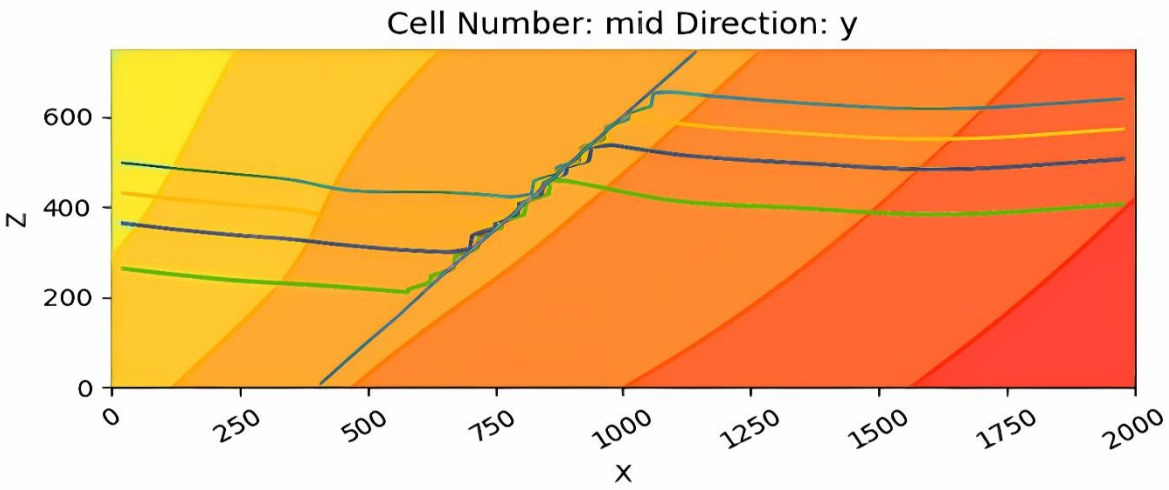


```
gp.plot_2d(geo_model, series_n=1, show_data=False, show_scalar=True, show_lith=False)
plt.show()
```

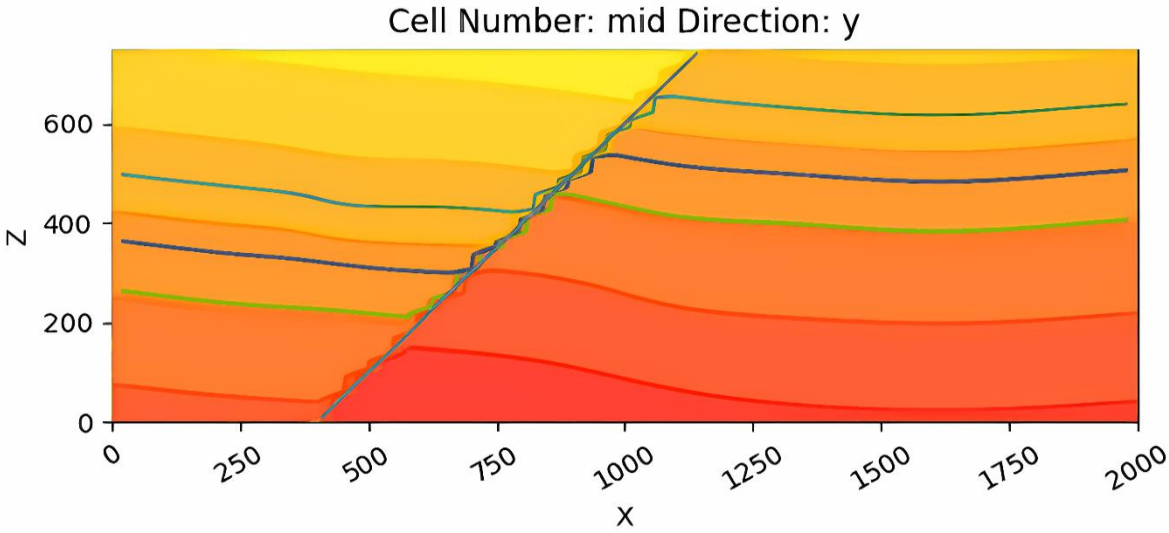

This is an excellent illustration of how folds have distorted the stratigraphy and how the fault has impacted the strata.

The following methods can be used to illustrate the fault network modeling solutions:

```
geo_model.solutions.scalar_field_at_surface_points
```

Out:

```
array([[0.03075848, 0.        , 0.        , 0.        , 0.        ],
       [0.        , 0.77174354, 0.72471042, 0.80357372, 0.83598092]])
```

```
gp.plot_2d(geo_model, show_block=True, show_lith=False)
plt.show()
```

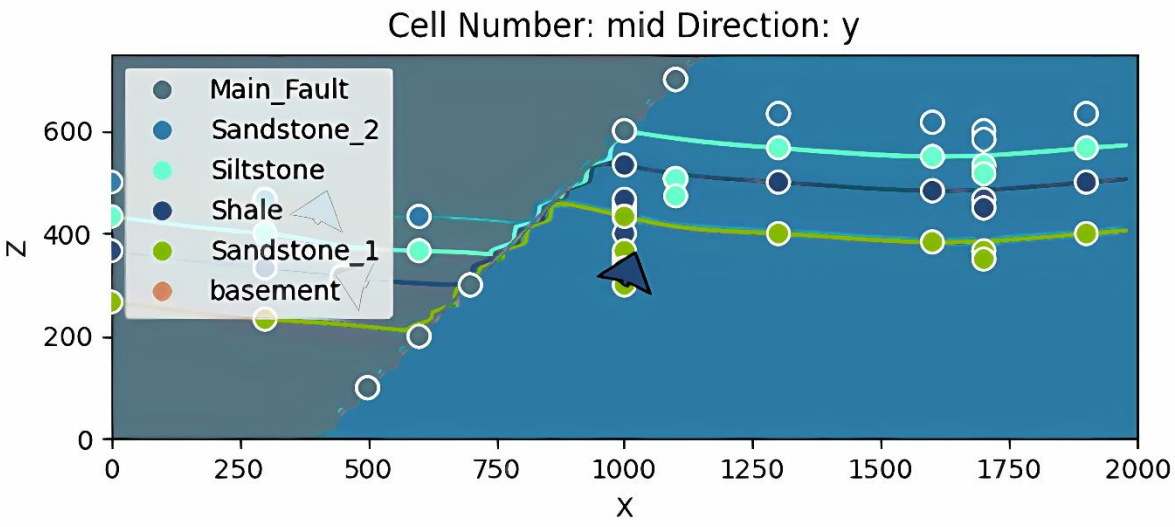


```
gp.plot_2d(geo_model, series_n=1, show_block=True, show_lith=False)
plt.show()
```

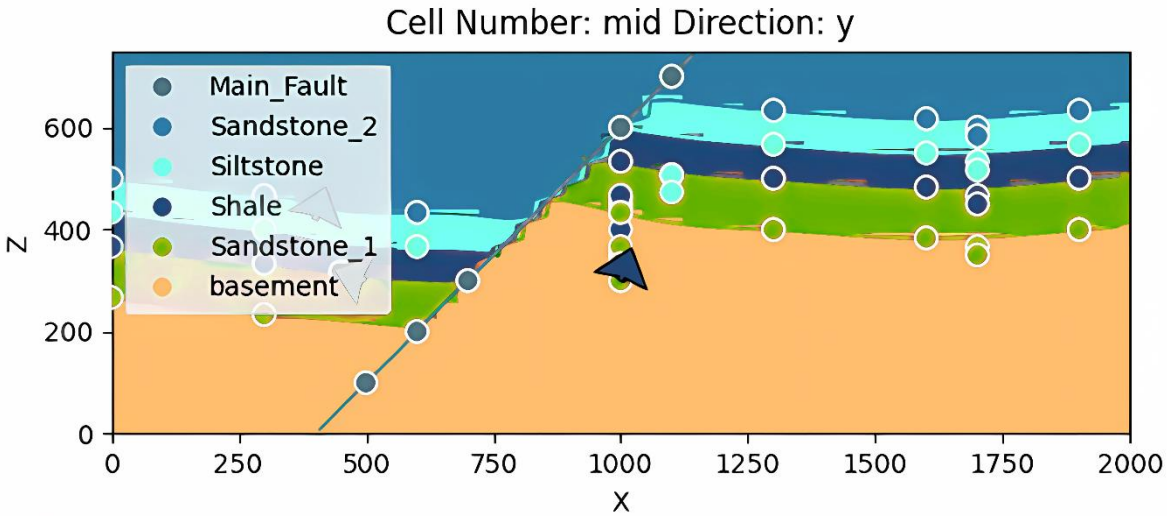

Marching cubes and VTK visualization

For 3D rendering, we can extract surfaces in addition to 2D sections. Surfaces are represented as 3D triangular complexes in VTK. To build these triangles, we have to select the proper vertices and simplices from the potential fields of faults and lithologies. This process is mechanized with the use of GemPy's get_surface function.

```
ver, sim = gp.get_surfaces(geo_model)
gpv = gp.plot_3d(geo_model, image=False, plotter_type='basic')
```

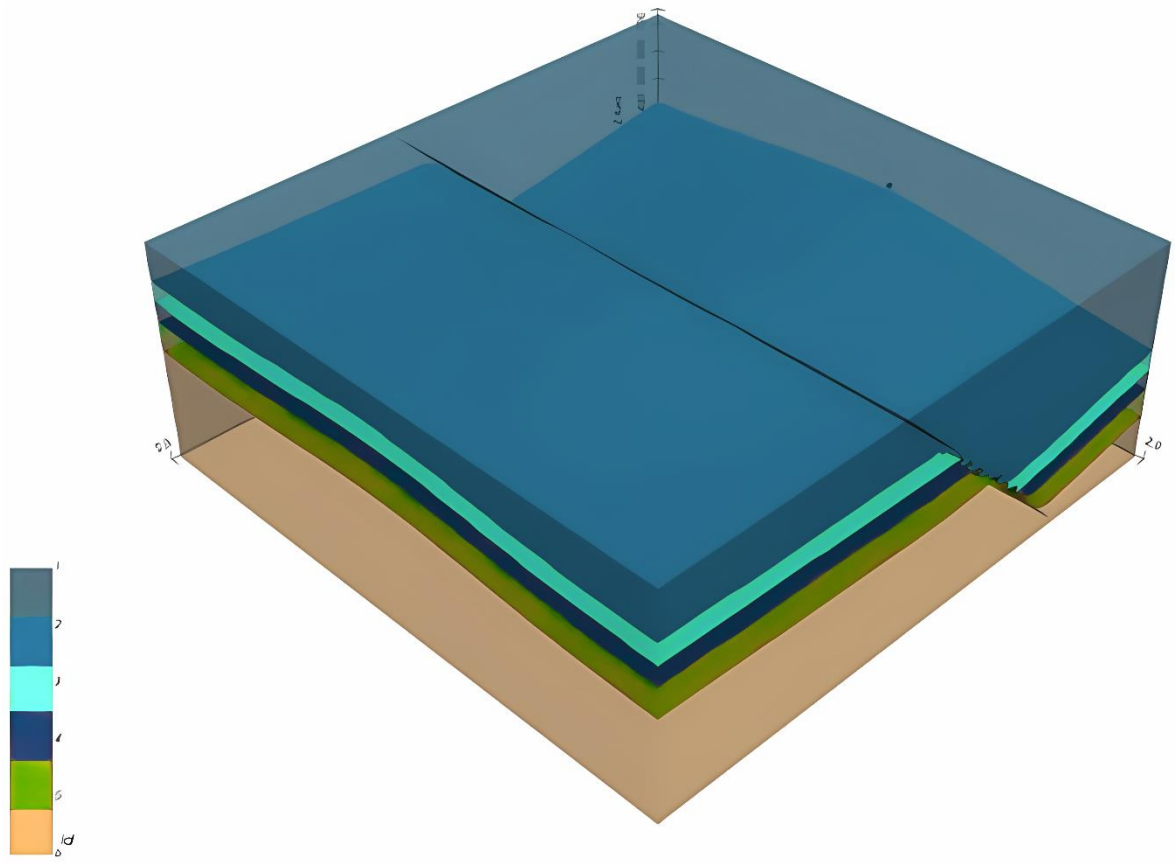

With the rescaled interpolation data, we can now run our 3D VTK visualization in an interactive mode, allowing us to make real-time modifications and updates to our model. The modifications, like the dynamic 3D representation of our input data, are permanently preserved (in the InterpolationInput.dataframe object). Real-time updates are also made to the geological models as a result. [50]

Adding topography

```
geo_model.set_topography(d_z=(350, 750))
```

Out:

```
Active grids: ['regular' 'topography']

Grid Object. Values:
array([[  20.        ,   20.        ,    7.5       ],
       [  20.        ,   20.        ,   22.5       ],
       [  20.        ,   20.        ,   37.5       ],
       ...,
       [2000.        , 1918.36734694,  423.48951452],
       [2000.        , 1959.18367347,  430.25455308],
       [2000.        , 2000.        ,  431.07163663]])
```

```
gp.compute_model(geo_model)
gp.plot_2d(geo_model, show_topography=True)
plt.show()


# sphinx_gallery_thumbnail_number = 9
gpv = gp.plot_3d(geo_model, plotter_type='basic', show_topography=True,
show_surfaces=True,
                 show_lith=True,
                 image=False)
```

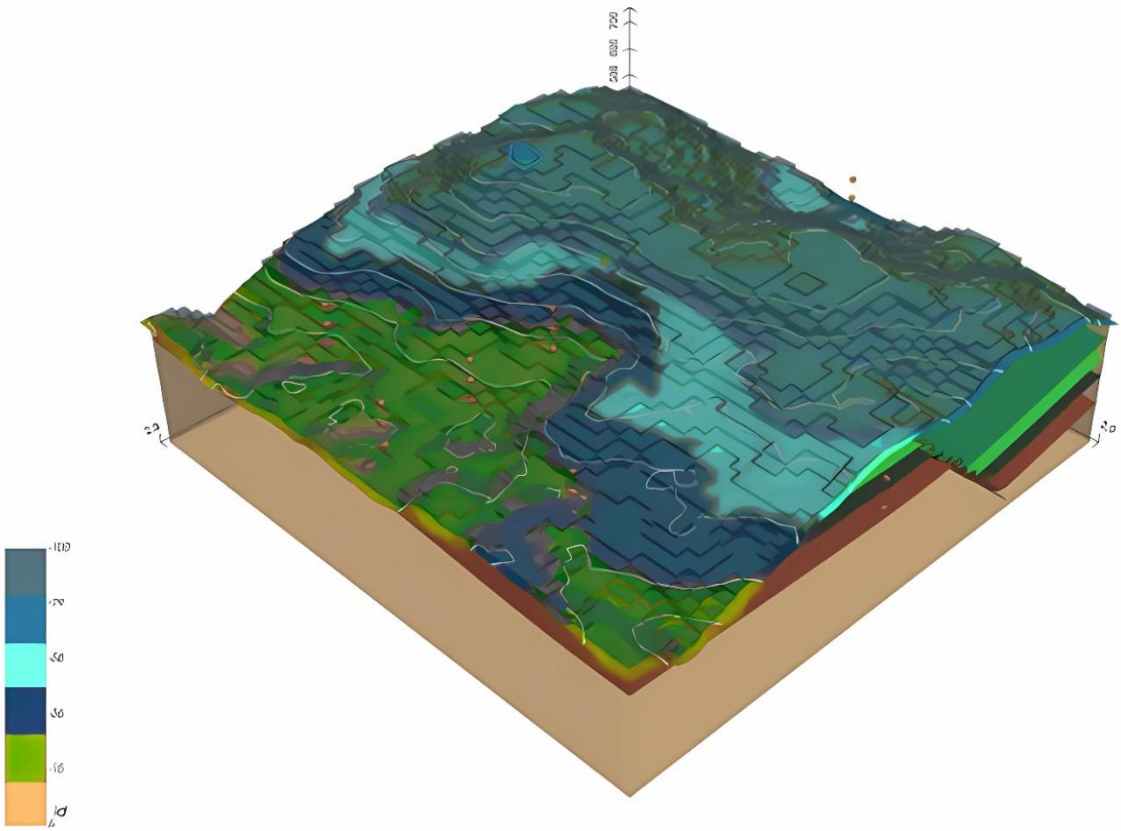

```
or-tuples-or ndarrays with different lengths or shapes) is deprecated. If you meant to
do this, you must specify 'dtype=object' when creating the ndarray.
  self.geological_map = np.array(
```

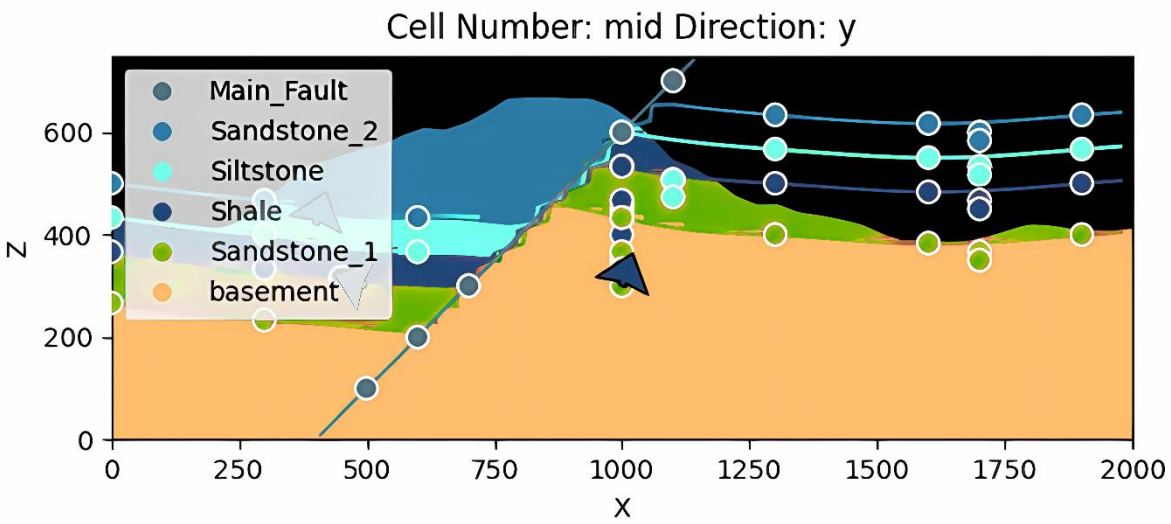

Out:

```
/WorkSSD/PythonProjects/gempy/gempy/core/solution.py:173: VisibleDeprecationWarning:
Creating an ndarray from ragged nested sequences (which is a list-or-tuple of lists-
```

Compute at a given location

Recomputing and changing the grid to a bespoke grid do this. The results are shown as grid + surfaces_points_ref + surface_points_rest locations, as you may have seen.

```
x_i = np.array([[3, 5, 6]])
sol = gp.compute_model(geo_model, at=x_i)
```

Out:

```
Active grids: ['custom']
/WorkSSD/PythonProjects/gempy/gempy/core/solution.py:168: VisibleDeprecationWarning:
Creating an ndarray from ragged nested sequences (which is a list-or-tuple of lists-
or-tuples-or ndarrays with different lengths or shapes) is deprecated. If you meant to
do this, you must specify 'dtype=object' when creating the ndarray.
  self.custom = np.array(
```

Consequently, if all we require is the value at x_i:

```
sol.custom
```

Out:

```
array([array([[6.]]), array([[0.18630133],
                             [0.63163565]])], dtype=object)
```

Saving the model

GemPy quickly stores temporary items using Python [pickle]. Consistency across module versions is necessary, though. Make sure you are using the same version of pickle and any dependant modules (like Pandas or NumPy) as when the data was first saved in order to load a pickle into GemPy. We can export the pandas for longer-term, more secure keeping.Using DataFrames to CSV.

```
gp.save_model(geo_model)
Out:
True
```

6. Numerical example and simulation

Using the associated parameter in Table (IV. 1), a numerical example analysis is conducted to investigate the stick-slip characteristics of the drill string system during torsional vibration movement.

Table IV. 1: Associated example parameters.

Variables	Values
Moment of inertia of top drive $\boldsymbol{J_r}$	900 $\boldsymbol{Kg.m^2}$
Moment of inertia of drill pipes $\boldsymbol{J_p}$	2780 $\boldsymbol{Kg.m^2}$
Moment of inertia of drill collars $\boldsymbol{J_c}$	690.53 $\boldsymbol{Kg.m^2}$
Moment of inertia of drill tool $\boldsymbol{J_t}$	1.1658 $\boldsymbol{Kg.m^2}$
Moment of inertia of drill Bit $\boldsymbol{J_b}$	465.2 $\boldsymbol{Kg.m^2}$
Stiffness between top drive and drill pipes $\boldsymbol{K_{rp}}$	1100 $\boldsymbol{Nm/rad}$
Stiffness between drill pipes and drill collars $\boldsymbol{K_{pc}}$	1175 $\boldsymbol{Nm/rad}$
Stiffness between drill collars and drill tool $\boldsymbol{K_{ct}}$	947 $\boldsymbol{Nm/rad}$
Stiffness between drill tool and drill bit $\boldsymbol{K_{tb}}$	814.3 $\boldsymbol{Nm/rad}$
Damping between top drive and drill pipes $\boldsymbol{C_{rp}}$	120.6 $\boldsymbol{Nm/rad}$
Damping between drill pipes and drill collars $\boldsymbol{C_{pc}}$	185.71 $\boldsymbol{Nm/rad}$
Damping between drill collar and drill tool $\boldsymbol{C_{ct}}$	170 $\boldsymbol{Nm/rad}$
Damping between drill tool and drill bit $\boldsymbol{C_{tb}}$	229.22 $\boldsymbol{Nm/rad}$
Viscous damping coefficient of top drive $\boldsymbol{C_r}$	415.3 $\boldsymbol{Nm/rad}$

Viscous damping coefficient of drill bit C_b	45 Nm/rad
WOB	90 KN
Radius of drill bit R_b	145.2 mm
Outer diameter of drill tool	164 mm
Dynamic friction factor factor μ_{sb}	0.7
Coulomb friction factor factor μ_{cb}	0.45
Conversion factor factor γ_b	0.45

6.1 Simulation results

A dynamic model of the drill string that has been built is used to replicate the motion of the drill bit and top drive while the top drive is moving at a constant speed of 6.54 rad/s.

We can see that the drill bit exhibits a stick-slip vibration phenomenon: the torque is initially constant before abruptly decreasing and increasing; the drill bit's angular velocity starts at zero before abruptly accelerating and then rapidly decreasing to zero.

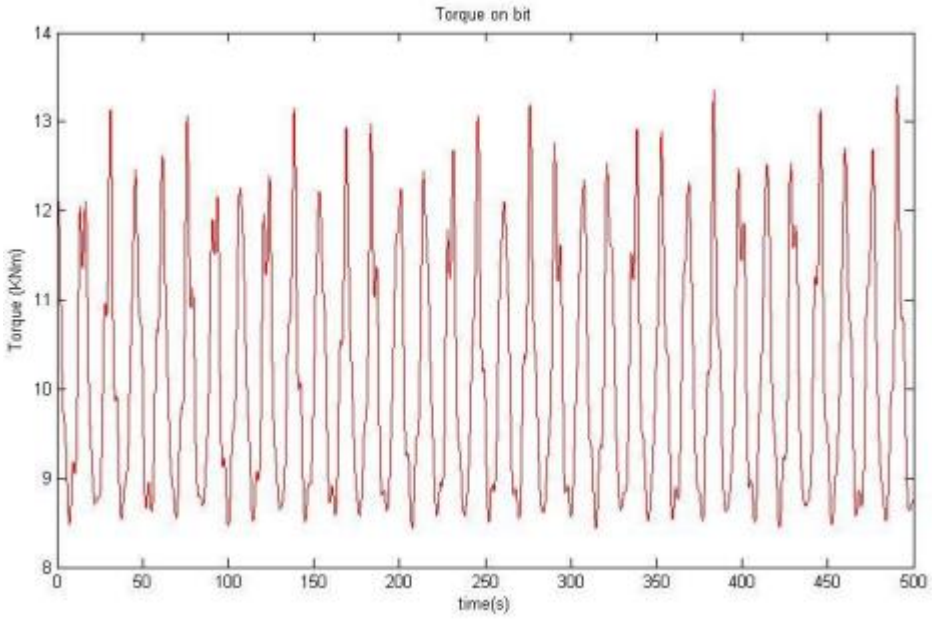

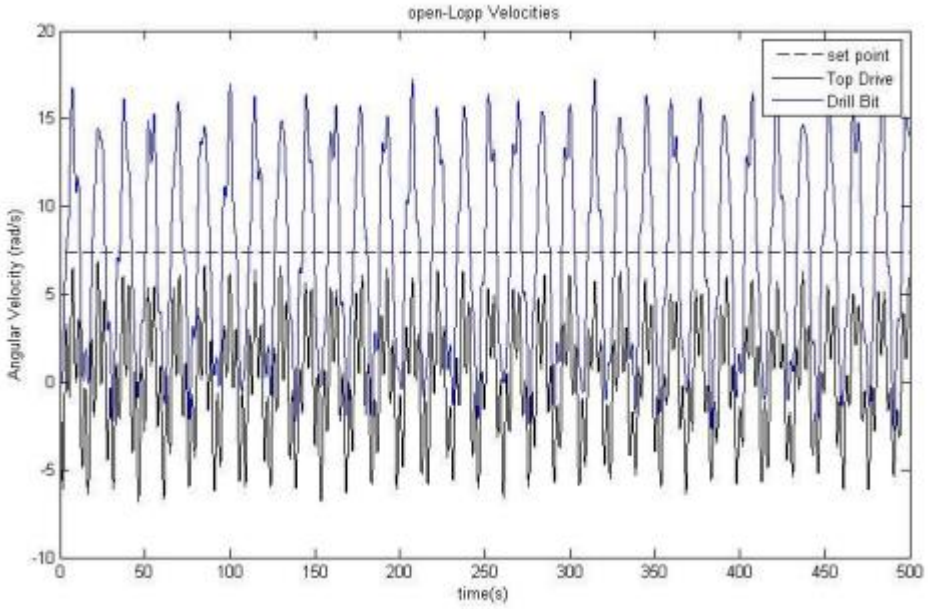

Figure IV. 18. Top drive torque, drill bit angular velocity, and torsional vibration.

6.2 Various WOBs outcomes

At different WOBs, the drill bit's angular velocity is approximated while the top drive operates at a steady 6.54 rad/s speed. At the selected WOB, the drill bit clearly displays stick-slip vibrations, as seen in Figure (IV. 19). The stick-slip vibration duration of the drill bit and the angular velocity fluctuation range both lengthen with increasing WOB. As WOB increases, the friction torque increases as well, leading to an unstable stick-slip behavior. Without a doubt, the drill bit will become caught if the WOB continues to rise.

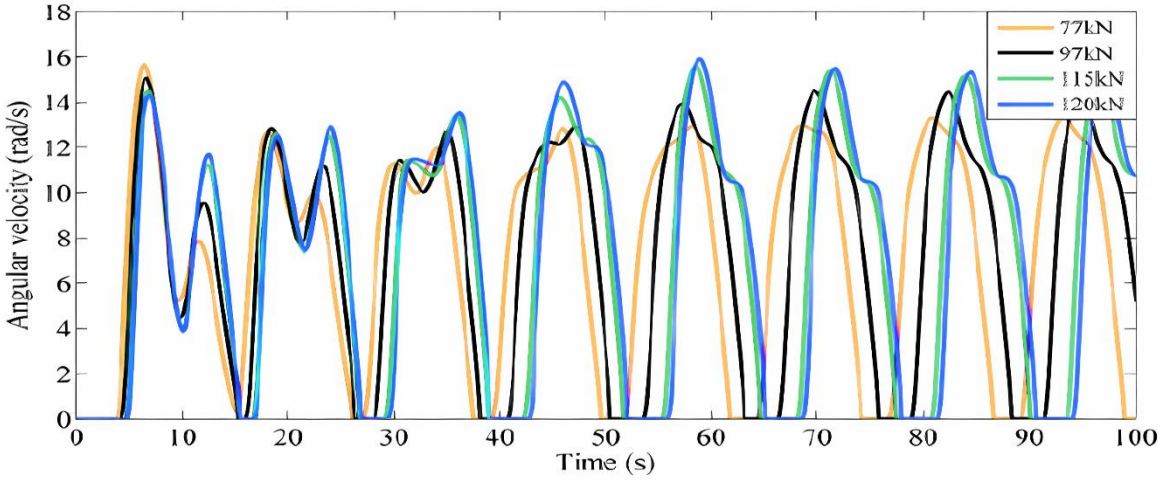

Figure IV. 19. Drill bit's angular velocity at various WOBs.

The results of the investigation indicate that the lower WOB and quicker rotation of the top drive will help mitigate some stick-slip vibrations. The nonlinear dynamic model and computing technique created in this part are integrated with the real field circumstances.

6.3 Various spinning rates' outcomes

Each drill bit's angular velocity is determined for a range of top drive rotating speeds. As seen in Figures (IV. 20, IV. .21, IV .22), the longer the drill bit's stick-slip vibration period and the larger the angular velocity variation, the lower the top drive's rotating speed. The numbers are 1 rad/s, 10 rad/s, and 50 rad/s, respectively. The stick-slip vibration period is longest and the drill bit nearly always gets stuck when the top drive's rotating speed is 1 rad/s, as shown in Figures (IV. 20, IV. .21, IV .22). The stick-slip vibrations are short when the rotational speed is 50 rad/s.

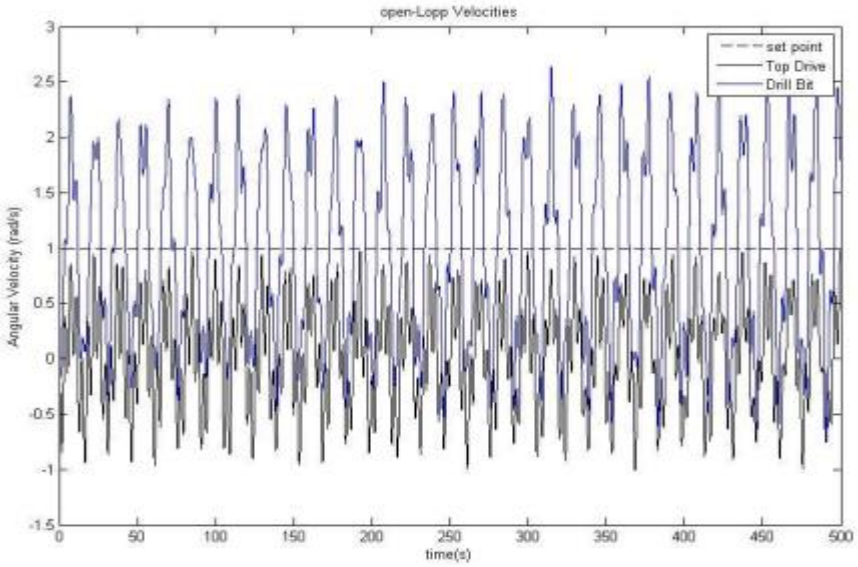

Figure IV. 20. Angular velocity at 1 rad/s.

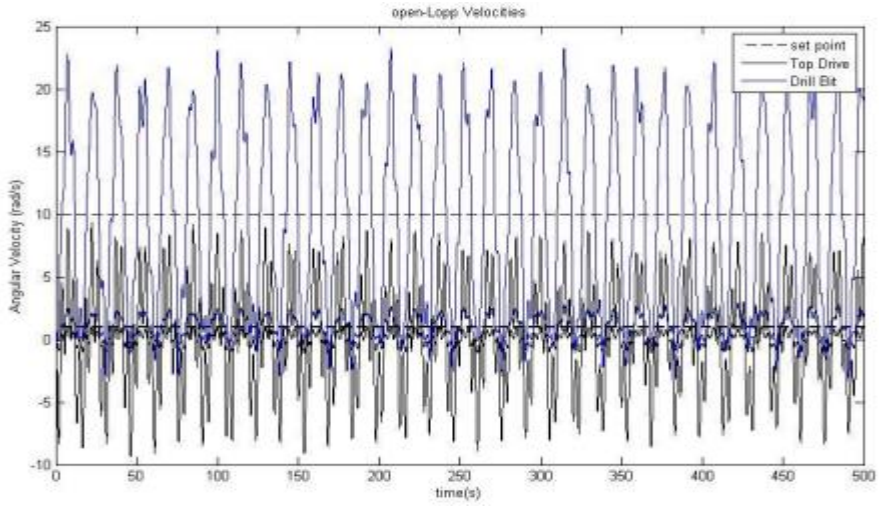

Figure IV. 21. Angular velocity at 5 rad/s.

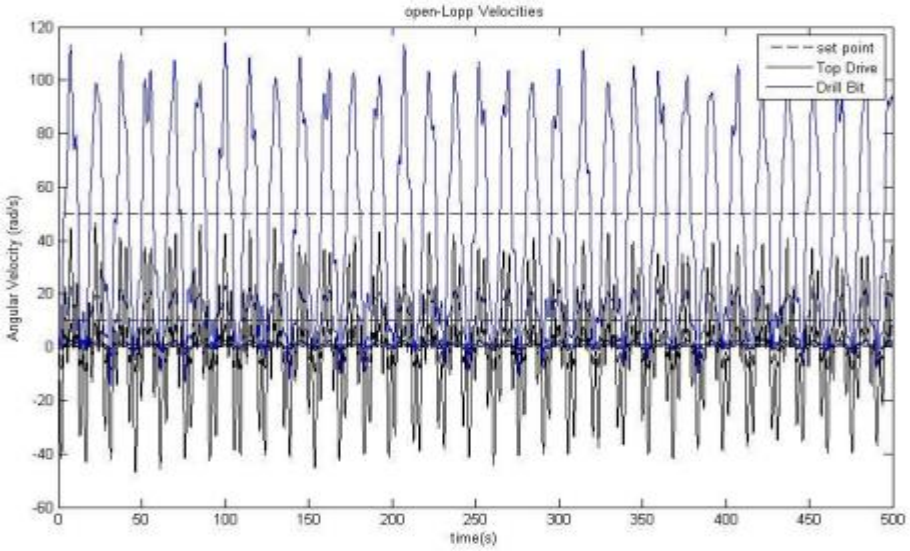

Figure IV. 22. Angular velocity at 50 rad/s.

7. Conclusion and recommendation

It is clear from the seismic analysis and simulation during drilling that uses drill bit stick-slip vibration as a source that this method is not very likely to improve subsurface imaging accuracy and resolution during drilling operations for Algerian oil fields.

It has been demonstrated that the stick-slip vibration model employed in Seismic While Drilling is superior to other techniques in terms of producing a higher quality seismic signal, which can improve the identification of hydrocarbon sources and lower the risk of drilling. There are a few restrictions to take into account, though. The kind of rock formation, the well's

depth, and the drilling circumstances are some of the variables that affect how successful SWD is. Sometimes the stick-slip vibration is too weak to produce the necessary seismic signal, or it gets in the way of other drilling activities.

The potential and limits of SWD employing drill bit stick-slip vibration as a source in the Algerian oil field cannot, therefore, be completely understood by more study and testing. It is probably not recommended otherwise until additional advancements in sophisticated data analysis and interpretation methods may contribute to a further increase in the precision and sharpness of subsurface imaging.

Ultimately, it is necessary to carefully evaluate specific drilling circumstances, high pressure zones and geological formations in order to assure the technique's efficacy and applicability.

GENERAL CONCLUSION

General Conclusion

The concluding section of this thesis synthesizes the findings from both the theoretical and practical chapters, highlighting the potential and limitations of using stick-slip vibrations as a source for Seismic While Drilling (SWD). This investigation has provided a comprehensive analysis of the mechanics of stick-slip vibrations, the propagation characteristics of the resultant seismic waves, and the practical aspects of acquiring and interpreting seismic data in real-time during drilling operations. The study has also specifically considered the geological complexities of the Algerian oilfields, which present unique challenges to the effective implementation of this technique.

Despite these promising aspects, the application of stick-slip-based SWD in the Algerian oilfields faces significant challenges. The geological conditions in this region are notably complex, with formations characterized by the presence of salts, anhydrite, and other challenging materials. These geological features can severely attenuate seismic signals, reducing the clarity and accuracy of the subsurface images obtained. Furthermore, the insufficient noise generation associated with stick-slip vibrations further complicates the acquisition of reliable seismic data. The low-frequency oscillations may not produce adequate seismic energy to penetrate deeply or travel long distances in such complex geological settings, hampering the ability to capture high-quality seismic data.

Given these limitations, the thesis concludes that it is currently difficult to recommend the widespread adoption of stick-slip-based SWD in the Algerian oilfields. The combination of complex geology and insufficient noise generation poses substantial obstacles that undermine the effectiveness of this technique. However, this conclusion does not diminish the potential of stick-slip vibrations for SWD in other geological contexts or with future advancements. The challenges identified in this study point to areas where further research and technological innovation are needed. Future research should focus on addressing these specific challenges, such as exploring new methods to amplify the seismic energy generated by stick-slip vibrations, improving the sensitivity and resolution of seismic sensors, and developing advanced data processing algorithms to better handle the complexities of seismic wave propagation in challenging geological formations.

Technological advancements in drilling equipment and seismic acquisition systems could also play a crucial role in overcoming the current limitations. Innovations such as high-frequency vibration sources, enhanced drill bit designs, and more robust data transmission technologies could significantly improve the feasibility of using stick-slip vibrations for SWD.

In conclusion, while stick-slip vibrations offer a novel and potentially valuable source for Seismic While Drilling, their application in the Algerian oilfields is currently constrained by significant geological and technical challenges, In contrast to VSP technology, which has consistently demonstrated its efficacy. The findings of this thesis underscore the need for continued research and innovation to unlock the full potential of this technique. With targeted efforts to address the identified limitations, stick-slip-based SWD could become a more viable and effective tool for subsurface imaging, contributing to safer and more efficient drilling operations in diverse geological settings.

Bibliography

[1] R. R. Stewart, An In-Depth Seismic Understanding, CANADA: DEPARTMENT OF GEOLOGY & GEOPHYSICS, UNIVERSITY OF CALGARY,, 2001.

[2] O. Obiegbu, PRINCIPLES AND APPLICATIONS OF VSP IN HYDROCARBON EXPLORATION, Department of Geology and Exploration Geophysics, 2013.

[3] D. K. Galybin et Leon Dahlhaus, Walkaway VSP - Going beyond imaging, ASEG Extended, 2013.

[4] J. Arroyo, L., Brenton, P., Dijkerman et H., Dingwal, Seismic Data from the Borehole, AAPG, 2003.

[5] T. KIMURA, Schlumberger Fiber Optics Technology, Southampton, UK.

[6] A. J. Greenwood, Application of Vertical Seismic Profiling for the characterisation of, Curtin University: Department of Exploration Geophysics, February 2013.

[7] S. T. Chen et L. J. Zimmerman, «Subsurface imaging using reversed vertical seismic profiling and crosshole tomographic methods,» SEG Library, vol. 55, n° %111, 2023.

[8] J. V. d. Toorn et Zaheer Ali Shah, Vertical Seismic Profile, Applied Techniques to Integrated Oil and Gas Reservoir Characterization, 2021.

[9] SLB, Explore the Energy Glossary, «vertical seismic profile (VSP),» SLB, 2024.

[10] C. Naville, ILLUSTRATION OF A LAND VSP FIELD OPERATION WITH VIBRATOR SOURCE AROUND THE DRILLING SITE, GRAND PARIS AREA, FRANCE., 2024.

[11] Salah Said Med AMEUR, Mohammed Abd El illah ABBOU et Amine DERGAOUI, Seismic While Drilling (SWD) Process Simulation Based on Stick-Slip Vibration Model in Algerian Petroleum Field, University of Kasdi Merbah., 2022.

[12] J. Azar et G. Robello Samuel., Drilling engineering, PennWell Corporation, 2007.

[13] B. Saldivar, I. Boussaada, H. Mounier, S. Mondi´e et S. I. Niculescu, An Overview on the Modeling of Oilwell Drilling Vibrations, 2014.

[14] M. Belem, Saldivar Márquez, Islam Boussaada, Hugues Mounier et Silviu-Iulian Niculescu, Analysis and Control of Oilwell Drilling Vibrations A Time-Delay Systems Approach, 2015.

[15] Ghasemloonia, Ahmad, D. Geoff Rideout et Stephen D. Butt, A review of drillsting vibration modeling and suppression methods, Journal of petroleum Science and Engineering, 2015.

[16] M. E. Hossain et M. R. Islam., Drilling Engineering Problems and Solutions A Field Guide for Engineers and Students.

[17] M. Kidouche, Mohamed Zinelabidine Doghmane, Samir Benammar et Kong Fah Tee, Rock–bit interaction effects on high-frequency stick-slip vibration severity in rotary drilling systems, 10 August 202.

[18] F. P. I. Nazionale, di Oceanografia et di Geofisica Sperimentale, SEISMIC WHILE DRILLING FUNDAMENTALS OF DRILL-BIT SEISMIC FOR EXPLORATION, Milan Italy: Francesco Miranda ENI E&P Division.

[19] W. Liu, Feilong Yang, Xiaohua Zhu et Xingwu Chen, Stick-slip vibration behaviors of BHA and its control method in highly-deviated wells, 04 March 2022.

[20] L. Tang, Wei He et Xiaohua Zhu, «The effect of high-frequency torsional impacts on the dynamic response of a drill string in a stick state,» Advances in Mechanical Engineering, 2019.

[21] A. J. A. Aziz, Ahmad Zakuan, et Petronas Carigali,, «Stick Slip Mitigation Plan to Improve Drilling,» Society of Petroleum Engineers, 2011.

[22] S. Chen et John Wisinger, «Identification and Mitigation of Friction- and Cutting-Action-Induced Stick/Slip Vibrations with PDC Bits,» Onepetro, 2020.

[23] Y. Shen, Zhengxin Zhang, Jie Zhao; et Wei Chen, «The Origin and Mechanism of Severe Stick-Slip,» Onepetro , n° %1SPE-187457-MS, 201.

[24] Aditya Sharma, Khizar Abid,, Saket Srivastava, et Andres Felipe Baena Velasquez,, «A review of torsional vibration mitigation techniques using active control and machine learning strategies,» keaipublishing, The University of Oklahoma, Norman, OK, USA, 2023.

[25] downhole nov, PosiTrack TVM, downhole nov, 2023.

[26] SLB, energy Glossary, antiwhirl bit, SLB, 2024.

[27] TURBO DRILL, Steady Scout STICK-SLIP MANAGEMENT TOOL, Texas: Turbo drilling, 2023.

[28] S. X. Wu, Luis Paez, Uyen Partin et Mukul Agnihotri, «Decoupling Stick-Slip and Whirl to Achieve Breakthrough in Drilling Performance,» Onepetro, n° %1SPE-128767-MS, 2010.

[29] C. .. NAVILLE, P .C. LAYOTTE, G . PIGNARD et J . GUESNON, WELL SEISMIC APPLICATION OF THE TRAFOR MWL?, Cedex, Franc e: Institut Frangais du Pétrole, Département Géophysique,, 1994.

[30] L. Wang, Huaishan Liu,, Siyou Tong et Yanxin Yin, Retrieving drill bit seismic signals using surface seismometers, China: Key Laboratory of Submarine Geosciences and Exploration Techniques, 2015.

[31] S. Putt, Considers the merits of seismic while drilling technology, USA, December 2019.

[32] W. Yang, Signal Detection of the Drill Bit Seismic Wave While Drilling, China : The Institute of Geophysics, 2007.

[33] H. W. et Rector, J, Radiation Pattern and Seismic Waves Generated by a Working Roller-Cone Drill Bit., Geoscienceworld, 1992.

[34] H. Chen, Stratigraphic Division of Volcanic Reservoir by Uniting of Well Data and Seismic Data-Taking Volcanic Reservoir of Member one of Yingcheng Formation in Xudong Area of Songliao Basin for an Example, Journal of Earth Science, 2014.

[35] O. S, Khaled, et Alaa M., «Seismic-While-Drilling in Kuwait,» GeoArabia, vol. 01, n° %104, 1996.

[36] Z. Wilczynski, Ayse Kaslilar, Monika Ivandic et Christopher Juhlin, Drill-bit position monitoring using seismic-while-drilling data;numerical and field examples from Sweden, Sweden: European Association of Geoscientists & Engineers., 27 January 2023.

[37] Thiago Pinotti, Seismic while drilling (SWD) experiences on the Peregrino field – a case study, Sociedade Brasileira de Geofísica: SBGf, 2013.

[38] Wajid Rasheed, Reservoir, drilling and real-time technologies increase Saudi Aramco reserves, production, Middel east: Drilling contarctor , 2007.

[39] R. Hastings-James, 3-D Land Seismic Acquisition in Saudi Arabia, GeoArabia, OCTOBER 01, 1996.

[40] A. M. Alkandari, Night Shot-Hole Drilling, A New Approach for Successful Completion of Mega Onshore 3D Seismic Survey, Manama, Bahrain,: Middle East Geosciences Conference and Exhibition, 2018.

[41] Arabnews, Saudi Aramco uses new technology to re-explore vast Empty Quarter, Arabnews, 2017.

[42] N. E. Heddadi, REDJEM Khaled et Manal Melisy, How can BIG DATA help Algeria Algerian Oil And Gas Companies, Algeria: Algerian Journal of Economics and Business studies, 2021.

[43] Geophysical Journal International, Algerian margin off Jijel: integrating wide-angle seismic modelling and multichannel seismic pre-stack depth migration, Geophysical Journal International, 2020.

[44] J. Bian, Aixin Liu et Shuo Yang, A Combined Method of Seismic Monitoring and Transient Electromagnetic Detection for the Evaluation of HydraulicFracturing Effect in Coal Burst Prevention, sensors MDPI, 2024.

[45] Smith, J. (2021). Simulating Complex Processes: MATLAB and Python Functions for Seismic Data Analysis. (Unpublished doctoral thesis). University of XYZ.

[46] SeisLab Documentation

[47] Gary F. Margrave, New seismic modelling facilities in Matlab.

[48] GemPy Documentation. GemPy: An Open-Source Python Package for 3D Geological Modeling. Retrieved from https://www.gempy.org/documentation

[49] Rami Riane, Mohamed Zinelabidine Doghmane, Madjid Kidouche, Kong Fah Tee, and Sofiane Djezzar, Stick-Slip Vibration Suppression in Drill String Using Observer-Based LQG Controller.

[50] Jialin Tian, Genyin Li,Liming Dai,Lin Yang, Hongzhi He, Shuhui Hu1, Torsional Vibration and Nonlinear Dynamic Characteristics of Drill String s and Stick-Slip Reduction Mechanism